Adenylyl cyclase 5/6 underlie PIP_3 dependent regulation

Dissertation

zur

Erlangung des Doktorgrades

der Naturwissenschaften

(Dr. rer. Nat.)

dem

Fachbereich Pharmazie der

Philipps-Universität Marburg

vorgelegt von

Raghavender Reddy Gopireddy

aus

Hyderabad, Indien

Marburg/Lahn **Juli 2015**

Erstgutachter: **Prof. Dr. Moritz Bünemann**

Zweitgutachter: **Prof. Dr. Jens Kockskämper**

Eingereicht am 12.06.2015

Tag der mündlichen Prüfung am 24.07.2015

Hochschulkennziffer: 1180

Table of contents

Abbreviations

AC	Adenylyl cyclase
ACh	Acetylcholine
AKAP	A-kinase anchoring protein
Akt or PKB	Protein kinase B
ATP	Adenosine 5’-triphosphate
BSA	Bovine serum albumin
Btk	Bruton’s tyrosine kinase
Ca^{2+}	Calcium
CaM	Calmodulin
cAMP	Cyclic adenosine-3’5’-monophosphate
CFP	Cyan fluorescent protein
cGMP	Cyclic guanosine-3’,5’-monophosphate
DAG	Diacylglycerine
DMEM	Dulbecco’s modified Eagle’s medium
EDTA	Ethylenediamine-N,N,N’N’-tetraaceticacid
Epac	Exchange protein directly activated by cAMP
Epac1-camps	FRET-based cAMP sensor which contains the Epac1-domain
FCS	Fetal calf serum
GAPDH	Glyceraldehyde-3-phosphate dehydrogenase

GPCR	G protein coupled receptor
G protein	Guanine nucleotide binding protein
HCN	Hyperpolarization-activated cyclic nucleotide-gated channel
HEK293	Human embryonic kidney cells
HeLa	Human uterine cervical carcinoma cells
IP_3	Inositol trisphosphate
Iso	Isoproterenol
M_2ACh-R	Muscarinic acetylcholine receptor (type 2)
NE	Norepinephrine
NO	Nitric oxide
PAGE	Polyacrylamid gel electrophoresis
PBS	Phosphate buffered saline
PCR	Polymerase chain reaction
PDE	Phosphodiesterases
PDGF	Platelet derived growth factor
PDK1	Phosphoinositide-dependent kinase-1
PH	Pleckstrin-homology
PI	Phosphatidylinositol
PI-3,4,5-P_3	Phosphatidylinositol-3,4,5-trisphosphate (PIP_3)
PI-3,4-P_2	Phosphatidylinositol-3,4-bisphosphate (PIP_2)
PI3-K	Phosphoinositide 3-kinase
PKA	Protein kinase A

PKC	Protein kinase C
PKG	Protein kinase G
PLC	Phospholipase C
PTEN	Phosphates and tensin homologue deleted on chromosome 10
PTX	Pertussis toxin
qPCR	quantitative polymer chain reaction
S.E.M	Standard error of the mean
sGC	Soluble guanylyl cyclase
SHIP	Src homology 2-conatining inositol 5'-phosphate
WT	wild type
YFP	Yellow fluorescent protein
α_{2A}-AR	α_{2A}-adrenoceptor
β-AR	β-adrenoceptor

1. Introduction

1.1 Signal transduction

To ensure proper function of tissues and organs within an organism, cells must be able to respond to signals, not only from their local environment but also from external sources (Cooper, 2013). The transfer of these signals from external sources to the cell interior leads to triggering of a signal-specific cellular response that is referred to as signal transduction. In general, an extracellular signal activates different signal transduction pathways with widely varied mechanisms. However, the activation of these signal transduction pathways rely on cell surface receptors that are able to receive or identify external signals. These cell surface receptors are in turn activated by extracellular messengers (known as first messengers) such as light, heat, peptides, nucleotides and amino acids (Erin *et al*., 2013). The receptor activation by these first messengers subsequently activates intracellular signaling cascades that ultimately activate intracellular signaling molecules (known as second messengers) (Alberts *et al*., 2012) including cyclic nucleotides like cyclic adenosine monophosphate (cAMP), cyclic guanosine monophosphate (cGMP) and lipids like Phosphatidylinositol bisphosphate (PIP_2) and also ions like Ca^{2+} (Scott *et al*., 2000). Intracellular signal transduction pathways are regulated by four important receptors, i) G protein coupled receptors ii) ligand-gated ion channel receptors iii) transcription factor receptors iv) enzyme-linked receptors (Scott *et al*., 2000; Gomperts *et al*., 2002). Since the focus of this work was on GPCRs, the detail descriptions about GPCRs are discussed below.

1.1.1 G protein coupled receptors (GPCRs)

GPCRs are also known as 7-TM (trans membrane) receptors. In signal transduction, GPCRs represent a major group of cell surface receptors (Jastrzebska *et al*., 2006; Fredriksson *et al*., 2003; Menzaghi *et al*., 2002). The human genome encodes more than 1,000 GPCRs, which constitutes approximately 2% of the entire human genome (Jiang *et al*., 2006). The GPCRs are implicated in a wide variety of diseases thus making these GPCRs as an important drug target for in the pharmaceutical industry and all clinical areas (Vassilatis *et al*., 2003).

A wide variety of ligands binds to and activates GPCRs, including hormones and neurotransmitters leading to diverse biological responses such as neurotransmission, cellular metabolism, cellular differentiation, immune responses and so on ((Pierce *et al*., 2002; Jacoby *et al*., 2006).

GPCRs are composed of a single peptide, usually 300-500 but also up to 1400 amino acids. The superfamily of GPCRs shares the similar architecture of 7TM-α helices, and this consists of an extracellular amino-terminal and an intracellular carboxy-terminal. Based on sequence homology and functional similarities, GPCRs can be further divided into five major classes: i) glutamate receptors ii) rhodopsin receptors iii) adhesion receptors iv) frizzled receptors v) secretin receptors. However, the amino acid sequence similarities between these families are less than 20% (Lagerström *et al*., 2008).

1.1.2 General mechanism of signal transduction through GPCRs

When ligand or agonist binds to GPCR, the receptor is activated. Upon receptor activation, GTP replaces GDP on the α subunit of the G protein. Upon exchange of GDP for GTP, a conformational change takes place in GPCRs, this leads to dissociation of Gβγ from Gα (Fig.1). The dissociated subunits can activate distinct downstream effector proteins, resulting in a considerable amplification of the signal (Roberts *et al.,* 2004) (Fig.2). Different variety of effector molecules including adenylyl cyclase (AC), phospholipase C (PLC), protein kinases, potassium and calcium channels are regulated by Gα. On the other hand variety of effectors such as adenylyl cyclase, phospholipase C-β (PLC-β), phosphoinositide 3-kinase (PI3-K) and β-adrenergic receptor kinases are regulated by Gβγ. Regulation of these effectors ultimately lead to production of second messengers, such as cAMP (Watts *et al*., 2005), cGMP, Ca^{2+} (Landry *et al*., 2006) and Inositol trisphosphate (IP_3) (Ohno-Shosaku *et al*., 2005), and thereby control many biological and physiological responses such as cellular immune responses and neuronal transmission (Roberts *et al.,* 2004).

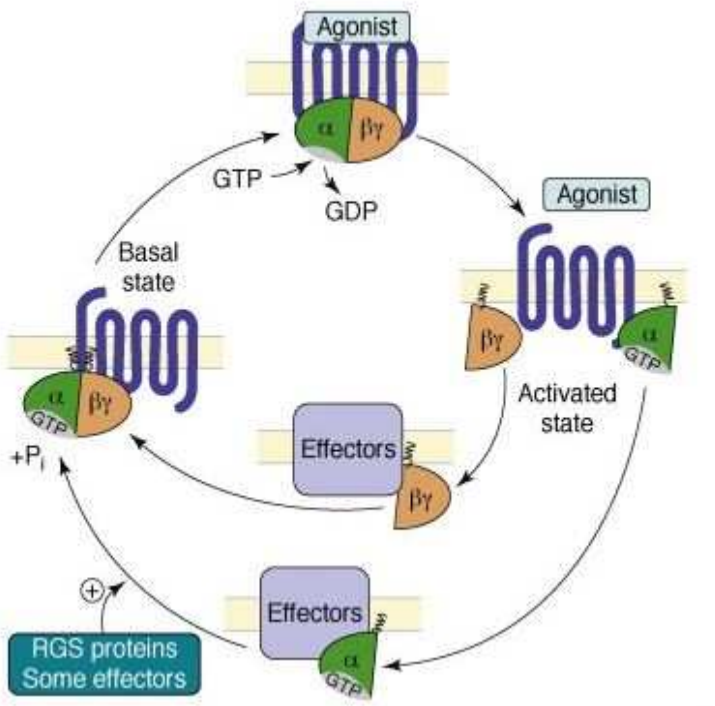

Figure.1. Model for signal transduction by activation/inactivation of heterotrimeric G proteins through GPCR. In the inactive state, the Gα subunit is associated with GDP the GDP is bound to Gα (Gα-GDP). Upon receptor activation with agonist, the receptor undergoes a conformational change and acts as a guanine nucleotide exchange factor (GEF) for the α subunit, stimulating the exchange of GDP for GTP. In active state, the GTP is bound to Gα (Gα-GTP). Upon binding of GTP, the Gα subunit dissociates from the Gβγ dimmer and these proteins are released from the receptor. Dissociated Gα and Gβγ subunits then interact with a variety of effectors respectively to further transmit the signals and initiate unique intracellular signaling responses. Upon termination of the signal, the Gα-GTPase activity hydrolyzes the bound GTP (Gα-GTP) to GDP and Pi and inactivates the G protein complex by re-associating Gα with Gβγ. In this state GDP is again bound to Gα (Gα-GDP) in G protein complex. RGS proteins can accelerate the deactivation by enhancing the GTPase activity. Adapted and modified from (Worzfeld *et al*., 2008).

Some second messengers such as cAMP, cGMP, and IP_3 are water soluble and can diffuse to some extent into the cytoplasm; whereas other second messengers such as DAG and phosphatidylinositol-3,4,5-trisphosphate (PIP_3) are water insoluble, which are membrane-associated lipids and diffuse in the plasma membrane (Rhee, 2001).

G proteins are important signal transducing molecules in cells and they transmit signals from outside the cell to the cell interior. G proteins are activated by GPCRs and inactivated by Gα-

GTP accelerating proteins (GAPs) such as RGS (regulators of G protein signaling) proteins. G proteins are composed by three distinct subunits α-, β- and γ-, where β- and γ- subunits form an undissociable complex and represent a functional unit. Based on their G protein coupling preference, GPCRs can be broadly sub-classified into Gs-, Gi/o-, Gq/11- and G12/13-coupled receptors (Pierce *et al.*, 2002). In this work $G\alpha_{i}$- and $G\alpha_{s}$- coupled receptors were used to study receptor-mediated changes in cAMP. Some of these receptors are briefly discussed below.

1.1.2.1 M_2-muscarinic receptor (M_2-R)

The muscarinic receptors are a subfamily of rhodopsin-like G protein coupled receptors. Muscarinic receptors are classified into five subtypes (M_{1-5}). Based on their coupling to the G proteins, the muscarinic receptor family is further categorized into two classes. M_2 and M_4 receptors couple predominantly to PTX-sensitive G_i proteins leading to inhibition AC and thus decreasing intracellular cAMP levels which results in reduced PKA activity. M_1, M_3, and M_5 receptors preferentially couple to G_q proteins to activate phospholipase C (PLC). Activation of $G\alpha_q$ leads to an activation of phospholipase C-β (PLC-β), which then triggers the breakdown of phosphatidyinositol-4,5-bisphosphate (PIP_2) to the second messengers inositol-1,4,5-trisphosphate (IP_3) and diacylglycerol (DAG). These receptors regulate primary functions of the central and peripheral nervous system (Gomeza *et al*., 2001). The M_2-R is highly expressed in the heart and it is the most important subtype in cardiac tissues, where it induces negative chronotropic, dromotropic and inotropic effects (Hulme *et al.*, 1990; Caulfield *et al*., 1993). M_2-receptor knockout mice show a decrease in smooth muscle contraction and a decrease in body temperature (Wess *et al*., 2003). M_2-receptor agonists including acetylcholine, carbachol, and pilocarpine are primarily used in ophthalmology to treat glaucoma (Zahn *et al*. 2002). These agonists bind to M_2-R and regulate physiological responses such as adenylate cyclase inhibition and potassium channel activation. Acetylcholine is an important neurotransmitter in the autonomic nervous system (Lee & Higginbotham, 2005). The release of acetylcholine from post vagal parasympathetic neurons has inhibitory effects on heart rate and contractility (Murad *et al.*, 1962; Löffelholz & Pappano 1985; Hartzell, 1988). These inhibitory effects can be attributed to inhibition of AC activity and cAMP production by a mechanism involving PTX-sensitive inhibitory G protein, G_i (Hazeki & Ui, 1981; Endoh *et al.*, 1985). In addition to the direct inhibition of cAMP responses via inhibitory G proteins, a second level of cAMP regulation via G_i proteins has

been reported (Gilmour & Zips, 1985): In cardiac myocytes, it was observed that muscarinic receptor activation is facilitated β-adrenergic responses which immediately followed the termination of vagal stimulation or suspension of M_2-receptor agonist (Hollenberg *et al*., 1965; Levy, 1971; Burke & Calaresu, 1971; Gilmour & zips, 1985). This stimulatory response can explain physiological phenomena such as post-vagal tachycardia and arrhythmogenic mechanisms (Wang & Lipsus, 1996). However, the underlying mechanism was not clear so far for this stimulatory effect. This issue was addressed in the present study. In addition to $G\alpha_i$, $G\beta\gamma$ activation via the M_2 and M_4 mAChR in the heart leads to activation of G protein coupled inward rectifying potassium channels (GIRKs) resulting in a decrease of the heart rate (Wickmann *et al*., 1999)

1.1.2.2 β_2-adrenoceptor (β_2-AR)

β_2-adrenoceptor is a subtype of β-adrenoceptor. β_2-adrenoceptor couple to G_s proteins leading to activation of adenylyl cyclase activity and thus increasing intracellular cAMP levels. The increase in cAMP leads to the stimulation of protein kinase A (PKA), which then alters cellular functions. The majority of β_2-AR mediated signaling occurs via $G\alpha_s$ proteins and subsequent cAMP-dependent mechanisms. However, there is an evidence of other signaling schemes including $G\alpha_i$ activated MAPK pathway (Azzi *et al*., 2003). In this study, β_2-AR is used to activate $G\alpha_s$.

β_2-ARs are ubiquitously expressed in most tissues and are involved in a variety of physiologically relevant functions in the human body. β_2-ARs are vastly distributed in muscle tissue including smooth muscle and striated muscle, where they relaxes myometrial smooth muscle in uterus. β_2-ARs also regulates cell metabolism in skeletal muscle. β_2-ARs are also expressed in the heart, where they increase (lesser extent compared to β_1-ARs) cardiac contractility and heart rate (Uhln *et al*., 2010). The β_2-ARs mediate vasodilation, glycogenolysis and lipolysis in the immune system. In the brain, β_2-ARs are vastly distributed in different regions and regulate working memory and other brain functions (Wang *et al*., 2010). In addition, β_2 agonists induce bronchodilation in patients suffering from chronic obstructive pulmonary disease (COPD) and asthma (Celli & Macnee, 2004). Furthermore, β_2 agonists increase intraocular pressure in the eye. Based on the mechanism of actions, β_2 agonists are divided into two types, short acting and long acting agonists. In this the study short acting β_2-receptor agonist Iso proterenol is used.

1.1.2.3 α_{2A}-adrenoceptor (α_{2A}-AR)

Based on their primary structure, α_2-AR is sub divided into three main subtypes (α_{2A-C}). α_2-AR activate inhibitory G proteins (G_i) thereby inhibits adenylyl cyclases, resulting in reduced levels of intracellular cAMP and PKA activity.

α_{2A}-AR is highly expressed in both central nervous system and peripheral tissues such as kidney, lung, eye and skeletal muscle. α_{2A}-AR is also involved in the synaptic brain function, where it controls the release of neurotransmitters (Hein *et al*., 1999). α_{2A}-AR plays prominent roles in the cardiovascular system to regulate heart rate, blood pressure sympathetic nervous system and also regulate central nervous system functions. In addition, adrenoceptor agonist and antagonists are used clinically for many years in the treatment of different diseases including asthma, heart failure, hypertension and depression (Guyton *et al*., 2006). Furthermore, activation of α_2-ARs causes platelet aggregation, and blood vessel constriction. In the spinal cord, α_2-ARs have been shown to regulate nociceptive processing, blood pressure and spinal reflex (Yaksh *et al*., 1985). In pancreatic islet, activation of α_2-AR leads to inhibition of insulin release from β cells (Nakaki *et al*., 1980). The α_{2A}-adrenoceptor is activated by α_{2A}-ARs agonists including clonidine, norepinephrine and epinephrine. The α_{2A}-AR agonist clonidine is an antihypertensive drug, lowers blood pressure and used for the treatment of hypertension (Engelman & Marsala *et al*., 2013). Epinephrine induces aggregation of human platelets. In this study α_{2A}-AR agonist norepinephrine is used to activate α_{2A}-adrenoceptor (Guyton *et al*., 2006).

1.1.3 G protein mediated signal transduction

G proteins are a family of proteins that are involved in transferring signals from GPCRs to a wide range of downstream effectors. G proteins are regulatory proteins that act as molecular switches in signal transduction pathways and they control a wide range of biological processes. The classical G proteins are subdivided into two main classes.

1) High molecular weight G proteins or heterotrimeric G proteins

2) Low molecular weight G proteins or Small GTPases

Since the focus of this work was on signaling through heterotrimeric G proteins. These heterotrimeric G proteins are discussed below.

1.1.3.1 Heterotrimeric G proteins as signal mediators

Heterotrimeric guanine nucleotide-binding proteins are also known as G proteins, which can be activated by GPCRs. The heterotrimeric G proteins are comprised of an α - subunit, a β - subunit and a γ - subunit. The β - and γ - subunits are tightly assembled into βγ - complexes and act as a functional unit. The Gα - subunit typically has a molecular weight of 36-56 kDa, Gβ - has a molecular weight of 35-36 kDa and Gγ - a molecular weight of 8-10 kDa (Nürnberg *et al*., 1995).

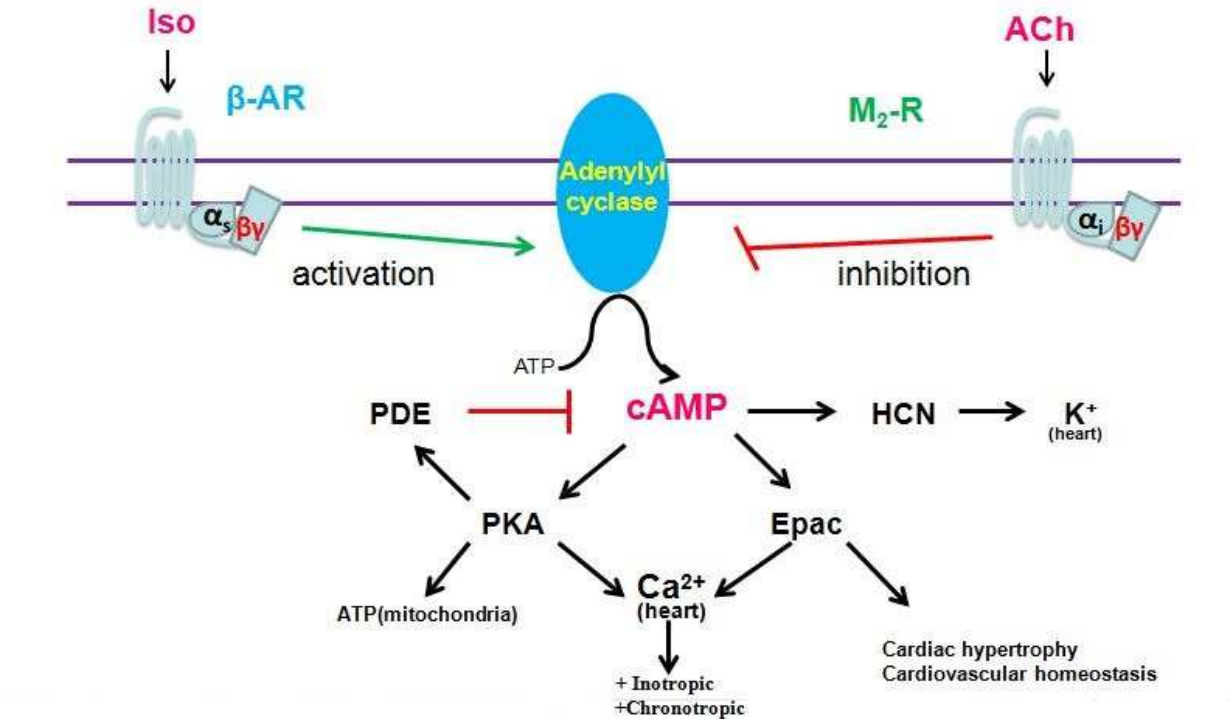

Figure 2: GPCR signaling pathway. Stimulation of a G protein coupled receptor (GPCR) by a hormone results in a conformational change and the activation of G proteins. G proteins are heterotrimeric and upon stimulation, the $G\alpha_s$ subunit becomes activated by GDP/GTP exchange. $G\alpha_s$ subsequently dissociates from the regulatory Gβγ subunits (which can themselves activate other signaling pathways) and activates adenylyl cyclase (AC) to generate cyclic AMP (cAMP) from ATP. On the other hand $G\alpha_i$ proteins inhibit AC and cAMP production. cAMP can be hydrolyzed by phosphodiesterases (PDE). cAMP generation can then activate downstream effectors of the pathway, such as protein kinase A (PKA), Epac or cAMP gated ion channels (HCN) which can ellicit a diverse range of cellular processes.

Upon ligand binding, GPCRs stimulate the α subunit of a heterotrimeric G protein to release GDP and to bind GTP in its place (Figure 1). In the GTP-bound form, Gα dissociates from Gβγ subunits, even though some data indicate that G protein activation may also lead to

subunit rearrangement rather than dissociation (Bünemann *et al*., 2003). However, the released and activated Gα-GTP and Gβγ further interact with their target downstream effector proteins, which then modulate a number of second messenger-generating pathways (Evanko *et al.*, 2005; Wall *et al.*, 1995; Forse, 2000).

1.1.3.1.1 Gα-subtypes and functions

Gα-subunits belong to a family of high molecular weight G proteins, having a molecular weight of 36-56 kDa. So far, 23 different Gα-subunits have been identified (McCudden *et al*., 2005). Based on downstream signaling, Gα subunits can be further divided into 4 major classes ($G\alpha_s$, $G\alpha_{i/o}$, $G\alpha_{q/11,}$ and $G\alpha_{12/13}$). The $G\alpha_s$ family includes $G\alpha_s$ and $G_{\alpha olf}$. These subunits stimulate the activity of adenylyl cyclase (AC) and cause an increase in intracellular cAMP levels. Increased cAMP further activates PKA and Epac (Ross *et al*., 1977). $G\alpha_s$ is the only subunit known to directly activate AC (Sutherland *et al*., 1960; Rall, 1977). $G\alpha_s$ is widely expressed in most tissue types. However, G_{olf} is expressed in olfactory neuroepithelial cells, brain, and pancreas. In addition to ACs, ion channels such as atrial voltage-gated sodium channels and dihydropyridine-sensitive calcium channels in skeletal muscle are also activated by $G\alpha_s$ (Sunahara *et al*., 1997).There are different bacterial toxins available to identify specific Gα-protein mediated signal transduction pathways, e.g., cholera toxin (CTX) and pertussis toxin (PTX). Cholera toxin is an enzyme released by *Vibrio cholera.* CTX catalyzes the transfer of ADP-ribose to $G\alpha_s$, which inhibits its intrinsic GTPase activity and thus makes $G\alpha_s$ constitutively active, which causes persistent activation of adenylyl cyclase (Merritt *et al*., 1995). $G\alpha_s$ proteins are known to be activated by receptors such as β_2-AR, Dopamine (D_1-R), etc.

PTX, the pathogenic toxin of *Bordetella pertussis*, induces ADP-ribosylation of Gα subunits of the $G_{i/o}$ family except $G\alpha_z$. $G\alpha_i$ thereby sequesters Gβγ-subunits, and fails to inhibit AC with a resulting increase in intracellular cAMP (Watts *et al*., 2005). The $G\alpha_i$ protein family is sensitive to PTX (Wu *et al*., 2005). The $G\alpha_{i/o}$ protein family consists of $G\alpha_i$, $G\alpha_o$, $G\alpha_z$, $G\alpha_t$ and G_{gust}. The $G\alpha_i$ proteins are further divided into three main subtypes: $G\alpha_{i1}$, $G\alpha_{i2}$ and $G\alpha_{i3}$. Almost all $G\alpha_i$ subunits inhibit adenylyl cyclase activity (ACs), thus promoting decreased intracellular cAMP. On the other hand, $G\alpha_i$ subunits activate phosphodiesterases (PDEs). Activation of $G\alpha_t$ leads to increased hydrolysis of cGMP, and activation of G_{gust} causes hydrolysis of cAMP.

Table 1: Classification and functional properties of Gα-subunit (Nürnberg, 2004)

Family	Subtype	Tissue distribution	Effectors	Receptors(examples)
G_S	$G\alpha_{s(s),s(1)}$[a]	ubiquitous	↑AC	β_1/β_2-AR, D_1-R A2-R etc.
	$G\alpha_{olf}$	olfactory epithelium, brain and pancreas	↑AC	V_2-R, odorant-R
G_i	$G\alpha_{i1}$	mostly neurons	↓ AC1,5,6 (↑GIRK[b], ↑PLCβ[b])	α_2-AR, M_2/M_4-R
	$G\alpha_{i2}$	ubiquitous	↓AC1,5,6 (↑GIRK[b], ↑PLCβ[b],↑PI3K[b])	α_2-AR, M_2/M_4-R
	$G\alpha_{i3}$	mostly non-neuronal	↓AC1,5,6 (↑GIRK[b], ↑PLCβ[b],↑PI3K[b]?)	D_2-R, A1-R, μ-OR
	$G\alpha_{o1,2,3}$[c]	neurons	↓AC? ↑VDCC[b] ↓GIRK[b] ↓PLCβ[b])	LPA-R, SSTR
	$G\alpha_{t(r)}$	retinal rods	↓cGMP-PDE	Rhodopsin
	$G\alpha_{t(c)}$	retinal cones	↑cGMP-PDE	
	$G\alpha_{gust}$	taste cells	↑PDE	
	$G\alpha_z$	neurons, endocrine, platelets	↑AC1,AC 5(↑GIRK[b], ↓VDCC[b])	AT II-R, ET-R
G_q	$G\alpha_q$	ubiquitous	↑PLC-β, Rho-GEF	M1/M3-R, V_1-R
	$G\alpha_{11}$	widely	↑PLC-β	P_{2Y}-R
	$G\alpha_{14}$	testis and hematopoietic	↑PLC-β	
	$G\alpha_{15/16}$[d]	cellshematopoietic cells and tissues	↑PLC-β	
G_{12}	$G\alpha_{12}$	ubiquitous	↑Rho-GEF,↓Btk, ↑Gap1[m], cadherin	TxA_2-R, LPA-R
	$G\alpha_{13}$	ubiquitous	↑Rho-GEF, radixin	

Table 1: Classification and functional properties of Gα-subunit. Abbreviations for the text used in the table. α/β-AR= adrenergic receptors; $V_{1/2}$= vasopressin receptors; $D_{1/2}$= dopamine receptors; $A_{1/2}$= adenosine receptors; $M_{1\text{-}4}$-R= muscarinic receptors; SSTR= somatostatin receptors; μ-R= opioid receptors; TR= taste receptors; LPA-R= lysophosphatidicacid receptors; AT II-R= angiotensin II receptors; B_2R= bradykinin receptors; P_{2y}= purinergic receptors; TxA_2-R= thromboxane receptors. a: (s) and (l) indicate short and long splice variants of $G\alpha_s$. b: Regulation of effector presumably depends on direct interaction with Gβγ-dimers resulted from PTX-sensitive G protein. c: $G\alpha o_3$ corresponds to deamidated $G\alpha o_1$, representing 30% of total Gαo in brain. d: $G\alpha_{15}$ and $G\alpha_{16}$ are the mouse and human homologues of GNA15 gene product, respectively. ↑ Stimulation: ↓ inhibition; AC: adenylyl cyclase, Btk: Bruton's tyrosine kinase, cGMP-PDE: cGMP-phosphodiesterase, Gap1m: Ras GTPase-activating protein, GIRK: G-protein-regulated inward rectifier K^+-channel, PLC-β: phopholipase C-β, PI3K: phosphatidylinositol-3-kinase, Rho-GEF: guanine nucleotide exchange factor of the monomeric GTPaase Rho, VDCC: voltage-dependent Ca^+-channel. Table was adapted and modified from Claus *et al*., 2000; Nürnberg, 2004.

$G\alpha_{i2}$ and $G\alpha_{i3}$ proteins are very closely related. Adenylyl cyclases are stimulated directly by forskolin, and these stimulatory effects can be inhibited by $G\alpha_{i2}$. Similar to $G\alpha_{i2}$, $G\alpha_{i3}$ also inhibits $G\alpha_s$-stimulated AC activity (Obadiah *et al*., 1999). Other $G\alpha_i$ subunits such as $G\alpha_o$ and $G\alpha_z$ proteins also have an inhibitory effect on ACs. Furthermore, $G\alpha_i$ and $G\alpha_o$ are associated with Gβγ proteins which then regulate G protein-gated inwardly rectifying K^+ (GIRK) channels. $G\alpha_t$ represents the Gα subunit of transducin which can be activated by visual receptor rhodopsin. On the other hand, $G\alpha_z$ is defined as the α subunit of gustducin. $G\alpha_i$ and $G\alpha_o$ proteins are predominantly expressed in the brain and heart, whereas $G\alpha_t$ and $G\alpha_z$ proteins have restricted tissue distribution but $G\alpha_t$ mediates the light response in retinas and $G\alpha_z$ proteins are involved in calcium mobilization (Liu *et al.*, 2003). $G\alpha_i$ proteins are known to to be activated receptors such as M_2-R, α_2-ARs.

The $G\alpha_q$ proteins are widely expressed. The $G\alpha_q$ protein family consists of $G\alpha_q$, $G\alpha_{11}$, $G\alpha_{14}$, $G\alpha_{15}$ and $G\alpha_{16}$ subtypes. $G\alpha_q$ activate phospholipase C β (PLCβ), which generates second massagers such as diacylglycerol (DAG) and inositol-1,4,5-trisphosphate ($Ins(1,4,5)P_3$) (IP_3). PLCβ, is an enzyme that catalyzes the hydrolysis of the phosphatidylinositol(4,5)-bisphosphate ($PI(4,5)P_2$) (Pavan *et al.*, 2007; Rhee *et al*., 2000). Activated DAG stimulates protein kinase C (PKC), while the other second messenger IP_3 triggers intracellular Ca^{2+} release by activation of receptors in the endoplasmic reticulum (ER) (Macrez-Lepretre *et al*., 1997). Furthermore, Bruton's tyrosine kinase (Btk) is also activated by $G\alpha_q$ both *in vivo* and

in vitro (Jing *et al*., 1998). The $G\alpha_q$ proteins are known to be activated by receptors such as muscarinic receptors (M_1, M_3, and M_5-R) and Histamine receptors (H_1-R).

The last family of α subunits of G protein is $G\alpha_{12}$. This family was not well characterized and also has relatively low sequence homology to the other heterotrimeric G proteins. The $G\alpha_{12}$ family is comprised of $G\alpha_{12}$ and $G\alpha_{13}$ (Strathmann *et al*., 1991). $G\alpha_{12}$ proteins do not interact with ACs, but mainly activate the small G protein RhoA and its downstream effectors, which further affects cellular morphology including cell migration and invasion (Kristelly *et al*., 2004). The $G\alpha_{12}$ family is widely expressed and can induce different signaling pathways, which lead to activation of downstream effectors such as phospholipase C, phospholipase D or MAP kinase activation (Buhk *et al*., 1995; Gohla *et al*., 1999; Cvejic *et al*., 2000). It has been shown that $G\alpha_{12/13}$ interacts with various other proteins like Btk, Ras GTPase-activating protein (Gap1m) and cadherin (Meigs *et al*., 2002). It has been also reported that extracellular signal-regulated activated kinase (ERK) is activated by $G_{12/13}$ proteins.

1.1.3.1.2 Gβγ-subtypes and functions

Gβγ is an integral part of heterotrimeric G proteins. Gβγ is a tightly complexed dimeric protein consisting of one Gβ- and one Gγ- subunit. Five Gβ (1-5) and twelve Gγ (1-12) subunits have been identified, which are expressed in humans. $G\beta_{1-4}$ subunits share between 80 and 90% amino acid sequence homology while the various Gγ- isoforms are much less conserved. Gβγ-dimers bind directly to GPCRs and enhance the binding of Gα-subunit to GPCRs. Gβγ proteins preferentially bind certain receptors or activate specific signaling pathways (McCudden *et al*., 2005). In addition, current evidence indicates that Gβγ is a possible therapeutic drug target in several diseases including heart failure, inflammation and leukemia (Lin *et al*., 2011; Runne *et al*., 2013; Williams *et al*., 2004).

Table 2: Gβγ-mediated regulated effectors (Nürnberg, 2004)

Effector	Gβγ response
AC 1, AC 3, AC 5, AC 6, AC 8	↓
AC 2[a], AC 4[a],AC 7[a]	↑
G protein regulated inward rectifier K^+ channels (GIRK1-4)	↑
G-protein coupled receptor kinase (GRK2,3)	↑
Phosphatidylinositol-3-kinase-β-γ (PI3K-β[b],-γ)	↓
Phospholipase C β1-3	↑
Phospholipase A	↑
RAF 1 Protein kinase	↑
Bruton's-tyrosine kinase (Btk)	↑
Interleukin-2(IL-2)-inducible tyrosine kinase (TSK)	↑
T-type voltage dependent Ca^{2+}-channels	↑
N-type calcium channels	↓
Tsk tyrosine kinase	↑

Table 2: Gβγ-mediated regulated effectors. a: AC activity is super activated by Gβγ only if co-activated by $G\alpha_s$. b: Stimulation has been demonstrated under in vitro conditions only. P140Ras-GEF: guanine-nucleotide exchange factor of the Ras GTPase, Raf-1: member of the ras subfamily of serine protein kinases. ↑: stimulation, ↓: inhibition. Table was adopted and modified from Nürnberg, 2004).

The βγ-dimers do not only act as an anchor for Gα subunits to form the functional heterotrimer; they also possess regulatory functions. The most significant βγ-mediated regulation is on ACs. The effect of Gβγ on adenylyl cyclases is dependent on the type of

ACs. Some of them are activated, and others are inhibited by Gβγ. Of all mammalian ACs, only AC2 and AC7 isoforms are activated by Gβγ dimers. Upon activation of ACs, Gβγ stimulates cAMP via activated $G\alpha_s$ coupled receptors (Gao *et al*., 1991; Tang *et al*., 1991). On the other hand AC1, 3 and AC6 are inhibited by Gβγ dimers, thereby inhibiting cAMP production (Diel *et al.,* 2006; Steiner *et al*., 2006).

However, there are some contradictory reports about the Gβγ regulation of AC5. Some reports stated that AC5 was inhibited by Gβγ (Smrcka *et al*., 2008; Pavan *et al*., 2009) via activation of $G\alpha_s$ or activation of $G\alpha_i$ (Gao *et al*., 2007), while others reported that AC5 is conditionally stimulated by Gβγ (Sadana *et al*., 2009). Most of the Gβγ-effectors are regulated by $G\alpha_i$-mediated subunits.

In addition, the $G\alpha_i$-mediated Gβγ dimer activates or inhibits many other effectors, including GIRK channel and N-type Ca^{2+} channels (Li *et al,* 1999). Furthermore, the G protein signaling effectors PLCβ and mitogen-activated protein kinase 1-3 (ERK1/2) are directly regulated by Gβγ, resulting in activation of PKC through IP_3. PKC activation leads to stimulation of AC5 (Watson *et al*., 1994; Wu *et al*., 1993). Some classes of phosphatidylinositol 3-kinases such as PI3Kγ and PI3Kβ are directly activated by Gβγ-dimers (Maier *et al.,* 2000). Mitogen-activated protein kinases are also activated by Gβγ (Yamauchi *et al*., 1999).

1.1.4. The main effector systems of GPCRs signaling

Binding of the ligand to a GPCR activates heterotrimeric G proteins thereby activating specific isoforms (ACs), multiple second messengers (cAMP, cGMP and IP_3), and second messenger-derived mediators (PKA, Epac, PKC, PI3K, PDE and Ca^{2+}).

1.1.4.1 Adenylyl cyclases (ACs)

Adenylyl cyclases (ACs) are a family of enzymes which are regulated by GPCRs. ACs are important effectors for GPCRs, and are mainly responsible for cAMP synthesis. These enzymes play an important role in various cellular signal transduction processes, including cardiac contraction, smooth muscle relaxation and hormone secretion (Seamon *et al*., 1981; Coppe *et al*., 1978). In mammals, AC isozymes are central and important components of signal transduction pathways and these isozymes are encoded by at least ten independent genes (AC 1-10). Most of the AC isoforms are expressed at a limited number in tissues and are highly expressed in brain. AC2, 3, 4, 5, 6 and AC8 are highly expressed in heart

(Feinstein *et al*., 1991; Bakalyar *et al*., 1990; Gao *et al*., 1991; Ishikawa *et al*., 1992; Yoshimura *et al*., 1992), whereas AC1 is expressed only in adrenal gland (Krupinski *et al*., 1989) and AC7 is expressed in platelets (Krupinski *et al.,* 1992). AC10 is expressed in testis (Buck *et al.,* 1999). Among the ten AC isoforms, nine of them are membrane-bound, and these are closely related. The type 10AC isoform encodes a soluble isoform also referred as sAC (Gancedo *et al*., 2013). The nine membrane-bound AC isoforms are divided into five distinct categories based on their amino acid sequence similarity and regulatory properties. Group one consists of Ca^{2+}/CaM-stimulated AC forms such as AC1, 3 and AC8; group two consists of Gβγ-stimulated AC isoforms such as AC2, 4 and 7; group three consists of G_i/Ca^{2+}- inhibited AC isoforms including AC5 and AC6. Group four is the most divergent of the membrane-bound family and consists of forskolin-insensitive AC9 (Sosunov *et al*., 2001). AC10 isoform is found in cyanobacteria and also in mammalian cells (Fraser *et al*., 2005). Adenylyl cyclases are also regulated by free metal ions, P-site inhibitors and protein phosphorylation (Cooper, 2003).

1.1.4.1.1 Adenylyl cyclase structure

Adenylyl cyclases are large integral membrane glycoproteins having molecular weights of approximately 119 to 175 kDa. All nine mammalian transmembrane ACs share a common structure that consists of two cytoplasmic domains (C1 and C2) and two transmembrane domains (M1 and M2) each containing six membrane-spanning α- helices. The C1 and C2 regions can be subdivided further into catalytic domains C1a and C1b and regulatory domains C2a and C2b. The catalytic subdomains C1a and C1b are most conserved and highly homologous to each other to form a functional unit. The C1 and C2 domains have 230 amino acid regions (Tang *et al.,* 1991; Linder *et al*., 2006). The C1a and C2b regions resemble each other in each adenylyl cyclase (roughly 50% similar and 25% identical) (Tang *et al*., 1995). The C1a and C2a domains contribute to ATP binding. Membrane bound AC isoforms are regulated by G protein Gα- and Gβγ- subunits, forskolin, substrate inhibitors and P-site inhibitors (Cooper, 2003).

Table 3: Regulation of mammalian adenylyl cyclases (Hanoune *et al.*, 2001)

AC isoforms[a]	**$G\alpha_s$**	**$G\alpha_i$**	**$G\beta\gamma$**	**Forskolin**	**Ca^{2+}/CaM**	**Protein Kinases**	**Putative function**
AC1	↑	↓Ca^{2+}/CaM-stimulated	↓	↑	↑	↑PKC(week) ↓CaM kinase IV	Learning memory,synaptic plasicity
AC2	↑		↑	↑		↑PKC	
AC3	↑	↓	↓	↑	↑ (in vitro)	↑PKC	olfaction
AC4	↑		↑	↑		↑PKC	
AC5	↑	↓		↑	↓	↓PKA ↑PKC	
AC6	↑	↓		↑	↓	↓PKC, PKA	
AC7	↑		↑	↑		↓PKC	Drug dependency
AC8	↑	↓Ca^{2+}		↑	↓	→PKC	Learning memory
AC9[b]	↑	↓		→	↓calcinurin		
sAC[c]	→	→		→			Sperm capacitation

Table 3. Regulation of mammalian adenylyl cyclases. ↑ positive regulatory response; ↓ negative regulatory response; → no regulatory response. a: all isoforms except sAC inhibited by P-site inhibitors. b: inhibited by calcineurin. c: stimulated by bicarbonate. Adapted and modified from (Hanoune *et al*., 2001; Sunahara *et al*., 2002).

The full length sAC molecular weight is approximately 187 kDa. The isoform contains tandem catalytic C1 and C2 domains (Buck *et al*., 1999). The catalytic core is highly similar to that of transmembrane ACs. The sAC is stimulated by calcium and bicarbonate. Importantly, sAC is not known to be regulated by heterotrimeric G proteins (Chen *et al*., 2000; Jaiswal *et al*., 2003).

1.1.4.2 Regulation of adenylyl cyclases

1.1.4.2.1 Regulation of adenylyl cyclases by free metal ions.

ACs requires the binding of metal ions for catalytic activity (Dessauer *et al*., 1997). Some of the mammalian adenylyl cyclases are activated by free metal ions, including magnesium (Mg^{2+}). Previously it was reported that AC5 and AC6 are physiologically inhibited by free Ca^{2+} (Scholich *et al*., 1997). However, the precise pharmacological contribution of manganese (Mg^{2+}) in comparison to Mn^{2+} on AC is still unknown.

1.1.4.2.2 Regulation of adenylyl cyclases by P-site inhibitors

Most of the P-site inhibitors are monophosphates and represent physilogicol regulators of ACs. P-site inhibitors are analogs of AMP. The AMP directly binds to an inhibitory site on adenylate cyclase. P-site inhibitors such as deoxy-adenosine phosphate, adenine and AMP which inhibit AC activity. Recently it was reported that AMP was accumulated by metformin therby inhibits adenylyl cyclases (Madiraju *et al*., 2014). Metformin is an antidiabetic drug which is known to activate AMP activated protein kinase (AMPK). Previously it was reported that AC1, 3, 5, 7 and 8 are inhibited by P-site inhibitors such as adenine and 9-(tetrhydro-2-furyl)-adenine, and there is no effect on other ACs (Johnson *et al*., 1997; Sunahara *et al*., 2002)

1.1.4.2.3 Regulation of adenylyl cyclases by forskolin

Forskolin is a cAMP activator and potentially activates all isoforms of mammalian membrane-bound ACs except AC 9 and sAC because of a Ser → Ala and a Leu → Tyr change in the binding pocket (Permont *et al*., 1996; Iyengar, 1993). Forskolin binds to the C1 and C2 heterodimers and then activates AC (Tesmer *et a*l., 1997). The interaction between AC and forskolin is predominantly by hydrophobic interactions and hydrogen bonds. The stimulation of cAMP-production by forskolin is likely to involve direct activation of adenylyl cyclase and facilitation and/or enhancement of receptor-mediated activation of AC. Stimulation by forskolin directly activates AC2, AC4, AC5, AC6 and AC7 with $G\alpha_s$-

mediated co-activation whereas, stimulation by forskolin activates AC1, AC3, and AC7 in cooperation with Ca^{2+}-CaM (Tang *et al*., 1991; Insel *et al*., 2003).

1.1.4.2.4 Regulation of adenylyl cyclases by Gα-subunits

The mammalian AC activation occurs primarily through receptors coupled to the stimulatory G protein $G\alpha_s$. All mammalian ACs (except AC10) are predominantly activated by GTP-$G\alpha_s$. In addition to $G\alpha_s$, $G\alpha_{olf}$ also stimulates AC (Jones *et al*., 1989). Crystallographic studies suggest that the interaction between $G\alpha_s$ and AC occurs through an α-helix that is highly mobile throughout the GTPase cycle of G proteins (Feldmann *et al*., 2002). The primary binding site for $G\alpha_s$ on AC is located on the C2 domain where it is formed by the α2' and α3' helices. The N-terminal portion of the catalytic domain C1 also contributes to $G\alpha_s$ binding (Tesmer *et al*., 1997).

The inhibitory G protein family $G\alpha_{i1}$, $G\alpha_{i2}$, $G\alpha_{i3}$, $G\alpha_z$ and $G\alpha_o$ selectively inhibit AC5 and AC6 (Taussig *et al*., 1994). However, $G\alpha_i$ does not compete with $G\alpha_s$ for the binding to the enzymes because the forskolin-stimulated activity is also inhibited (Wittpoth *et al*., 1999). Instead, structural modeling and mutagenesis experiments suggest a binding site for $G\alpha_i$ which is located in the crevice formed by α2 and α3 of C1, symmetrically opposite of the binding site of $G\alpha_s$ (Dessauer *et al*., 1998). In addition, the N-terminus of AC5 directly interacts with the C1 domain which has been implecation in the $G\alpha_i$-mediated inhibition as well $G\alpha_s$-mediated activation of AC5. Furthermore, the calmodulin-activated AC1 is inhibited by $G\alpha_i$ proteins. However, forskolin-stimulated AC1 is only partially inhibited by $G\alpha_i$ (Taussig *et al*., 1994). Furthermore, $G\alpha_o$ inhibits AC1 and AC8, although it is not as potent as other $G\alpha_i$-subunits on AC5 and AC6 (Evanko *et al*., 2005). However, all other ACs are not sensitive to $G\alpha_i$.

1.1.4.2.5 Regulation of adenylyl cyclases by Gβγ-dimers

Adenylyl cyclases are conditionally regulated by heterotrimeric G protein βγ-subunits. Gβγ-subunits may show stimulatory effects on ACs, as in the case of AC2, AC4 and AC7, or inhibitory effects on ACs, as in the case of AC1, AC3, and AC8. Gβγ potently stimulates the AC activity of AC2, AC4, and AC7 but only in the presence of $G\alpha_s$, suggesting that Gβγ enhances the capacity of $G\alpha_s$ to activate AC (Sunahara *et al*., 2002). In the C2 domain, amino acids 956 to 982 of AC2 have been mapped as the interaction site for Gβγ-subunits and $G\alpha_s$-GDP. Despite the high degree of sequence conservation among AC catalytic domains, this

sequence is not found in other AC isoforms not modulated by Gβγ. However, when Gβγ is released upon activation of $G\alpha_s$ coupled receptors, Gβγ neutralizes AC1 and AC8 stimulation by $G\alpha_s$ in some cell lines. However, the Gβγ-dimers are negative regulators of AC1 and AC8 and can significantly inhibit effects of forskolin, $G\alpha_s$ and Ca^{2+}/CaM on AC activity. The AC2 family is stimulated conditionally by Gβγ. Gβγ potentiates $G\alpha_s$-stimulated activity of AC4 and AC7 by up to 5- to 10-fold (Bayewitch *et al*., 1998). However, this activity was observed only in the presence of $G\alpha_s$, and there is no AC potentiating effect of Gβγ alone (Tang *et al*., 1991; Tausig *et al*., 1995; Sadana *et al*., 2009). In addition, it has been reported previously that Gβγ overexpression has a tendency to lower cAMP levels in cells expressing AC5 or 6 (Bayewitch ML *et al*., 1998).

1.1.4.2.6 Regulation of adenylyl cyclases by Ca^{2+}/Calmodulin

Ca^{2+}/CaM are key regulators of group I ACs. Ca^{2+}/CaM activate isoforms of AC1 and AC8. The binding sites for calmodulin have been identified in the C1b of AC1 and C2b of AC8. Calmodulin conditionally stimulates AC3 via calcium-dependent calmodulin kinase II and calcineurin/PP2B (Tang *et al*., 1991). However, this AC3 stimulation occurs only in the presence of $G\alpha_s$ or forskolin (Choi *et al*., 1992). Furthermore, the Ca^{2+}/CaM-stimulated phosphoprotein-phosphatase calcineurin has an inhibitory effect on AC9 via an unknown protein kinase (Paterson *et al*., 2000). In addition, almost all AC isoforms are inhibited by non-physiological (high) concentrations (millimolar) of Ca^{2+} whereas (micromolar) Ca^{2+} concentrations inhibit AC5 and AC6 enzyme activity (Baker *et al*., 1998; Cali *et al*., 1994). In addition, CaM kinase 2 inhibited AC3 by phosphorylating it at Ser-1076 (Weij *et al*., 1996).

1.1.4.2.7 Regulation of adenylyl cyclases by protein kinases and other proteins

There are different protein kinases and proteins which directly regulate ACs, including protein kinase A or C. Protein kinase A negatively regulates AC5 and 6 activities by phosphorylation of these isoforms (Iwami *et al*., 1995). On the other hand, PKC regulates ACs either by inhibition or stimulation. AC2 and AC5 are activated by PKC, whereas AC4 and AC6 are inhibited by PKC. Interestingly, PKC has opposite effects on the $G\alpha_s$-stimulated AC2 (enhanced by PKC) and AC4 (inhibited by PKC). The stimulatory effect of Gβγ on AC2 and AC4 is lost by PKC phosphorylation (Kawabe *et al*., 1994). However, AC9 is inhibited by PKC (Cumbay *et al*., 2004). PIP_3 (product of PI3-K) activated atypical PKC isoform (PKCζ) can also stimulate AC5/6 (Nguyen *et al*., 2005). Additional kinases, such as tyrosine kinases indirectly stimulate AC5 activity by phosphorylation of $G\alpha_s$ (Poppleton *et al*., 1996).

Furthermore, AC3 is inhibited by CaM kinase II (Weij *et al*., 1996). Additionally, some other G proteins also regulate ACs (specifically AC3), including RGS proteins. However, a direct association between RGS proteins and AC3 has so far not been demonstrated. Furthermore, nitric oxide also may inhibit AC5 and AC6 (Hill *et al*., 2000).

1.1.5 Cyclic nucleotide signaling

The cyclic nucleotides (cAMP and cGMP) are identified as important intracellular signal transduction molecules, acting as second messengers between extracellular signal such as a hormone or neurotransmitter and the elicited intracellular response. Cyclic nucleotide signaling is a key regulator of many cellular processes such as cell migration, proliferation, growth and apoptosis.

1.1.5.1 Cyclic adenosine monophosphate (cAMP)

cAMP is a ubiquitous intracellular second messenger, which transmits signaling information from receptors to many different effector proteins within the cells. cAMP was first discovered in 1957 as a intracellular mediator of the glycogenolytic action of epinephrine and glucagon in the liver (Sutherland, 1960). Intracellular cAMP levels are not only regulated by AC but also cAMP specific phosphodiesterases (PDEs), which degrade intracellular cAMP (Omori, 2007). cAMP can elicited a wide range of cellular processes including cell differentiation, proliferation, neurotransmission, and transcription (Houslay *et al.*, 1997). The transduction of intracellular cAMP into a cellular response can be achieved by several cAMP effectors proteins (Beavo *et al*., 2002).

1.1.5.2 cAMP effectors

There are several different cAMP effectors in cAMP signal transduction, including cyclic-dependent protein kinase (PKA), cAMP-dependent guanine nucleotide exchange factor (cAMP-GEFs) or exchange protein directly activated by cAMP (Epac) and cAMP nucleotide-gated ion channels (CNG) such as hyperpolarized cyclic nucleotide gated channel (HCN). The detail description of these effectors discussed below.

1.1.5.2.1 Protein kinase A (PKA)

PKA is an important cAMP effector in GPCR signaling. The majority of cAMP downstream signaling effects are occurring through PKA (Tasken & Aandahl *et al*., 2004). cAMP activated PKA is one of the major mechanisms by which cellular events are controlled. PKA is a heterotetramer, which is composed by two catalytic (C) subunits and two regulatory (R)

subunits. Each subunit has multiple isoforms with 4 regulatory (RIα, RIβ RIIα and RIIβ) and 3 catalytic (Cα, Cβ, Cγ) subunits. The catalytic subunit contains a domain that binds ATP and one which binds the regulatory subunit. The regulatory (R) subunit contains two domains, which binds cAMP. The catalytic subunits are bound to the regulatory subunit dimer and are inactive when cyclic AMP levels are low. The catalytic subunits are active when cAMP binds to the regulatory subunits, leading to an allosteric change in conformation. Then the free catalytic subunits are active and start to phosphorylate their targets. The PKA holoenzyme can be classified in to two types. Type I (RIα and RIβ dimers) and type II (RIIα and RIIβ dimers). Type 1 is soluble and located in the cytoplasm and more sensitive to cAMP than Type II. Type II is associated with sub-cellular structures, being anchored by scaffolding proteins called A-kinase anchoring proteins (AKAPs) (Michel *et al.,* 2002). PKA phosphorylation activates Ca^{2+} channels, resulting an increase in intracellular [Ca^{2+}] level and an increase in myocytes contraction in the heart. Furthermore, PKA can phosphorylate complex 1 of the respiratory chain of mitochondria, thereby regulates oxidative energy production (Papa *et al.,* 2012).

1.1.5.2.2 Exchange protein directly activated by cAMP (Epac)

Apart from PKA, cyclic AMP also activates cAMP regulated guanine nucleotide exchange factor (cAMP-GEF). It is also called as Epac (Holz *et al*., 2006). Epac regulates vital processes, including cell proliferation, differentiation, calcium handling and neuronal signaling. There are two isoforms of Epac identified so far: Epac1 and Epac2. Epac1 is expressed ubiquitously, whereas Epac2 is predominantly expressed in the brain (Kawasaki *et al*., 1998; de rooji, 1998). Ras superfamily has small GTPases such as Rap1, and Rap2 and both are stimulated by cAMP activated Epac proteins. Both Epac1 and Epac2 share extensive sequence homology and both contain an N-terminal regulatory region and a C-terminal catalytic region. Epac2 has an additional N-terminal cyclic nucleotide-binding domain (CNB), the function of this extra domain is not clear. The C-terminal catalytic region of Epac2 consists of Ras association domain (RA) and a CDC25-homology domain. The N-terminal regulatory region of Epac1 and Epac2 shares a Dishevelled-Eg1-10-Pleckstrin (DFP) domain followed by a CNB domain (Fig. 3) (de Rooji, 2000).

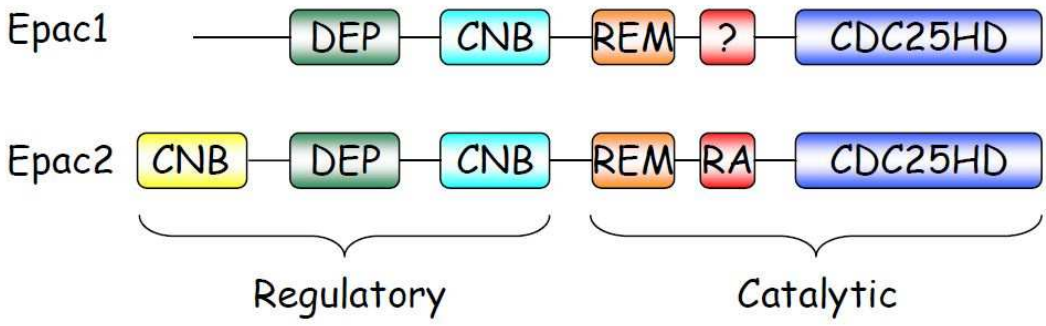

Figure 3: Domain structure of exchange protein directly activated by cAMP (Epac). The domain structure of Epac1 and Epac2 indicating a cyclic nucleotide binding domains (CNB) and a catalytic region with CDC25 homology domain (CDC25HD), which is responsible for the guanine nucleotide exchange activity. The DFP (Disheveled/Eg1-10/pleckstrin) (DEP) domain that is involved in membrane localization, the Ras exchange motif (REM) which stabilizes the catalytic helix of CDC25HD and Ras-association domain (RA). The figure was adopted and modified from (Johannes, 2006).

Epac modulates intracellular Ca^{2+} in the heart (Emily *et al.*, 2009). Epac proteins regulate a wide variety of cellular functions, such as cell adhesion, cell differentiation, proliferation, gene expression and apoptosis (Kiwmayer *et al*., 2005; Qiao, *et al*., 2002). Epac attributes to the secretion of insulin (Gloerich *et al*., 2010). Furthermore, neuronal functions including neuronal differentiation, neurite outgrowth, and axon regeneration are also regulated by Epac (Chistensen *et al*., 2003). Most leukocytes express the Epac1, which directly controls inflammation by regulating the immune response of leukocytes (Metrich *et al*., 2010). Epac1 signaling regulates inflammatory responses of vascular endothelial cells (Sands *et al.*, 2006). Furthermore, recent pieces of evidence indicated that Epac is being involved in renal diseases (Patschan *et al.*, 2010).

1.1.5.2.3 Hyperpolarization-activated cyclic-nucleotide-gated channel (HCN)

Hyperpolarization-activated cyclic-nucleotide-modulated channels are cation channels that are directly activated by intracellular second messengers such as cAMP and cGMP. HCN channels are widely expressed in the heart and central nervous system (CNS). HCN channel family comprises four members (HCN1-4) (Kaupp *et al.*, 2002). HCN channels are regulated by many neurotransmitters, including norepinephrine and ACh. For example, norepinephrine activates β-adrenergic receptors which increases levels of cAMP which activate HCN channels and leads to a positive chronotropy in the heart (Ludwig *et al*., 1998). Neuronal

excitability, dendritic integration of synaptic potentials and synaptic transmissions are also controlled by HCN channels. Some recent reports indicate that HCN channels may contribute to mechanisms of epilepsy and pain (Postea *et al*., 2011; Nobels *et al*., 2012).

1.1.5.3 Cyclic guanosine monophosphate (cGMP)

cGMP is also an important intracellular second messenger which mediates a wide variety of cellular processes. cGMP is generated by two important guanylyl cyclases (GCs), one is nitric oxide (NO)-sensitive soluble guanylyl cyclase (sGC) and the other one is natriuretic peptide (NPP)-activated plasma membrane-bound particulate guanylyl cyclase (PGC) (Waldman & Murad, 1988; Bryan *et al.*, 2009). These two guanylyl cyclase isoforms are widely expressed in many cells and tissues (Bryan *et al.*, 2009). The generation of cGMP further activates downstream signaling pathways such as cyclic guanosine monophosphate-dependent kinases (PKGs), cGMP-gated cation channels and PDEs (Hofmann, 2005; Lohmann & Walter, 2005; Lincoln *et al*., 2006). PKG is positively regulated by cGMP. In addition, cGMP also regulates intracellular concentrations of cAMP by activating or inhibiting cAMP-specific PDEs. It has been reported that PDE3 and PDE1 are inhibited by cGMP. This prevents cAMP breakdown and thereby indirectly increases intracellular cAMP levels (Hofmann *et al.*, 2000).

1.1.5.4 Phosphodiesterases (PDEs)

PDEs are a family of enzymes. The intracellular levels of second messengers such as cAMP and cGMP are regulated through degradation by PDEs. The diverse family of cyclic nucleotide PDEs are important regulators of signal transduction and they influence ion channel function, muscle contraction, learning and many other cellular responses. PDEs have been identified as important drug targets for treatment of several diseases, including heart failure, depression, asthma and inflammation (Conti *et al*., 2000; Torphy *et al*., 1998). Based on amino acid sequences, regulatory properties and catalytic characteristics, mammalian PDEs are so far grouped into eleven families (PDE1-11) (Thompson *et al.*, 1979; Beavo *et al*., 1982). Some of these enzymes only hydrolyze cAMP (PDE4, PDE7 and PDE8) while others only hydrolyze cGMP (PDE5, PDE6 and PDE9) and the remaining PDEs show mixed specificity (PDE1, PDE3, PDE10 and PDE11). PDEs contain three functional domains: a conserved catalytic core, a N-terminal regulatory and a C-terminal domain. The N-terminal portions of PDEs are widely divergent and contain structural determinants that allow PDEs to respond specific regulatory (Martinez *et al*., 2002). This region contains additional binding domains for calmodulin in case of PDE1, for cyclic GMP in case of PDE2 as well as

phosphorylation sites for various protein kinases in cases of PDE1-5, and a transducin binding domain in case of PDE6 (Card *et al*., 2004; Jeon *et al*., 2005). Intracellular cAMP/cGMP levels are increasing upon PDE inhibition, which in turn regulates various physiological functions. Among 11 PDEs, PDE4 and PDE7 have a higher specificity for activation by cAMP than cGMP or Ca^{2+}/calmodulin (Conti & Zin., 1998). In addition, PDE4 is particularly sensitive to inhibition by rolipram. PDE4 inhibition results in accumulation of intracellular cAMP, and thereby downstream activation of PKA, which subsequently phosphorylates transcription factor cAMP-response element binding protein (CREB) (Wachtel, 1982). PDE4 is expressed in many but not all cell types, and it has been considered as suitable drug target for the treatment of respiratory disease such as asthma and chronic obstructive pulmonary disease (COPD) (Rabe *et al.,* 2011). PDE3 is also able to hydrolyze cGMP with high affinities (Degermann *et al.,* 1997).

The cGMP-dependent PDEs regulate cAMP response in several cell types. In vascular smooth muscle cells (VSMCs), nitric oxide (NO) activates PKA signaling through cAMP-dependent inhibition of PDE3 leads to elevations of cAMP (Manganiello *et al.,* 1995; Beavo, 1995). However, in cardiac myocytes, cGMP-dependent PDEs also regulate cAMP responses. It has been reported that cGMP-inhibits PDE3, increases cAMP in human atrial myocytes (Kiristein *et al*., 1995).

1.1.5.5 Protein kinase C (PKC)

Protein kinase C (PKC) is a family of protein kinases which phosphorylate serine and threonine residues in many target proteins (Benjamin *et al*., 2000). PKC plays an important role in many cellular functions such as cell proliferation, differentiation and apoptosis (Maioli *et al*., 2006).

PKC family can be divided into three main subtypes: PKC-α, PKC-β and PKC-γ. All these three subtypes are activated by DAG and calcium. Binding of ligand such as hormone or neurotransmitter to GPCR, activates heterotrimeric G protein $G\alpha_{q/11}$ (Calpham & Neer, 1997). Upon activation of G protein $G\alpha_{q/11}$, PLC-β get activated and cleaves $PI(4,5)P_2$ resulting generation of second messengers such as $InsP_3$ or IP_3 and DAG. DAG stimulates the PKC together with elevated [Ca^{2+}]. IP_3 stimulates intercellular Ca^{2+} release from ER and thereby alters many cellular processes including cell proliferation, gene activation and cell death. On the other hand Gβγ subunit of G proteins also directly couples to PLC, PI3K and K^+. It's been reported previously that Gβγ directly stimulates PLC-β, and thereby activate PKC, which then stimulates AC5/6 in a Gs dependent manner (Calpham & Neer, 1997).

1.1.5.6 Phosphatidyl inositol phosphatases (PtdInsPs or PIPs)

Phosphatidyl inositol phosphates (PtdIns) are a family of phospholipids in cell membranes. PtdInsPs interact with many different proteins through a common binding domain and triggers downstream signaling. There are mainly four species of PtdIns in D3 position: PI3P, $PI(3,4)P_2$, $PI(4,5)P_2$, $PI(3,4,5)P_3$, which are present in cells (Fig. 4). PtdIns3P is found in lower eukaryotes, like yeasts, whereas $PI(3,4)P_2$ and $PI(3,4,5)P_3$ are found in almost all eukaryotic cells (Michell *et al*., 2007).

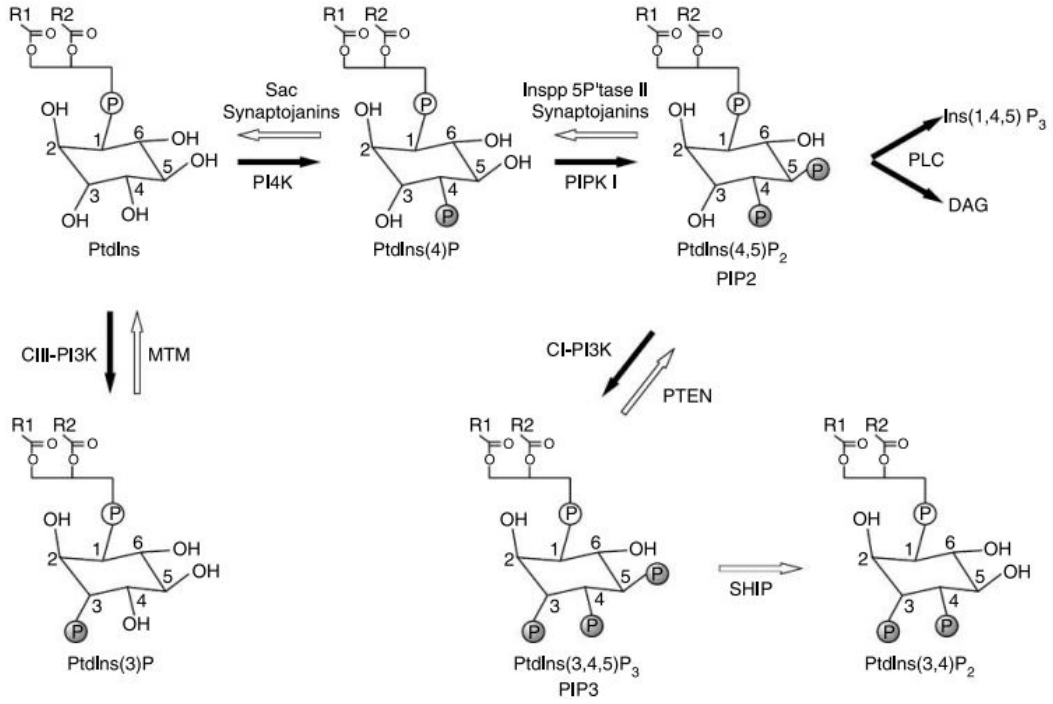

Figure 4: Structure of selected phosphoinositides. A schematic of PtdIns and some of it's phosphorylated derivatives. Black arrows indicate that kinase is involved; conversely, a white arrow indicates that phosphatase is involved. (Adapted from Hirsch *et al*., 2006).

1.1.5.6.1 Phosphoinositide 3-kinases (PI3Ks)

PI3Ks are lipid kinases that are activated by the binding of growth factors, insulin and cytokines to cell surface receptors and the subsequent activation of the GPCR or tyrosine kinase receptor. The activated PI3K catalyse the phosphorylation of phosphatidylinositol at the at the 3' position of the inositol ring, producing secondary messenger lipids, which control cellular activities including cell growth and proliferation (Engelman *et al.,* 2006). Signaling through PI3 kinase regulates glucose and lipid metabolism and also induce lipogenesis and glucose uptake/metabolism in both muscle and adipose tissues (Kahn, 1995). There are three classes of PI3 kinases: Class I PI3K, class II PI3K, and class III PI3K. Among

three classes of PI3Ks, class I PI3K is known as the best-characterized type so far. Based on sequence similarity, class I PI3Ks are further divided into two subgroups, Class IA and Class IB. Class IA PI3Ks are activated by stimulation of different receptors including tyrosine kinase receptor. Class IA PI3K are heterodimers, which contain a catalytic (p110α, p110β, and p110δ) and a regulatory subunit (P85α, p85β, p55α, p55γ, and p50α). P85α regulatory and p110α and p110β catalytic subunits are the most widely expressed subunits. There are 3 isoforms in class IA including PI3Kα, PI3Kβ and PI3Kδ with the respective p110γ catalytic subunit bound to the p85 regulatory subunit. PI3Kα and PI3Kβ are ubiquitously expressed, while PI3Kδ is limited but preferentially found in leukocytes, and PI3Kγ has been found recently in the cardiovascular system (Hirsch *et al*., 2006). Among all classes of PI3 kinases, only class IB PI3K is directly activated by GPCR via heterotrimeric G proteins. The class IB PI3Kγ is composed of p101 regulatory subunit and p110γ catalytic subunit. The p101 regulatory subunit responds to specific GPCR-associated G protein, βγ subunits and a γ P110 (p110γ) catalytic subunit, thus activating the class IB PI3K and production of $PI(3,4,5)P_3$ (Walker *et al*., 1999). In addition, the X-ray crystallographic studies reveled that PI3K inhibitors such as wortmannin and LY294002 and the broad-spectrum protein kinase staurosporine are bound to p110γ subunit (Suire *et al*., 2005). These inhibitors effectively inhibit or block the enzymatic activity of all PI3K via Gβγ subunits (Kurosu *et al*., 1997; Maier *et al.*, 1999; Stephens *et al.*, 1997; Walker *et al*., 1999).

1.1.5.6.2 Regulation of $PI(3,4,5)P_3$ and $PI(3,4)P_2$ phosphatases

All class I PI3Ks preferentially phosphorylates $PI(4,5)P_2$, generating $PI(3,4,5)P_3$ and $PI(3,4)P_2$. In these two phospholipids, PIP_3 is an important signaling molecule and act as second messenger. Activation of PIP_3 further triggering the activation of its downstream effectors such as PDK1 (phosphoinositide-dependent kinase-1), Akt/ Protein kinase B (PKB) and mTOR (mechanistic target of rapamycin) through plekstrin-homology (PH) (Wymann *et al*, 2005). These effectors facilitate cellular processes.

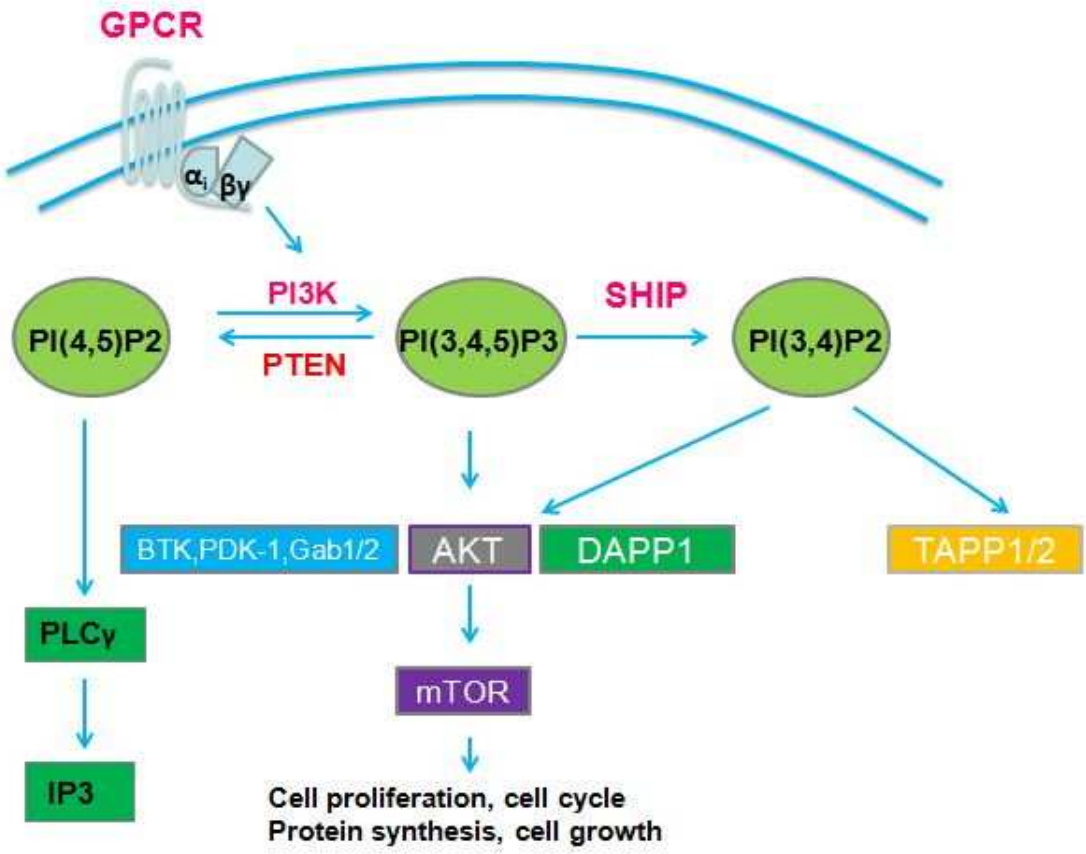

Figure 5: The PI3K/PIP_3/Akt pathway. Binding of growth factors to G protein coupled receptors, recruits and activates PI3K. Activated PI3K phosphorylates PI(4,5)P_2 to PI(3,4,5)P_3, which leads to phosphorylation of Akt by PDK1. Phosphorylated Akt is active on a wide range of substrates. One of its most important targets is mTOR, which is involved in cell growth, proliferation and cell survival. SHIP is a phosphotase which catalyzes conversion of PIP_3 to PI(3,4)P_2, which also activates Akt, DAPP1 and TAPP1/2, and thus regulate pivotal cellular processes including cell proliferation and cell growth. PTEN is a tumor suppressor gene that negatively regulates the pathway by removing the 3-phosphate from PIP_3, thus converting it back to PI(4,5)P_2. Further, PLCγ converts PI(4,5)P_2 to IP_3 and DAG (Cully *et al*., 2006).

The activation of PIP_3 is regulated by tumor suppressor protein phosphates and tensin homologue deleted on chromosome 10 (PTEN) (Li & Sun, 1997, Li, *et al*., 1997, Stock, *et al*., 1997), which dephosphorylates and thus negatively regulates PIP_3-dependent signaling (Maehama & Dixon, 1998). In addition, PTEN dephosphorylates downstream effectors of PIP_3, including PDK1 and Akt/PKB (Cantely & Neel, 1999).

PI(3,4)P_2 is another phospholipid and also acts as second messenger. PI(3,4)P_2 is generated by dephosphorylation of PIP_3 on the 5´ phosphate of the inositol ring by SHIP. PI (3,4)P_2 bind and activates PDK1, Btk (Bruton tyrosine kinase), Akt/PKB and tandem PH-domain-

containing proteins (TAPP1/2) (Aman *et al*., 1998; Bolland *et al*., 1998; Cully *et al*., 2006). However, $PI(3,4)P_2$ is also dephosphorylated by the phosphatase INPP4B on 5 prime position of the inositol ring (Kalesnikoff *et al*., 2003).

SHIP (Src homology 2-containing inositol 5' phosphatase) is a lipid phosphatase, which hydrolyzes at 5 prime position of inositol ring from inositol 1,2,4,5-tetraphosphate and PIP_3 and converts $PI(3,4,5)P_3$ to $PI(3,4)P_2$ (Damen *et al*., 1996; Lioubin *et al*., 1996).

1.1.5.6.3 PI3K downstream effectors

Generation of $PI(3,4,5)P_3$ from $PI(4,5)P_2$ by PI3K, further triggers several important downstream signaling mechanisms via specific lipid-binding domains such as PH domain containing proteins. Many, though not all PH domains containing proteins binds to PIs. One of the major downstream signaling events triggered by PI3K is the activation of members of the serine/threonine kinases such as PDK1 and PKB/Akt. Binding to PIP_3 triggers the activation of PDK1, which can phosphorylate the threonine 308 of PIP_3-bound PKB/Akt. Phosphorylation of Akt further activates the rictor-mTOR protein complex, which further phosphorylates its target substrates and regulates cellular responses including gene transcription and cell proliferation (Brazil *et al*., 2004). In addition, activation of PDK1 phosphorylates and activates atypical PKC, PKC-ζ, resulting stimulation of AC5/6 (Dessauer *et al.,* 2006; Romy *et al*., 2013). However, a wide numbers of proteins (75 substrates have been described so far) are phosphorylated by PKB/Akt. Among, the best-characterized substrate is glycogen synthase kinase3 (GSK3). Furthermore, PH domain-containing tyrosine kinases including Tec and Btk are triggered by PI3K (Lindvall, 2002).

1.2. Real-time FRET (Fluorescence or Förster resonance energy transfer) measurements.

Förster resonance energy transfer (FRET) was first discovered by a German scientist, Theodor Förster in 1946. In recent years, FRET has become an extremely powerful tool for identifying molecular interactions between fluorescently labeled molecules use conformational changes of those in living cells. It can be used in a variety of molecular techniques including microscopy, flow cytometry and ELISA. FRET is a non-radiative transfer of energy between nearby fluorophores, these fluorophores often referred as acceptor and donor. FRET is basically dependent on the distance between acceptor and donor fluorophores. When the energy is transferred from the donor fluorophore to an acceptor fluorophore, the donor fluorescence is loose, whereas acceptor fluorescence is gained. The energy transfer can be monitored using any fluorescence microscope or fluorometer.

However, FRET does not occur, if the distance between two fluorophores exceeds 10 nm. In addition, there are three key conditions to allow the Föster mechanism are

- The donor and acceptor molecules must be in close proximity to each other (approximately 1-10 nanometers).
- The absorption spectrum of the acceptor must overlap with the emission spectrum of the donor.
- The relative orientation of the dipole moment of donor and acceptor should be parallel.

Förster showed that the efficiency of FRET (E_{FRET}) depended on inverse sixth power of distance between the pair of molecule(r)

$$E_{FRET} = 1/(1 + (r/R_0)^6$$

Where R_0 is known as Forster distance, r is actual distance between pair.

Before FRET experiments can be performed successfully, it is important to choose the right fluorescent pairs. The most commonly used FRET pair for FRET studies is cyan fluorescent protein (CFP) and yellow fluorescent protein (YFP) (Tsien, 1998). This CFP-YFP pair has strong spectral overlap, and this allow high resolution for FRET recordings. By genetic engineering, these FRET pair can be easily incorporated into proteins, which allows to measure GPCR signaling kinetics such as second messenger breeding, receptor G protein coupling, receptor activation and ligand binding in live cells (Ferrandon *et al*., 2009; Janetopoulos *et al*., 2001).

There are three different methods for measuring FRET efficiency. 1, FRET acceptor photobleaching 2, Sensitized emission 3, FLIM-FRET. These methods are discussed briefly in sections below.

1.2.1 FRET-acceptor Photo-bleaching (AB): For acceptor photobleaching, the FRET acceptor molecule of the FRET pair is bleached, the resulting donor fluorescence is unquenched after photobleaching of the acceptor. The difference of fluorescence intensity of the donor pre and post-photobleaching gives direct FRET efficiency. This method is suitable only for steady state experiments.

1.2.2 Sensitized Emission (SE): The second possibility is to measure FRET by sensitized emission, and it is one of the most used method for determining FRET dynamics. In this method, donor molecule is excited and measured in the acceptor channel. In our FRET experiments CFP- is excited, the CFP- and YFP-fluorescence were recorded simultaneously and the subsequent ratio of YFP-over CFP fluorescence was calculated. Before the occurrence of FRET, a strong CFP- and weak YFP- emission resulting in a low YFP/CFP ratio is observed. Upon the occurrence of FRET, a strong YFP- and a weak CFP- emissions resulting a high YFP/CFP ratio will be observed (Figure 6). This method is most frequently used for live cell experiments.

In this study, the generation of cAMP in GPCR signaling pathway is investigated by sensitized emission method.

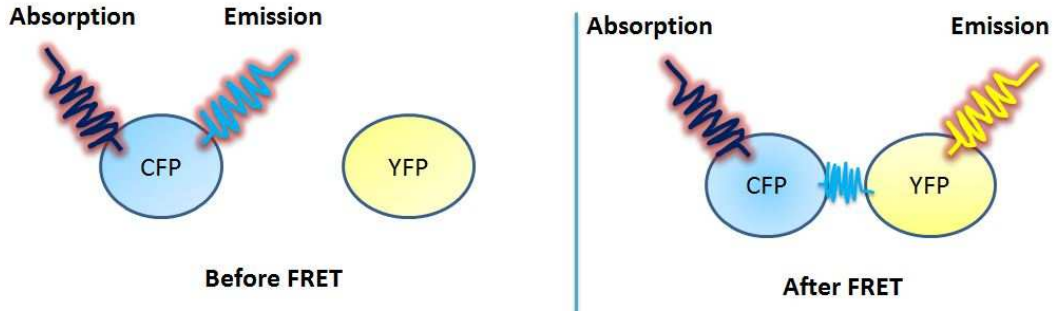

Figure 6: FRET-changes during sensitized emission. The sketch indicates that FRET only occurs if the acceptor (YFP) is close enough to the donor (CFP).

1.2.3 Fluorescence life time imaging: Fluorescence lifetime imaging is also known as FLIM. FLIM is more frequently used in FRET-based protein interaction methods. FLIM-FRET measures the change in decay function of FRET donor. When energy is transferred from donor molecule to acceptor molecule, the lifetime of donor will decrease, this change in fluorescence lifetime of donor is used to calculate FRET efficiency. FLIM-based FRET measurement does not face problems like donor bleed-through or direct excitation of acceptor. However, there are some disadvantages of this method. This system is not suitable to measure faster imaging because the imaging system is slow and this system is somewhat destructive because the excitation energy is too strong result a photobleaching over time.

1.3 Real-time cAMP measurements by FRET

To study real-time dynamics of cAMP signaling in living cells, a number of FRET-based biosensors have been developed in recent years including PKA-camps and Epac1-camps (Ponsioen *et al.*, 2004; Nikolaev *et al*., 2004).

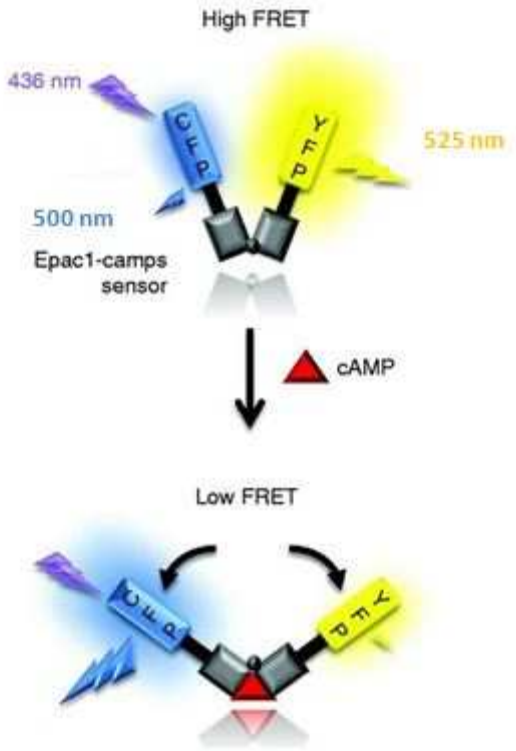

Figure 7: Structure of a single-chain cAMP FRET sensor (Epac1-camps). The Epac1-camps sensor reports intracellular levels of cAMP based on FRET between CFP and YFP. It consists of CFP and YFP fuses to a single cAMP-binding domain derived from Epac1 protein. In absence of cAMP, the two fluorophores are in close proximity, and strong FRET signal is observed. Upon cAMP binding to sensor, the distance between two fluorophores increases, leading to decrease in FRET. (Adapted and modified from Nikolaev *et al*., 2011)

These sensors measure relative fluorescence of two fluorescent proteins used as donor and acceptor fluorophores, typically cyan (CFP) and yellow (YFP) fluorescent proteins. PKA based sensors have some limitations and also show slower kinetics. Therefore, in this study we used Epac based FRET biosensor to measure real-time cAMP levels.

Epac1-camps biosensor is one of the most sensitive cAMP sensors to measure real-time cAMP levels in intact cells and cardiac myocytes. The standard FRET pair CFP and YFP as donor/acceptor are fused to a single cAMP binding domain of the Epac protein. This

biosensor displays faster activation of kinetics and high dynamic range compared to earlier cAMP FRET biosensors.

In the inactive state, the cAMP sensor has a closed confirmation, where the two fluorophores (CFP- and YFP-) are in close proximity, result a high FRET is observed. When binding of cAMP to the sensor leads to conformational change results a decrease in FRET signal as reflected by a decrease in YFP- and increase in CFP- fluorescence and the distance between two fluorophores is increased, which indicates increasing cAMP concentrations.

2. Aim of the study

The theoretical background of this work is originated from the previous findings that the cAMP rebound stimulation was observed after termination of Gi/o-stimulation in HEK293T cells expressing AC5 (Milde *et al*., 2013). Similar cAMP rebound stimulation was observed immediately following after termination of vagal stimulation or withdrawal of exposure to muscarinic receptor agonist ACh in cardiac myocytes (Burke & Calaresu, 1972; Gilmour & Zipes 1985). However, the underlying mechanism for these cAMP rebound stimulation was unclear. Therefore, we choose a FRET-based approach to investigate the possible mechanisms for muscarinic receptor-induced cAMP rebound stimulation. There were previous reports speculated that PTX-sensitive G protein/adenylate cyclase/cAMP pathway might be a possible mechanism for muscarinic receptor-induced cAMP rebound stimulation (Wang *et al*., 1995; Bett *et al*., 2001). Most reliable FRET-based cAMP biosensor (Epac1-camps) was chosen to monitor real-time cAMP levels and by using heterologous expression system, we therefore intend to study possible involvement of G protein/adenylyl cyclase/cAMP-dependent pathway on muscarinic receptor-induced cAMP rebound stimulation in cardiac myocytes and other intact cells. However, the main aim of this research was to reveal possible mechanisms underlying the muscarinic receptor-induced cAMP rebound stimulation.

3. Materials and experimental procedures

3.1 Materials

3.1.1 List of manufactures and distributors

Aldrich	Hamburg, Germany
Applichem	Darmstadt, Germany
Applied Biosystems	Waltham, USA
Biochrom	Berlin, Germany
Bio-Rad Laboratories	München, Germany
Calbiochem-Novabiochem	Darmstadt, Germany
Carl Roth	Karlsruhe, Germany
Carl Zesis	Oberkochen, Germany
Cell signaling Technology	Leiden, Netherlands
Chem rock technologies	Lafayette, USA
Chroma	Foothil Ranch, USA
Hartenstein	Würzburg, Germany
Image J	Bethesda, USA
Invitrogen	Darmstadt, Germany
Life technologies	Darmstadt, Germany
Merck Millipore	Darmstadt, Germany
Milteny Biotec	Bergisch Gladbach, Germany
Nikon	Tokyo, Japan
Neuvitro	Braunschweig, Germany
Olympus	Tokyo, Japan

Origin Pro	Northampton, USA
Paa	Cölbe, Germany
Perkin Elmer	Waltham, USA
Promega	Mannheim, Germany
Qiagen	Hilden, Germany
Roche	Mannheim, Germany
Santa Cruz	Heidelberg, Germany
Sarstedt	Nürnbrecht, Germany
Sigma-Aldrich	Steincheim, Germany
Thermo scientific	Karlsruche, Germany
Tocris	Bristol, United Kingdom
Visitech	Bristol, United Kingdom
Visitron	Puchheim, Germany

3.1.2 Reagents

[^{3}H]-clonidine hydrochloride	Sigma-Aldrich
Acetic acid	Sigma-Aldrich
Acetylcholine	Sigma-Aldrich
Adenosine 5’-triphosphate (ATP)	Sigma-Aldrich
Agarose	Biochrom
Alprenalol	Sigma-Aldrich
AS1949490	Tocris
Bovine serum albumin (BSA)	Sigma-Aldrich
Calcium chloride ($CaCl_2$)	Sigma-Aldrich

Cilostamide	Santa Cruz
Dimethyl sulfoxide (DMSO)	Sigma-Aldrich
Dopamine	Sigma-Aldrich
Ethanol	Carl Roth
Ethidium bromide (10mg/ml)	Promega
Ethylenediaminetetraacetic acid (EDTA)	Applichem
EDTA free tablet	Roche
Forskolin	Sigma-Aldrich
Gallein	Tocris
H-89 dihydrochloride hydrate,	Cell signal
Isoproterenol	Sigma-Aldrich
KT5720	Santa Cruz
Magnesium chloride ($MgCl_2$)	Sigma-Aldrich
HEPES	Sigma-Aldrich
Norepinephrine	Sigma-Aldrich
Pertussis Toxin (PTX)	Sigma-Aldrich
Platelet derived growth factor BB (PDGF BB)	Milteny Biotec
PMA	Santa Cruz
Potasium chloride (KCl)	Sigma-Aldrich
Rolipram	Santa Ccruz
SH-5	Santa Cruz
Sodium chloride (NaCl)	Sigma-Aldrich

Sodium dihydrogen phosphate (NaH_2PO_4)	Sigma-Aldrich
Sodium dodecyl sulfate (SDS)	Carl Roth
Staurosporin	Sigma-Aldrich
TrIS-(hydroxymethyl)-aminomethane (Tris)	Sigma-Aldrich
TURBO DNAse	Life technologies
Tween	Sigma-Aldrich
Wortmannin	Sigma-Aldrich
Yohimbine hydrochloride	Sigma-Aldrich
β-Mercaptoethanol (β-ME)	Sigma-Aldrich

3.1.3 Plasmids

The fallowing plasmids were either already published or available in the lab.

Plasmid	**Species**	**Origin**	**Vector/Resistance**
Epac1-camps	human	Viacheslav O. Nikolaev (Nikolaev *et al*., J.Biol.Chem. 2004)	pcDNA3/Amp+
HCN2-camps	human	(Nilolaev *et al*., *Circ Res*. 2004)	pcDNA3/Amp+
AKAR4	human	(Depry *et al*., Mol Biosyst. 2011)	pcDNA3/Amp+
Eevee-PKC	human	(Komatsu *et al*., *Mol Biol Cell*. 2011)	pcDNA3/Amp+
AKT-PH-YFP	human	Dominik Oliver	pcDNA3/kanamycine
AC4	mouse	Viacheslav O.Nikolaev	pcDNA3/Amp+
AC5	human	Carmen W. Dessauer (Sadana *et al*., *Mol pharm*. 2009)	pcDNA3/Amp+

AC6	human	Viacheslav O. Nikolaev	pcDNA3/Amp+
$G\alpha_s$	rat	(Hein *et al*., *J.Biol.Chem*. 2006)	pcDNA3/Amp+
$G\beta_1$-wt	human	(Bünemann *et al*., Proc.Natl.Acad.U.S.A. 2003)	pCMV/Amv+
$G\gamma_2$-wt	bovine	(Bünemann *et al.*, Proc.Natl.Acad.U.S.A.2003)	pcDNA3/Amp+
α_{2A}-AR	mouse	(Bünemann *et al*., Proc. Natl.Acad. U.S.A. 2003)	pcDNA3/Amp+
M_2ACh-R	human	(Roseberry *et al*., *Mol.Pharamcol*. 2001)	pGES/Amp+
D_1-R	human	Obtained fromMissouri S&T cDNA Resource Center	pcDNA3/Amp+
PcDNA3		Invitrogen	pcDNA3/Amp+
AC5Δ 66-137	human	(Sadana *et al*., *Mol pharm*. 2009)	pcDNA3/Amp+
PTEN	human	Dominik Oliver	pGES/Amp+
$G\alpha_{i1}$	human	Moritz Bünemann	pcDNA3/Amp+
$G\alpha_{i2}$	rat	Moritz Bünemann	pcDNA3/Amp+
$G\alpha_{i3}$	rat	Moritz Bünemann	pcDNA3/Amp+
PLCβ2	human	Moritz Bünemann	pcDNA3/Amp+
M_3ACh-R	human	Obtained fromMissouri S&T cDNA Resource Center	pcDNA3/Amp+
Gβ-Cer	human	(Frank *et al*, *J. Biol. Chem*. 2005)	pcDNA3/Amp+

Gq-YFP	mouse	(Hommers *et al, J. Biol. Chem.* 2010)	pcDNA3/Amp+

Table 4: Plasmids used during the study

3.1.4 Kits used

Product Name	Company
Plasmid Midi kit	Qiagen
RNase free DNase kit	Qiagen
BCA protein assay kit	Thermo scientific
RNA extraction kit	Qiagen
iScript cDNA synthesis kit	Bio-Rad
iTaq^{TM} Universal SYBER Green Supermix	Bio-Rad

Table.5 Kits used during the study

3.1.5 Cell culture, cell culture media and supplements

Bacteriological culture plates	Sarstedt
Cover slips	Neuvitro
Dulbecco's modified eagle's medium (DMEM)	Biochrom
Dulbecco's phosphate buffered saline (PBS)	Biochrom
Fetal calf serum (FCS)	Biochrom
L-glutamine	Biochrom
Luria-Bertani (LB) medium	Applichem
Penciline/streptomycin	Biochrom
Trypsin/EDTA	Biochrom

Poly-L-lysin hydrobromid	Sigma-Aldrich
Effectene	Quiagen
6-well cell culture plates	Sarstedt
Petridishes	Hartenstein
Eppendorf tubes (1.5ml)	Sarstedt
Pipettes	Sarstedt

3.1.6 Cells and Cardiac myocytes

Human cervical cancer cells (HeLa)	Obtained from Prof. Dr. Robert Grosse, Germany
Human embryonic kidney cells, stables (HEK293T)	European collection of animal cell cultures
Mouse atrial cardiac myocytes	Obtained from Prof. Dr. Viacheslav O. Nikolaev, Germany

3.1.7 Software's

The fallowing software was used for the assigned purpose:

1. Exporting Data from samples
    - Visitron software (from fluroscence microscopy)
    - Visitech software (from confocal microscopy)
2. Data analysis and statistics
    - Microsoft Excel 2007 or newer
    - GraphPad Prism 5
    - Origin Labs Origin Pro 9
3. Image analysis and modification
    - Image J 1.46r (http://imagej.nih.gov/ij/)

- Corel Photo-Paint X4

4. Figure optimization
    - CorelDraw X4

3.1.8 Microscopes

The following microscopes were used in our study

- Fluroscence Microscope (Zesis)
- Confocal Microscope (Olympus)

3.2 Experimental procedure

3.2.1 Molecular biological methods

3.2.1.1 Generation of electro competent cells (E coli)

A stock of bacterial cells were streaked onto an LB plates and grown overnight. Next day a single colony was selected for the starter culture and inoculated into 200ml of LB medium. Cells were allowed to grow at 37^{o}C with shaking at 250-300 rpm, until density reached OD_{600} of 0.3-0.6. 200ml of LB culture medium was splitted into four 50ml tubes. The cells were then centrifuged at 5000 rpm for 10min at 4^{o}C. Supernatant was removed, and pellets were resuspended into 25ml ice-cold TSB. Tubes were incubated for 2-3hrs on ice. Aliquots (300µl in 1.5ml tubes) were frozen in liquid nitrogen and stored at -80^{o}C.

3.2.1.2 Transformation of E. coli

The aliquot frozen cells were taken from liquid nitrogen and transfer into a 37^{o}C heat block. 100µL competent cells were added in 20µl of 5X KCM-buffer and 80µl of water. 2µl of DNA was added into the buffer mixture and incubated for 20min on ice and then incubated for 10min at room temperature (RT). 1ml of LB-broth was added to the buffer mixture and incubated for 50min shaking at 37^{o}C. 60-100µL of the mixture was plated on ampicilin or neomycin contained LB-agar and incubated overnight.

3.2.1.3 Amplification and plasmid preparation

Medium-scale plasmid preparations were carried out according to Qiagen's manufactures Plasmid Midi kit with 100ml of bacterial suspension grown overnight.
Yield and purity of plasmid DNA were determined by using a Nano Photometer (Implen GmbH, München, Germany) with 1 cm path length, and the DNA concentration was calculated according to Beer's law. Plasmid DNA solutions were then diluted to a standard concentration of 1µg DNA/µl.

3.2.1.4 Standard Polymerase chain reaction (PCR)

DNA isolation by PCR fallowing protocol:

Amount	Ingredient
0.5µL	Template DNA(0-1µg/µl)
2µL	Buffer 10X with $MgSO_4$
1µL	dntp mix (2mM)
0.4µL	Forward primer (10µM)
0.4µL	Reverse primer (10µM)
20µL	ddH_2O
0.5-1µL	DNA polymerase

Table.6 The PCR machine programming according to the manufacturer's protocol

3.2.1.5 Agarose gel electrophoresis

Agarose gel electrophoresis was used to analyzing DNA. The DNA was seen in the gel by addition of fluorescent dye ethidium bromide that binds strongly to DNA.

In this study, 0.7 %-1% of agarose was used in agarose gels.

Generally 1% gel shows good separation (resolution) of large DNA fragments (5-10kb). 1% agarose was prepared from 3.5g of agarose and 350ml of TAE (40mM Tris-acetate (pH 8.0), 1mM EDTA). Agarose was added into a flask containing 1xTAE. Then it was heated in a microwave until it was dissolved. The amount of water lost through boiling was supplemented. The flask was then cooled to 50°C in a water bath. The agar was simultaneously poured into the electrophoresis chamber. The gel was allowed to polymerize. The gel chamber was filled with 1xTAE buffer. The wells of the gel were loaded with 10µl of required samples and DNA marker. The voltage was set to 80 V and the gel was run for approximately 60min. In order to observe the DNA under a UV lamp at 260nm, the gel was stained with ethidium bromide solution (10mM Tris-HCl, 1mM EDTA, 1mg/ml ethidium bromide) for 10min and then washed with water to remove excess ethidium bromide. The

bands were then photographed with a ChemiDoc XRS Scanner and and the QuantitiyOne 4.6.5 software.

3.2.2 Transfection of HEK 293T cells and HeLa cells

The Effectene transfection reagent (Qiagen) was used to transfect HEK293T or HeLa cells according to the manufacturer's protocol. HEK29T or HeLa cells were seeded on the 10 cm dishes at a density of $6*10^5$. After cells reaching 80% confluence, cells were splitted from 10 cm dish to 6 cm dish. Then the cells were incubated at 37 ^oC and 5% CO_2. After 24h, the medium was replaced with the transfection mixture. The transfection mixture was prepared according to protocol bellow and incubated for 10min at RT.

Ingredient	Quantity
DNA	1µl
buffer	150µl
enhancer	8µl
effectene	10µl

Table 7: Transfection mixture

24h after transfection, the medium was replaced with normal medium or by yohimbine (100nM) containing DMEM medium for α_{2A}-AR transfected cells for 3 to 4h. Yohimbine was used to prevent potential serum-derived stimulation of α_{2A}-AR. Transfected cells were splitted on cover slips. Before splitting cover slips were coated with poly-Lysine (see below) to increase adherence of the cells. Cells were incubated overnight with 37^oC to allow the expression of construct. The next day cells were measured.

The following protocol was used for coating of glass cover slips:

Before coating, cover slips were dipped in to ethanol for 30min and then washed with PBS buffer to remove residual ethanol and then placed into 6-well plates. 200µl of poly-L-lysine (0.1mg/ml) was dropped onto each cover slip and left for 30min. The solution was then removed, and cover slips were washed with 1ml PBS buffer.

3.2.3 Fluorescence microscopy

3.2.3.1 FRET-based microscopy in intact cells

After 40-50h transfection, FRET measurements of transiently transfected intact cells were essentially performed at room temperature by using an inverted microscope (Axiovert 100, Zeiss) equipped with a PLAN/Apo N 60x/1.45 oil objective lens (Olympus), a SPOT Pursuit CCD-Camera (Spot Imaging solutions) and two cooled precisExcite LED illumination system (Visitron Systems, Germany). The following filters (Chroma, Semrock) were used for the FRET measurements: CFP-Excitation filter 436/20, YFP-Excitation filter 500/20, a long pass beam splitter to collect combined fluorescence of CFP and YFP 458LP (Semrock), 500LP a beam splitter to separate CFP and YFP emission, HC 470/24 (CFP) and HC 525/39 (YFP) emission filters (all from Semrock). CFP and YFP images were recorded by using a CCD camera. Cells were mounted on a home-built perfusion chamber and continuously super fused with Tyrode solution or agonist containing solution (see section 3.2.9.1) using pressurized perfusion system (Ala-VC³-8SP, Ala Scientific Instruments). CFP and YFP emissions were collected every 2s and illumination time was set to 30ms. Fluorescence of the cell was recorded at 440nm (F_{440} for CFP) and 500 nm (F_{500} for YFP). Later it was corrected for background subtraction, resulting in F_{YFP} and F_{CFP}. In order to determine FRET, additionally F_{YFP} was corrected for bleed-through (see section 3.2.3.3). The F_{YFP}/F_{CFP} ratio was calculated with the Visitron software, and represented in the intensity modulated display mode. For the quantification, the F_{YFP} and F_{CFP} intensities were exported to Excel software. The $F_{YFP}/_{CFP}$ values before stimulation were averaged and used as a reference. The ratio of raw F_{YFP}/F_{CFP} value to the reference value was defined as the normalized $F_{YFP}/F_{CFP.}$

3.2.3.2 Correction factors

To calculate the FRET ratio, two correction factors must first be determined: bleed through and false excitation. The tail of CFP emission spectrally overlaps with the emission of the YFP. Depending on the chosen emission filters, a part of the CFP emission is collected together with the YFP emission. This is called the bleed-through of the CFP into the YFP emission. Furthermore, EYFP is excited during FRET measurement with ECFP excitation. This phenomenon is called YFP-false excitation. In this study, these correction factors were used to subtract from original FRET traces.

3.2.3.3 CFP fluorescence bleed-through

In order to determine CFP-bleed through, HEK293T cells were transiently transfected with only one CFP-containing plasmid. CFP expressed cells were measured on the microscope as

described in (section 3.3.3.1). F_{470} and F_{525} were recorded and corrected for background fluorescence. The correction factor for bleed-through was calculated by dividing F_{525} by F_{470}. The resulting correction factor for bleed-through was 0.3335 (Protocol was adapted from Milde *et al*., 2013).

3.2.3.4 False excitation of YFP

In order to determine YFP-false excitation, HEK293T cells are transfected with a YFP-containing plasmid. The fluorescence F_{YFP} is recorded for excitation at 440±12 nm (filter setting 458LP) and 500±10 nm (filter setting CFP/YFP dual band filter). Both F-values were corrected for background fluorescence and $F_{525\ (440)}$ is divided by $F_{525\ (500)}$. The YFP false excitation value was 0.371 (Protocol was adapted from Milde *et al*., 2013).

3.2.4 cAMP measurements

To measure receptor-mediated cAMP levels, cells were transfected with wild-type receptor together with a FRET-based cAMP sensor, AC-wt. Then the cAMP levels were measured by FRET imaging as described previously (3.2.3.1).

3.2.5 Translocation measurements

Translocation experiments of transiently transfected HEK293T cells were performed about 40-50 h after transfection at room temperature by using an inverted confocal microscope (IX 71, Olympus) equipped with a 100x oil immersion objective (UPlanSApo 100x/1.40 oil, Olympus), a CCD camera (EM-CCD Digital Camera, Hamamatsu) and a confocal imaging system (VT-HAWK, VisiTech international). The following filters were used for the translocation experiments. T495lpxr, ET 470/40x and ET 535/30m (Chroma). Cells were mounted in a home-built perfusion chamber and continuously superfused with Tyrode solution or agonist-containing solution (see section 3.2.9.1) using a pressurized perfusion system (Ala-VC³-8SP, Ala Scientific Instruments). Samples were then illuminated with 491 nm laser (VisiTech International). By using the software VoxCell Scan (VisiTech international) the fluorescence recordings were measured. For translocation experiments, AKT-PH-YFP transfected cells were directly excited at 491 nm, and YFP fluorescence was recorded at 2 Hz. YFP emission images were collected every 5s with 250ms integration time. To analyze membrane translocation AKT-YFP two ROIs (region of interest) were defined one ROI in the cell cytosol ($F_{cytosol}$) and another ROI in the whole cell (F_{total}). Then the quotient $F_{cytosol}/F_{total}$ was calculated. The 20 time points of $F_{cytosol}/F_{total}$ values before the first stimulation were

averaged and used as a reference. The ratio of raw $F_{cytosol}/F_{total}$ to the reference value was defined as the normalized ($F_{cytosol}/F_{total}$).

3.2.6 Electrophysiology

These experiments were performed by Dr. Hariharan Subramanian in Dr. Viacheslav O. Nikolaev lab in a collaborative effort.

To monitor real-time cAMP levels in cardiac myocytes, atrial myocytes were isolated from the adult transgenic mice expressing cAMP FRET sensor (Epac1-camps) (Calebiro *et al*., 2009) by a Langendorff perfusion apparatus. FRET measurements of Epac1-camps expressed in isolated atrial myocytes were performed at room temperature using the Ti-S inverted fluorescence microscope (Nikon) with an x60 oil immersion objective (CFI P-Apo 60x Lambda, Nikon) and CCD camera (ORCA-03G, Hamamatsu Photonics). Cells were mounted in Ibidi perfusion chambers and superfused with Tyrode soultion or agonist containing solution (see section 3.2.10.1). CFP excitation was achieved by using a 440nm CoolLED light source with an ET436/30M excitation filter and a DCLP455 dichroic mirror. For CFP and YFP FRET recordings, it was used the 05-EM filter set containing the 505 cdxr dichroic mirror plus ET 480/30M and ET 535/40M emission filter for CFP and YFP, respectively. Ratiometric FRET measurements were performed by simultaneously recording YFP/CFP fluorescence via DV2 Dual view beam splitter (Photometrics). Cells were excited for 10-50ms once every 5 s. F_{YFP} was corrected for direct excitation and bleed-through. FRET ratios were calculated as ratio of corrected YFP over CFP emissions (F_{YFP}/F_{CFP}). The ratio of F_{YFP}/F_{CFP} value to the baseline value was defined as the normalized (F_{YFP}/F_{CFP}).

3.2.7 Total RNA extraction and Real-time PCR

3.2.7.1 RNA preparation from HEK and HeLa cells

HEK29T and HeLa cells were seeded on the 6 cm dish and transfected by using effectene transfection reagent. After reaching 80% confluence of the cells, cells were washed with ice-cold PBS and then snap frozen at -80^{o}C.

3.2.7.2 RNA extraction and reverse transcription.

Total RNA was isolated by using RNeasy mini kit (Qiagen) according to the manufacturer's protocol, 30µl of RNase-free water was used to elute the RNA (provided in the kit). Isolated RNA samples were treated with TURBO DNase (Ambion) to remove DNA contamination.

The concentration of RNA was determined by using a nano photometer. Reverse transcription was done by iScript cDNA Synthesis Kit (Bio-Rad) according to the manufacturer protocol. The reaction mix was incubated on thermal cycler. The program for thermal cycler was 25^{o}C for 5min, 42^{o}C for 30min, and 85^{o}C for 5min. After incubation, the cDNA was kept at 4^{o}C.

3.2.7.3 Real-time PCR

After reverse transcription, real-time PCR was performed by using an iTaq^{TM} Universal SYBER Green Supermix (Bio-Rad). The reaction mix was prepared according to the manufacturer protocol (Bi-Rad). The reactions were carried out in optical 96 well reaction PCR plates (Applied Biosystems) in StepOnePlus Real-Time PCR system (Applied Biosystems). The PCR program used was at 50^{o}C for 2min, 95^{o}C for 10 min, 95^{o}C for 15sec and 60^{o}C for 1 min with 40 repetitions. Samples were measured in triplicates. qRT-PCR data were processed and analyzed by $2^{-\Delta\Delta CT}$ method, where CT values were first normalized to internal control (GAPDH) and then to the mean of the control sample (defined as 1). Primers used are shown in Table 8. Transcripts of AC5 and AC6 were specific for human.

#	Type	Primer sequence	Gene
1	Forward	5′-GCACAGGAGCACAACATCAG-3′	
	Reverse	5′-CACGATGAGCACGTAGATGAG-3′	AC5
2	Forward	5′-CAAACAATGAGGGTGTCGAGT-3′	
	Reverse	5′-TGCTACCAATCGTCTTGATCTT-3′	AC6
3	Forward	5′-CCAGGCGCCCAATACG-3′	
	Reverse	5′-CCACATCGCTCAGACACCAT-3′	GAPDH

Table 8: Primer sequences of ACs (AC5 and AC6). GAPDH served as internal control

3.2.8 Ligand binding assay

The radioactive ligand binding experiments were performed by Alexandra Birk in a collaborative effort.

To determine receptor expression levels, cell membranes were prepared from HEK293T cells. HEK29T cells were seeded on 6 cm dish and transfected by using effectene transfection reagent. After reaching 80% confluence of cells, cells were washed once with warm PBS. Cells were then detached by using buffer 1 (see section 3.2.9.12) with EDTA and 1 tablet of protease inhibitor cocktail (Roche, Penzberg, Germany) Cell membranes were centrifuged at

14,000 rpm for 1h at 4^{o}C. Discard the supernatant and cell pellets were washed with buffer 2 (see section 3.2.9.13) and resuspended with the same buffer. Cells were then sonified. Membrane receptor-specific binding was determined by incubating saturating concentrations (700nM) of [^{3}H]-clonidine hydrochloride (Perkin Elmer, USA) overnight at 4^{o}C and 10µM yohimbine hydrochloride was used to determine nonspecific binding. GF/C glass fiber filters were used to separate bound and unbound ligand by vacuum filtration. Filters were washed four times with ice-cold buffer 3 (see section 3.2.9.14) and counted in a liquid scintillation counter (Packard 1600 TR).

3.2.9 Data analysis and statistics

Agonist-induced FRET-signal amplitudes and background signal intensities were obtained with the software. The obtained intensity values were exported and analyzed with Excel 2007 (Microsoft Corporation). All agonist-induced FRET-signals were corrected for photobleaching by subtracting background intensities. The corrected agonist-induced FRET-signals were normalized to the baseline value. Unless stated otherwise we compared Epac-based FRET signals to baseline referred as $\Delta(F_{YFP}/F_{CFP}$ norm.). In most of the figures (except Fig. 8 and 9), time points 'a' and 'b' are indicated. The indicated time point (b) was defined as the time when the maximally-evoked FRET-amplitude after withdrawal of G_i agonist was reached and the indicated time point (a) was defined as the time of before exposure of agonist.

Confocal images were evaluated in Image J and all statistics were obtained using GraphPad Prism and OriginPro by ANOVA with Bonferroni test.

3.2.9 Buffers

In our study most of the buffers were prepared in ultra-filtered water (Ultra clear UV plus Reinstwassersystem; SG Wasseraufbereitung, Barsbuttel, Germany)

3.2.9.1 Tyrode solution

Ingredient	Amount
NaCl	137mM
KCl	5.4mM
HEPES	10mM
$CaCl_2$	2mM
$MgCl_2$	1mM
ddH_2O	adjust to final volume of 1L

adjust pH to 7.4

3.2.9.2 5x BSA solution

Ingredient	Amount
BSA	10mM
ddH_2O	adjust to final volume

adjust pH 7.4

3.2.9.3 LB-broth

Ingredient	Amount
Peptone	1.0%
Yeast extract	0.5%
NaCl	1%
ddH_2O	adjust to finalvolume

3.2.9.4 LB-medium

Ingredient	Amount
Agar	1.5%
LB-broth	adjust to final volume

3.2.9.5 Transformation and storage buffer (TSB)

Ingredient	Amount
PEG 3000	10%
DMSO	5%
$MgCl_2$	20mM
LB-broth	adjust to final volume of 50mL

3.2.9.6 5x KCM buffer (for transformation of competent bacteria)

Ingredient	Amount
KCl	500mM
$CaCl_2$	150mM
$MgCl_2$	250mM
H_2O	adjust to final volume of 50mL

3.2.9.7 0.5 M EDTA

Ingredient	Amount
EDTA	35g
NaOH	-4g
H_2O	adjust to final volume of 200mL

adjust pH to 8.0 with NaOH

3.2.9.8 50x TRIS buffer

Ingredient	Amount
Tris base	242g
EDTA (0.5 M, pH8)	10mL
Glacial aceteic acid	57.1mL
H_2O	adjust to final volume of 1L

3.2.9.9 10x Agarose gel loading buffer

Ingredient	Amount
glycerol	40 %
EDTA	10mM
Tris	10mM
Orange G	0.25%
H_2O	adjust to final volume

3.2.9.10 50x TAE buffer (agarose gel electrophoresis)

Ingredient	Amount
Tris (base)	242g
Galcial acetic acid	57.1mL
EDTA (0.5 M)(see above)	10mL
ddH_2O	adjust to final volume of 1L

3.2.9.11 Tris Lysis buffer

Ingredient	Amount
Tris	20mM
EDTA	2mM
Protease inhibitor mix (Ultra Mini EDTA-free tablet)	1 Tablet
ddH_2O	adjust to final volume of 50mL

3.2.9.12 Buffer 1 (for ligand binding assay)

Ingredient	Amount
NaCl	50mM
NaH_2PO_4	20mM
$MgCl_2$	3mM
EDTA	1mM
ddH_2O	adjust to final volume of 10mL

adjust pH to 7.4

3.2.9.13 Buffer 2 (for ligand binding assay)

Ingredient	Amount
NaCl	100mM
Tris Base	20mM
ddH_2O	adjust to final volume of 50mL

adjust pH to 7.

3.2.9.14 Buffer 3 (for ligand binding assay)

Ingredient	Amount
Tris Base	50mM
ddH_2O	adjust to final volume of 1L

adjust pH to 7.4

4. Results

4.1. Muscarinic receptor-induced cAMP rebound stimulation in HEK293T cells.

The cAMP rebound stimulation was observed previously after termination of G_i-coupled receptor agonist in AC5 and Epac1-camps expressing HEK293T cells (Milde *et al.*, 2013). Therefore we first reproduced the well described cAMP rebound phenomenon after withdrawal of G_i-coupled receptor agonist in intact cells. In order to reproduce these rebound effects, HEK293T cells were transiently transfected with 0.25µg of FRET-based cAMP biosensor (Epac1-camps), 0.3µg of AC5-wt and 0.1µg of M_2-R. About 24h after transfection, cAMP levels were measured by FRET imaging.

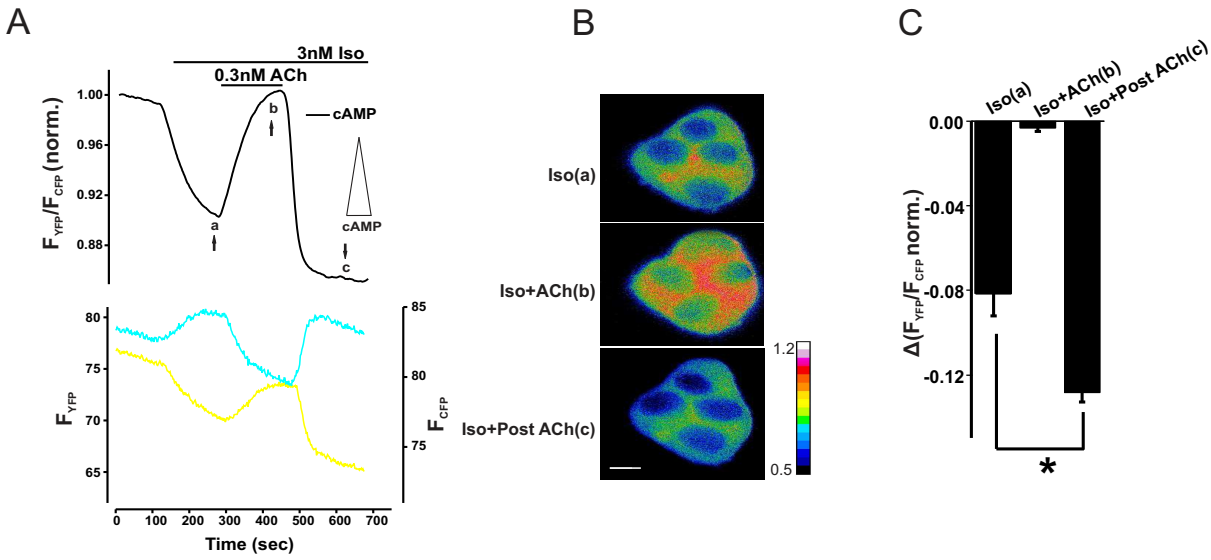

Figure 8: Acetylcholine induced cAMP rebound stimulation in HEK293T cells.

A, Representative FRET-based recording of G_i-induced cAMP alterations was measured in HEK293T cells transiently expressing the cAMP biosensor Epac1-camps, M_2-receptor and AC5. Fluorescence of the biosensor expressing cells was excited at 436±15nm, and emissions of cyan fluorescent protein (CFP) (470±24nm) and yellow fluorescent protein (YFP) (525±39nm) were detected using ratiometric imaging. Cells were exposed to isoprenaline (Iso) for 3 min then acetylcholine (ACh) for 3 min as indicated by black bars. *Top*, FRET ratio F_{YFP}/F_{CFP}, *Bottom*, corresponding CFP and YFP emissions. **B**, Pseudo-colored images of changes in FRET response (YFP/CFP) of M_2-R expressing HEK293T cells were taken at the indicated time points in Fig. A. Representative calibration bar indicates F_{YFP}/F_{CFP}. **C**, Quantification of iso (3nM)-evoked FRET changes as in *A*, calculated as F_{YFP}/F_{CFP} (norm.). Data are plotted for 3nM Iso prior to ACh (indicated with a in A), during costimulation with ACh (b) and after withdrawal of ACh (rebound stimulation indicated with c).

In order to see cAMP rebound responses, we first stimulated endogenous β_2-adrenergic receptors using isoprenaline (Iso) and then treated the cells simultaneously for a short time with a acetylcholine (ACh) concentration to account for the huge number of spare receptors expected for heterologously expressed $G\alpha_i$ coupled receptors**.** Upon stimulation of endogenous β-receptors with sub-threshold concentrations of Iso (3nM), cAMP concentrations increased to a submaximal level (indicated as *a* in Fig. 8A), as reflected by a decrease in FRET. This rise of cAMP was inhibited to baseline by the addition of 0.3nM ACh (indicated as *b* in Fig. 8A). The concentration of ACh was chosen based on the EC_{50} of the G_i/AC5-interaction studies (Milde *et al*., 2013). However, subsequent washout of ACh resulted in a rapid reversal of the inhibitory effect, leading to an increase in the cAMP concentration (defined as rebound response) (indicated as *c* in Fig. 8A). This increased cAMP concentration was substantially higher than that observed in the presence of Iso before exposure to ACh (c versus b in Figure 8A), and it was close to a maximally stimulating concentrations of Iso (10µM) alone. The rebound induced a decrease in Epac1-camps FRET of 10.2±1.4% compared to 6.1±1.6% (comparing a to c in Fig. 9). In principle, the use of Epac1-camps should allow an absolute quantification of cAMP concentrations in intact cells. It was attempted to translate changes in FRET ratio measured in HEK cells into cAMP concentrations by establishing a concentration-response curve for changes in Epac1-camps FRET measured in vitro. The calibration procedure was described in Nikolaev *et al.*, 2004. Based on the dynamic range of Epac1-camps, it was estimated that the ACh rebound increased the cAMP concentration from 0.9 by 3.1µM.

4.2 Muscarinic receptor-induced cAMP rebound stimulation in cardiac myocytes.

Several previous reports showed muscarinic receptor-induced cAMP rebound stimulation after withdrawal of agonist in cardiac myocytes (Wang & Lipsius, 1995; Belevych *et al*., 2001). In order to observe a similar cAMP rebound phenomenon in cardiac myocytes, atrial myocytes were isolated from transgenic mice expressing the cAMP biosensor Epac1-camps (Calebiro *et al*., 2009), and cAMP concentrations were measured by FRET. The cAMP rebound stimulation experiments in cardiac myocytes were performed in collaboration with the group of Viacheslav O. Nikolaev. M_2-R, β_2-AR, and ACs are predominantly expressed in cardiac tissues (Dhein *et al*., 2001; Defer *et al*., 2000). Upon exposure to sub-threshold concentrations of the β-adrenergic receptor agonist Iso (3nM), increased but submaximal cAMP concentrations were observed as indicated by a decrease of the FRET signal (shown as *a* in Fig. 9A). Subsequent addition of 10µM of the muscarinic agonist ACh for 2 min

antagonized this response as indicated by increase in the FRET signal (b in Fig.9A). Furthermore, washout of ACh resulted in a rapid reversal of its inhibitory effect as indicated by a drop of the FRET signal significantly below the values reached prior to the exposure of ACh (c versus b in Figure 9A), indicating a robust increase in the cAMP concentration which represents the well documented cAMP rebound phenomenon (Wang & Lipsius, 1995). The underlying mechanism for this muscarinic receptor-induced cAMP rebound response was not clear.

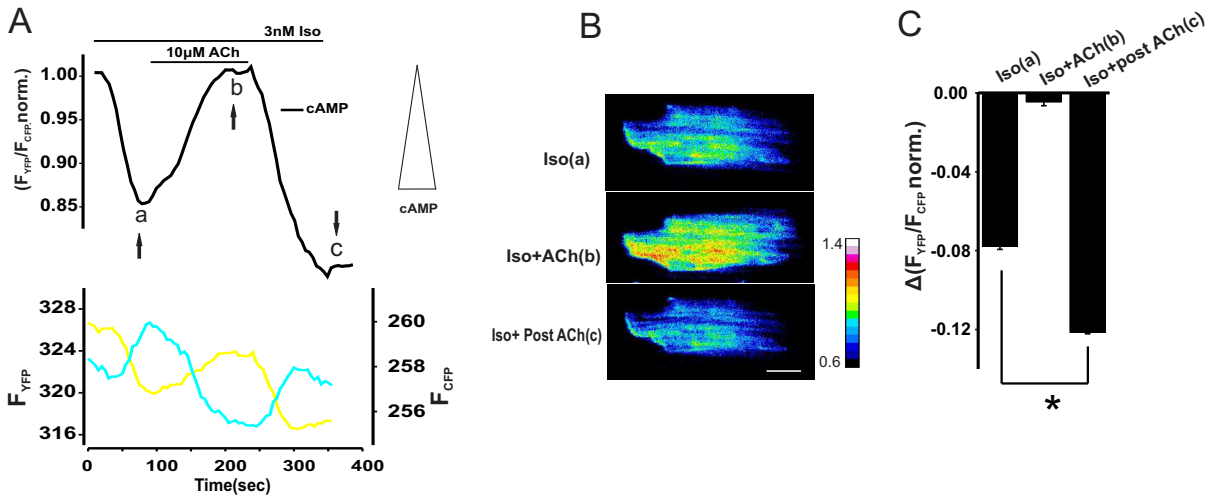

Figure 9: Acetylcholine induced cAMP rebound stimulation in adult atrial myocytes isolated from murine hearts.

A, Representative FRET recording of cAMP was measured in single freshly isolated atrial cells from mice transgenically expressing the cAMP biosensor Epac1-camps. Fluorescence of the biosensor-expressing atrial cells was excited at 436±15nm, and emissions of cyan fluorescent protein (CFP) (480±15nm) and yellow fluorescent protein (YFP) (535±20nm) were detected using ratiometric imaging. Cells were exposed to Iso and followed by ACh as indicated by black bars. *Top*, FRET ratio F_{YFP}/F_{CFP}, *bottom*, corresponding CFP and YFP emissions. The emission ratio (*top*, *black trace*) of F_{YFP} (corrected for bleed-through of CFP, *bottom*, *yellow trace*) over F_{CFP} (*bottom*, *blue trace*) was normalized to its initial value and plotted over the time course of the experiment. **B**, Pseudo-colored images of changes in FRET response (YFP/CFP) of a mouse atrial myocytes were taken from at the indicated time points in Fig. A. Calibration bar indicates F_{YFP}/F_{CFP}. **C**, Quantification of Iso (3nM)-evoked FRET changes as in A was calculated as F_{YFP}/F_{CFP} (norm.) and plotted for 3nM Iso prior to ACh (shown with a in A), during costimulation with ACh (b) and after withdrawal of ACh (rebound stimulation shown with c).

However, other groups speculated that two possible signaling mechanisms involved in muscarinic receptor-induced cAMP rebound responses are (i), $G\alpha_s$-stimulated AC5/6 and (ii),

Gβγ facilitation of $G\alpha_s$-stimulated AC4 and possibly AC7 (Belevych *et al.*, 2001, Bett *et al.*, 2001).

4.3 Muscarinic receptor-induced cAMP rebound stimulation is specific for AC5 and AC6 in HEK293T cells.

We first asked whether the $G\alpha_s$-stimulated AC5/6 signaling pathway is involved in muscarinic receptor-induced cAMP rebound stimulation. In order to investigate AC5/6 involvement, Epac1-camps and M_2-R were expressed in HEK293 cells together with or without AC5. Cells transfected with AC5 showed cAMP rebound stimulation (red trace) after termination of ACh. However, cells transfected with empty vector (pcDNA3) instead of AC5 showed significantly lower muscarinic-induced cAMP rebound stimulation (black trace).

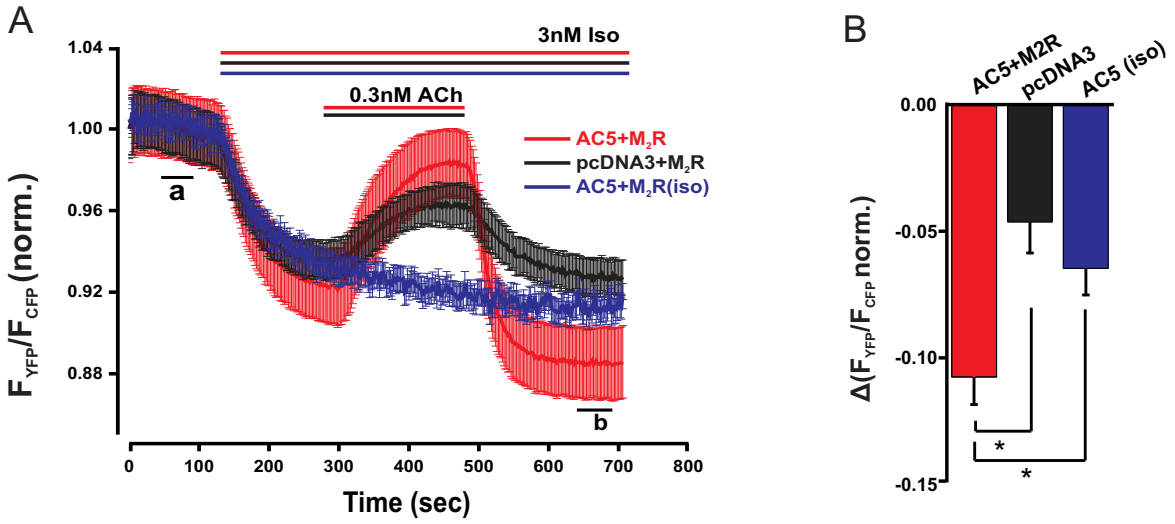

Figure 10: Acetylcholine induced cAMP rebound responses in AC5 expressing HEK293T cells.

Representative traces of FRET recordings of muscarinic receptor-induced cAMP rebound responses were measured in HEK293T cells transfected with Epac1-camps together with M_2-R with or without AC5-wt. Cells were subjected to the indicated agonist exposure protocol in order to elicit cAMP rebound responses. **A,** Average traces were obtained from 8-10 single FRET recordings from cells that were transfected with M_2-R and AC5 (red and blue) or M_2-R and empty pcDNA3 (black). Only cells expressing AC5 produced rebound stimulation as reflected by a decline in the Epac1-camps-FRET ratio after withdrawal of ACh (red versus black, time interval indicated with *b*). Cells expressing AC5 and M_2-R produced a higher FRET signal upon exposure to only Iso but not ACh (blue trace). **B**, Experimental data derived from ***A*** were quantified with respect to Iso-mediated alterations of F_{YFP}/F_{CFP} (norm.) after withdrawal of ACh (F_{YFP}/F_{CFP} at time point b - F_{YFP}/F_{CFP} at time point a). All results are plotted as mean±S.E.M.

Cells transfected with pcDNA3 showed slightly reduced β_2-AR mediated cAMP production and weak inhibitory effects upon exposure to ACh, which reveals a dependency on AC5 for both the β_2-AR mediated rise in cAMP and its M_2-R mediated attenuation (Fig. 10). These results indicated that muscarinic receptor-induced cAMP rebound responses are likely AC5 mediated. It was also suggested previously that AC6 might involved in muscarinic receptor-induced cAMP rebound responses. Therefore, we next asked whether AC6 is involved in muscarinic-induced cAMP rebound stimulation. In order to test this, Epac1-camps and M_2-R were transfected into HEK293T cells along with or without AC6-wt. Similar to cells transfected with cDNA for AC5, cells transfected with cDNA for AC6 but not cells transfected with empty pcDNA3 vector produced cAMP rebound stimulation after termination of ACh (Fig. 11), which revealed a dependency on AC5/6 for muscarinic receptor-induced cAMP rebound stimulation. These results support the hypothesis that muscarinic receptor-induced cAMP rebound effects were mediated by AC5/6.

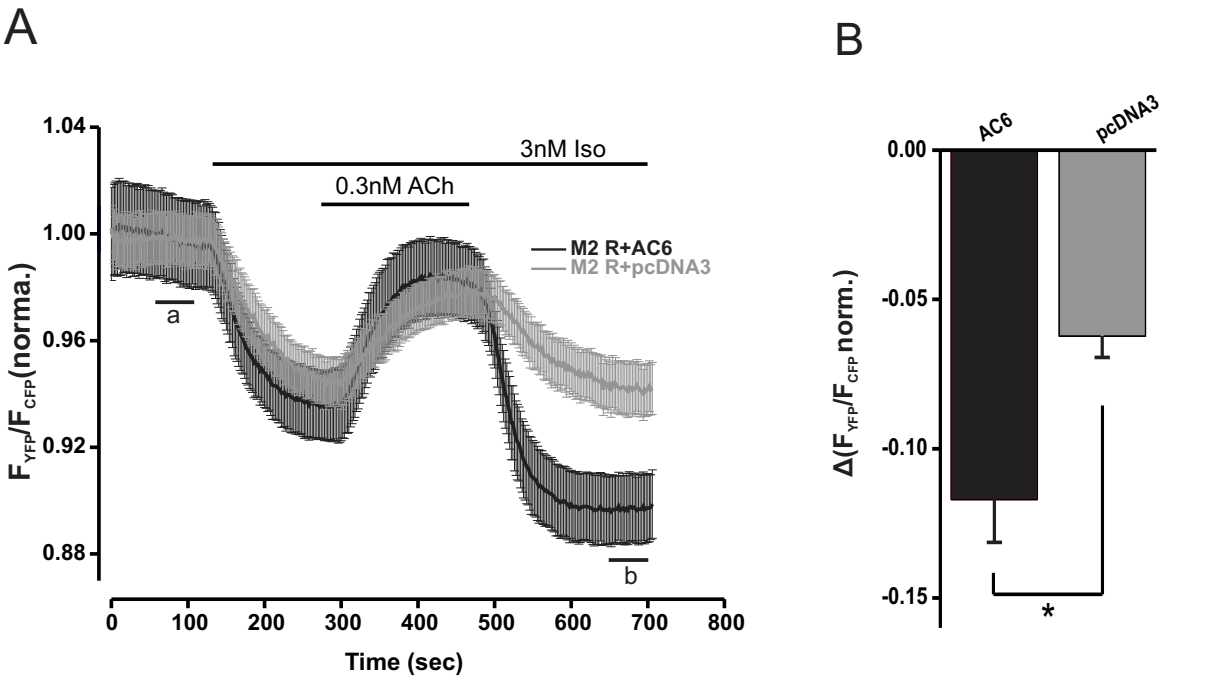

Figure 11: Acetylcholine induced cAMP rebound responses are mediated by AC6 in M_2-R expressing HEK293T cells.

A, Representative averaged FRET recordings showing alterations in cAMP induced by application and subsequent withdrawal of 0.3nM ACh in HEK293T cells transfected with Epac1-camps and M_2-R with (black) or without (grey) AC6 as indicated (n=6-7). The FRET signal of Epac1-camps was normalized to initial values. **B**, Iso-evoked alterations in FRET of the experiments shown in *A* were quantified as (F_{YFP}/F_{CFP} norm. at time point *b*) - (F_{YFP}/F_{CFP} norm. at time point *a*). All results are plotted as mean±S.E.M.

In addition, cells expressing a different G_i-coupled receptor, the α_{2A}-AR, also produced similar cAMP rebound responses in an AC5/6-dependent manner (Fig. 12)

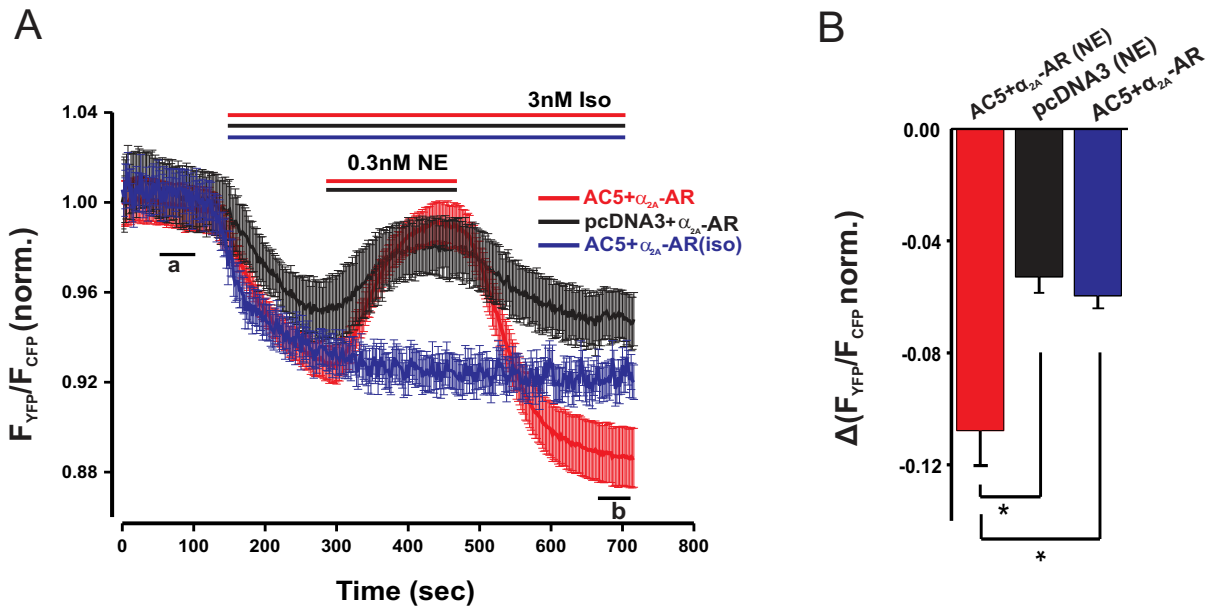

Figure 12: Norepinephrine induced cAMP rebound stimulation in α_{2A}-AR expressing HEK293T cells.

A, Depicted are averaged FRET recordings (n=7-8) measured from cells that were transfected with α_{2A}-AR and AC5 (red and blue) or with α_{2A}-AR and empty pcDNA3 (black). Only AC5-expressing cells produced rebound responses as reflected by the decline in Epac1-camps-FRET ratio after withdrawal of norepinephrine (NE) (red versus black, time interval indicated with *b*) indicating cAMP rebound response. AC5 and α_{2A}-AR expressing cells only exposed to Iso, but not to NE (blue trace) exhibited a higher FRET signal at the time interval indicated with *b*. **B**, Experimental data derived from *A* were quantified with respect to Iso-mediated alterations of F_{YFP}/F_{CFP} (norm.) after withdrawal of NE (F_{YFP}/F_{CFP} at time point b - F_{YFP}/F_{CFP} at time point a). All results are plotted as mean±S.E.M.

Thus, heterologously expressed $G\alpha_i$-coupled receptors produced cAMP rebound stimulation after withdrawal of agonist. We also determined (α_{2A}-AR) expression levels by means of radioligand binding. The expression of α_{2A}-AR was 11.0±0.9pmol/mg membrane protein, and no specific binding of [^{3}H]-clonidine hydrochloride could be detected in untransfected control cells.

Next we asked whether cAMP rebound stimulation can be attributed to specific β_2-receptor. In order to test this, the dopamine D_1 receptor (D_1-R) was used. Dopamine (D_1) receptors couple to $G\alpha_s$- which stimulates ACs resulting in an increase in cAMP. We measured G_i-induced cAMP responses in HEK293T cells which co-expressed the D_1-R in combination

with the α_{2A}-AR. Dopamine was used to activate the D_1 receptor, which stimulates AC5 resulting in an increase of cAMP via $G\alpha_s$-, and NE was used to antagonize the dopamine response. A cAMP rebound response was produced after termination of NE superfusion. However, cAMP rebound responses were observed only in cells expressing AC5 (red trace) but not in cells transfected with empty vector instead of AC5 (black) (Fig. 13). By comparing G_i-induced cAMP rebound stimulation in cells expressing different G protein coupled receptors (α_{2A}-AR, M_2-R, and D_1-R), it can be concluded that G_i-induced cAMP rebound responses are not receptor-specific.

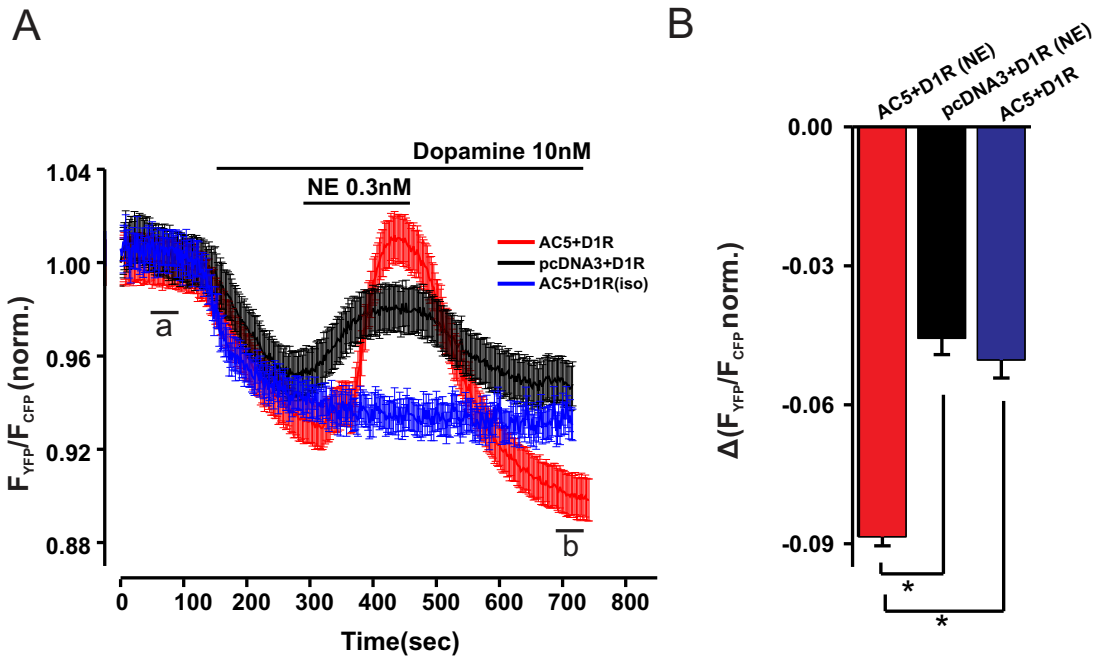

Figure 13: Dopamine induced cAMP rebound responses in D_1-R expressing HEK293T cells.

A, Averaged FRET recordings showing alterations in cAMP induced by application and subsequent withdrawal of 0.3nM NE was measured in HEK cells transfected with Epac1-camps, D_1-R and α_{2A}-AR with or without AC5 as indicated (n=6-7). The FRET signal of Epac1-camps was normalized to its initial value. FRET recordings derived from cells that were not treated with NE are shown in blue. **B,** Amplitudes of dopamine-evoked alterations in FRET of the experiments shown in *A* were quantified as (F_{YFP}/F_{CFP} norm. at time point *b*) - (F_{YFP}/F_{CFP} norm. at time point *a*) for all three conditions. All results are plotted as mean±S.E.M.

4.4 AC5 and AC6 dependent G_i-induced cAMP rebound responses are PTX-sensitive.

AC5 and AC6 isoforms are predominantly expressed in the heart and many cells and antagonize $G\alpha_s$-stimulated cAMP responses by activating inhibitory G_i-proteins (Hartzell *et al.*, 1988). However, based on previous findings these isoforms are not only inhibited by G

proteins ($G_{i/o}$) but also by physiological concentrations of Ca^{2+} (Dessauer *et al.*, 1998; Murthy *et al.*, 1998). In addition, Wang & Lipsius showed that ACh-induced rebound stimulation in atrial myocytes are attenuated by pertussis toxin (PTX) treatment (Wang & Lipsius, 1995). Therefore, it was tested whether PTX can inhibit the cAMP rebound responses. In order to test the effect of PTX, HEK293T cells transfected with Epac1-camps, AC5-wt and α_{2A}-AR were pre-treated with pertussis toxin (30ng/ml) (an inhibitor of $G_{i/o}$) for 3 to 5 hours and the effect of the cAMP rebound investigated by FRET. As expected, PTX treated cells were effectively uncoupled from $G\alpha_i$-proteins and also showed significantly attenuated cAMP rebound levels upon withdrawal of α_{2A}-AR stimulation (Fig. 14). These results are consistent with earlier findings and further confirm that G_i-induced cAMP rebound effects are mediated by a mechanism involving PTX-sensitive G_i-proteins in addition to AC5/6.

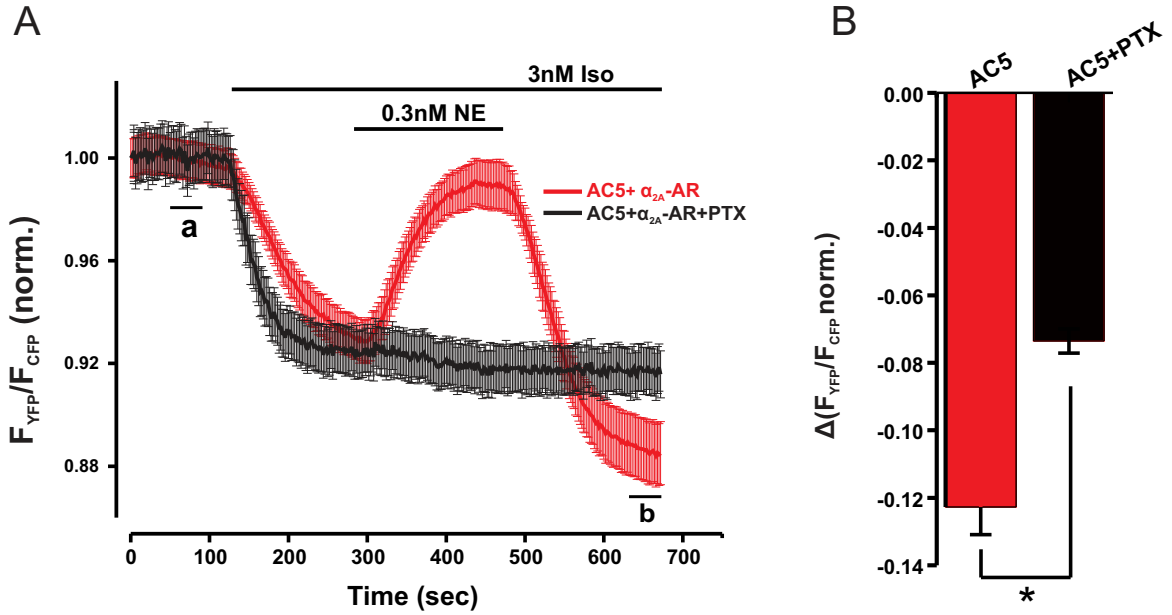

Figure 14: G_i-induced cAMP rebound responses were mediated by PTX-sensitive G proteins (G_i).

Averaged FRET recordings of G_i-induced cAMP rebound responses were measured in HEK293T cells transfected with Epac1-camps together with M_2-R and AC5-wt. **A**, Treatment of AC5 and α_{2A}-AR expressing cells with PTX (30ng/ml >4h, black) attenuated both the initial NE-induced decline in cAMP and the subsequent rebound response compared to untreated cells (red) (n=6-8). **B**, Experimental data derived from *A* were quantified with respect to Iso-mediated alterations of F_{YFP}/F_{CFP} (norm.) after withdrawal of NE (F_{YFP}/F_{CFP} at time point b - F_{YFP}/F_{CFP} at time point a). Results are plotted as mean±S.E.M.

The above results showed that the cAMP rebound responses were induced by PTX-sensitive G_i-proteins. Therefore, we next asked whether any specific G_i-proteins are mediating this rebound effect. In order to investigate this, HEK cells were transfected to overexpress $G\alpha_{i1}$ or $G\alpha_{i2}$ or $G\alpha_{i3}$ together with Epac1-camps, α_2-AR and AC5, and G_i-induced cAMP levels were measured. We observed no significant changes in $G\alpha_i$-induced cAMP rebound stimulation in cells transfected with different $G\alpha_i$-proteins ($G\alpha_{i1}$, $G\alpha_{i2}$ and $G\alpha_{i3}$) compared to control conditions (red, blue and green versus black trace) (Fig. 15) indicating that G_i-induced cAMP rebound responses are not specific for $G\alpha_{i1}$, $G\alpha_{i2}$ and $G\alpha_{i3}$ proteins.

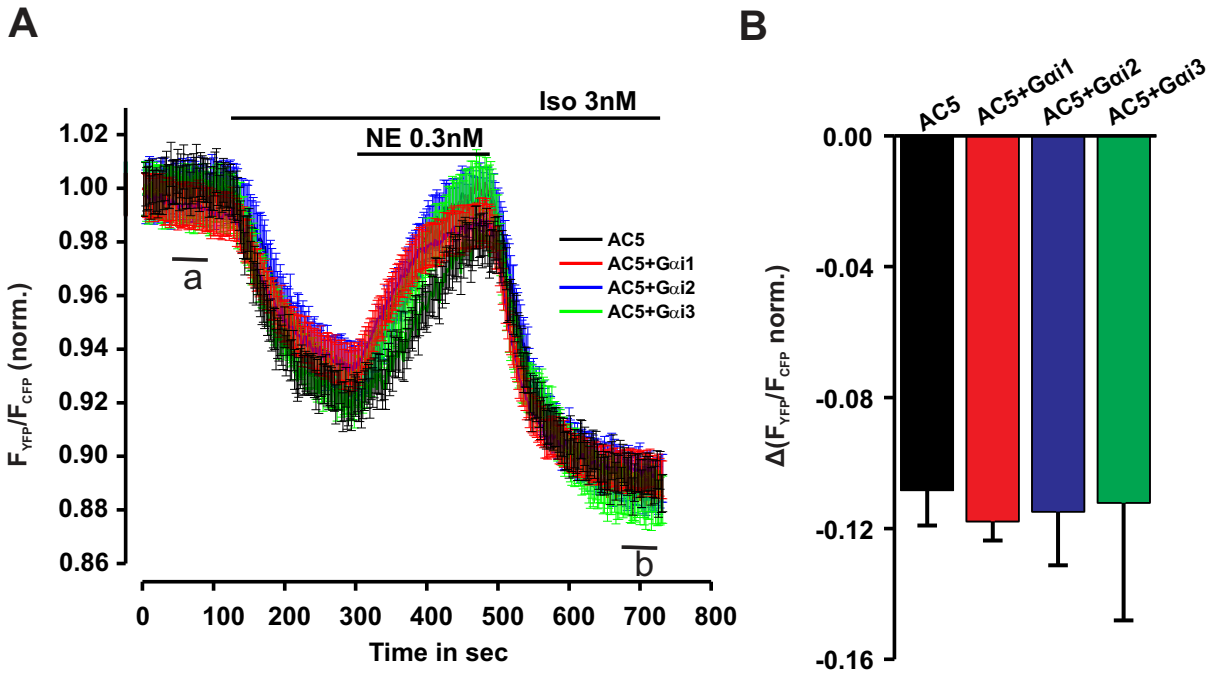

Figure 15: cAMP rebound responses were observed independent of the $G\alpha_i$-subtype

A, Averaged FRET recordings showing G_i-mediated alterations in cAMP induced by application and subsequent withdrawal of 0.3nM NE in HEK293T cells overexpressing $G\alpha_{i1}$ or $G\alpha_{i2}$ or $G\alpha_{i3}$ together with Epac1-camps, α_2-AR and AC5. The FRET signal of Epac1-camps was normalized to initial values. **B,** Iso-evoked alterations in FRET of the experiments shown in *A* were quantified as (F_{YFP}/F_{CFP} norm. at time point *b*) - (F_{YFP}/F_{CFP} norm. at time point *a*) for all four conditions. All results are plotted as mean±S.E.M. (n=5-6).

4.5 G_i-induced cAMP rebound responses in HeLa cells

The experiments described so far showed that heterologously expressed AC5 and AC6 isoforms produced cAMP rebound responses in HEK293T cells. Therefore, we next asked whether these cAMP rebound responses were restricted only to HEK cells. In order to

investigate this, HeLa cells were chosen and transfected to express Epac1-camps and M_2-R together with or without AC5-wt. Cells transfected with AC5 produced cAMP rebound stimulation after termination of muscarinic receptor agonist ACh (black trace). On the other hand, cells expressing empty vector (pcDNA3) produced significantly lower cAMP levels (gray trace) (Fig. 16). In addition, the onset of the G_i-inhibitory effect after application of the muscarinic agonist ACh on cAMP concentrations was more rapid in HeLa cells compared to HEK293T cells. It is likely that this rapid G_i-inhibitory effect is due to high phosphodiesterase activity in HeLa cells which degrade cAMP very rapidly.

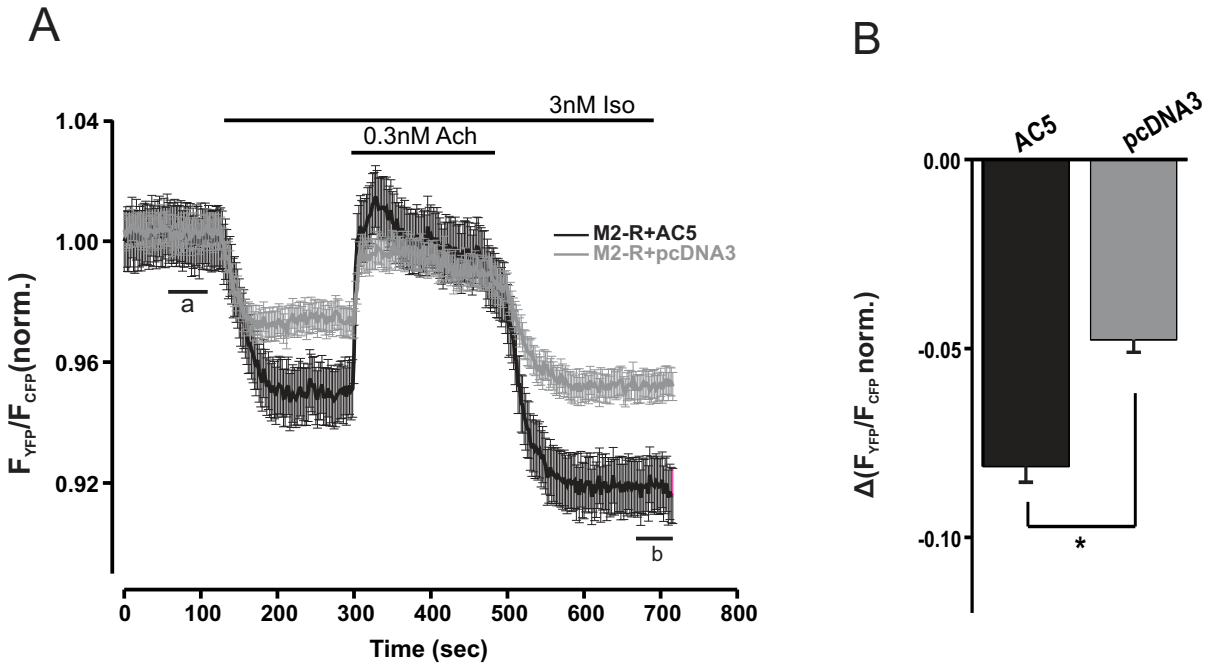

Figure 16: Acetylcholine induced a cAMP rebound responses in HeLa cells.

G_i-induced cAMP rebound responses were measured in HeLa cells transfected with Epac1-camps together with M_2-R and AC5-wt. **A,** Averaged FRET recordings showing alterations in cAMP induced by application and subsequent withdrawal of 0.3nM ACh in HeLa cells (n=6-7). The FRET signal of Epac1-camps was normalized to its initial value. **B**, Experimental data derived from ***A*** were quantified with respect to Iso-mediated alterations of F_{YFP}/F_{CFP} (norm.) after withdrawal of ACh (F_{YFP}/F_{CFP} at time point b - F_{YFP}/F_{CFP} at time point a). All results are plotted as mean±S.E.M.

From these experiments, it is concluded that G_i-induced cAMP rebound responses are similar irrespective of different receptors or cell types.

AC5/6 dependent G_i-induced cAMP rebound stimulation was measured in intact cells by using heterologous overexpression system. However, the AC5/6 protein expression levels

were not determined. Therefore, we next asked whether AC5/6 are overexpressed in intact cells or not. Due to a lack of suitable specific antibodies for AC5 and AC6, it was impossible to determine the expression of ACs on the protein level. Instead, AC5 and AC6 mRNA levels were measured in HEK and HeLa cells by qRT-PCR. Considering the transfection efficiency, (40-50% for HEK cells and 10-20% for HeLa cells) AC5 and AC6 mRNA were found to be at least eight-fold increased in AC-transfected cells compared to control cells (Fig. 17).

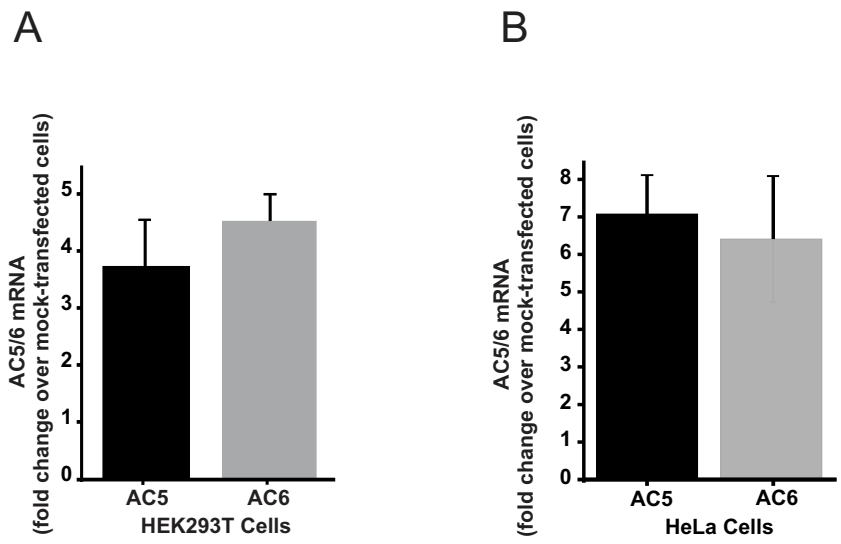

Figure 17: Relative mRNA expression levels were incresed in AC5 and AC6 transfected HEK and HeLa cells.

A, HEK293T cells were transfected to express Epac1-camps and the α_{2A}-AR together with ACs (AC5 or AC6) or pcDNA3. The relative mRNA expression levels of AC5 or AC6 were measured by qRT-PCR and normalized to the internal control (GAPDH) and are shown relative to control cells. Bar graphs represents the mean ± S.E.M from three independent transfections. **B**, Relative mRNA expression levels of AC5 and AC6 in HeLa cells. Representative data are relative to control cells. Bar graphs represent the mean±S.E.M from 2 independent transfections.

4.6 Effects of PDE3 and PDE4 inhibition on G_i-induced cAMP rebound stimulation.

The concentration of intracellular cAMP is not only dependent on cAMP generation by AC, but also on the action of cAMP-phosphodiesterases (Baillie & Houslay, 2005). However, it has been reported earlier that a PDE3-dependent NO-cGMP pathway is involved in the G_i-induced cAMP rebound increase in atrial myocytes (Wang & Lipsius, 1995 and 1998). Therefore, it was tested whether PDE3 and PDE4 inhibitors have any effect on G_i-induced cAMP rebound responses in HEK cells. Before investigating this possible mechanism, it was

necessary to examine the effects of PDE inhibitors on cAMP levels. It is known that PDE3 and PDE4 inhibitors generate cAMP via $G\alpha_s$. In order to test the effects of PDE inhibition on cAMP levels, cells were transfected with Epac1-camps, AC5, and α_{2A}-AR. Prior to the experiment, cells were pre-incubated with PDE3 or PDE4 inhibitors (cilostamide and rolipram, respectively). As expected, cells in which PDE3 or PDE4 had been inhibited produced higher cAMP levels upon Iso treatment compared to control conditions (Fig. 18).

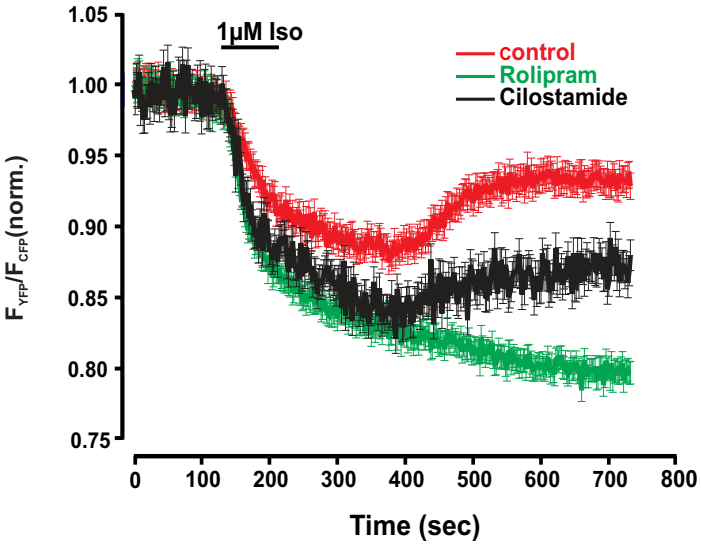

Figure 18: PDE inhibition induced cAMP accumulation

In order to explore the effectiveness of PDE inhibition in Epac1-camps expressing HEK293T cells we followed the time course of cAMP decline after withdrawal of 1µM Iso (as indicated) by means of FRET. Averaged data are shown for cells continuously exposed to 10µM of the indicated inhibitors (n=5-6).

The above results showed a clear participation of PDE3 and PDE4 to cytoplasmic cAMP degradation upon β-adrenergic stimulation (Fig. 18). Therefore, it was decided to check the effects of these PDE inhibitors on G_i-induced cAMP rebound responses. To test this, HEK293T cells were transfected to express Epac1-camps, AC5, and α_{2A}-AR. In order to avoid saturation of sensor upon treatment of PDE inhibitors, cells were pre-incubated with the inverse β-receptor agonist alprenolol for 20 to 30min. Treatment of these cells with 10µM cilostamide (a PDE 3 inhibitor) in combination with a submaximal concentration of Iso for 3 min led to an increase of cAMP levels, and these increased cAMP levels were reduced to basal levels by addition of 0.3nM NE. Furthermore, subsequent washout of NE resulted in

cAMP rebound stimulation. However, the G_i-induced cAMP rebound stimulation was not attenuated in these cells (Fig. 19).

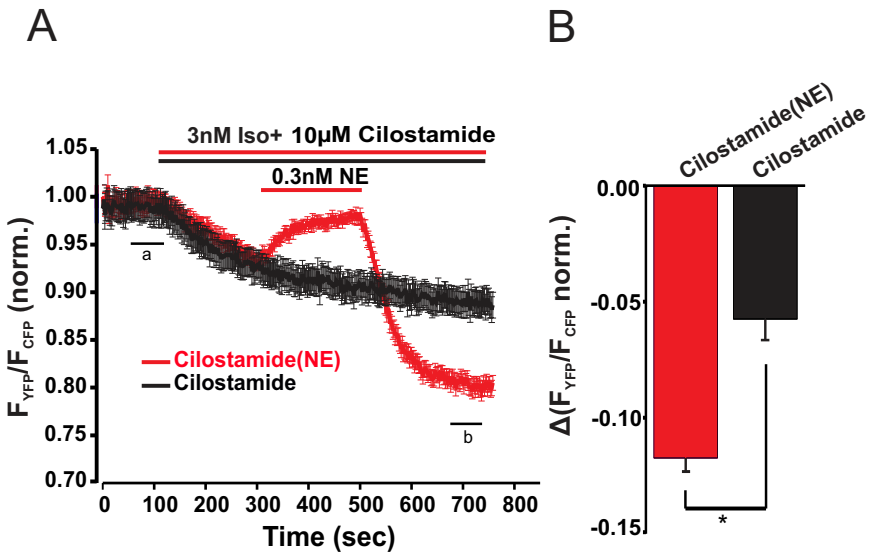

Figure 19: PDE3 inhibition did not attenuate G_i-induced cAMP rebound stimulation.

Exploring the effects of PDE3 inhibition on cAMP rebound stimulation was measured in HEK293T cells expressing Epac1-camps, AC5 and α_{2A}-AR. **A,** Averaged FRET data showing that the cAMP rebound stimulation after withdrawal of NE-induced α_{2A}-AR activation was not sensitive to inhibition of PDE3 with cilostamide. The FRET signal of Epac1-camps was normalized to initial values. **B,** Alterations in FRET of the experiments shown in *A* were quantified as (F_{YFP}/F_{CFP} norm. at time point *b*) - (F_{YFP}/F_{CFP} norm. at time point *a*). All results are plotted as mean±S.E.M. (n=7-8). To avoid saturation of the sensor upon treatment of PDE3 inhibitor, cells were pre-incubated with the inverse β-receptor agonist alprenolol for 20 to 30min.

These results indicate that PDE3 inhibitor cilostamide did not affect G_i-induced cAMP rebound stimulation. These data are in line with earlier findings in ventricular myocytes that PDE3 inhibition failed to inhibit G_i-induced cAMP rebound stimulation (Belevych *et al.*, 2001). These results also indicate that PDE3-dependent NO-cGMP signaling does not represent a major mechanism for ACh-induced inhibition in cAMP rebound stimulation. In addition, very similar results were observed in the presence of the PDE4 inhibitor rolipram. Rolipram also did not affect G_i-induced cAMP rebound stimulation (Fig. 20). These results argue against a major contribution of PDEs in the generation of the G_i-induced cAMP rebound stimulation (Wang & Lipsius, 1995). Therefore, it was concluded that PDE3-dependent NO-cGMP signaling pathway is not involved in G_i-induced cAMP rebound levels.

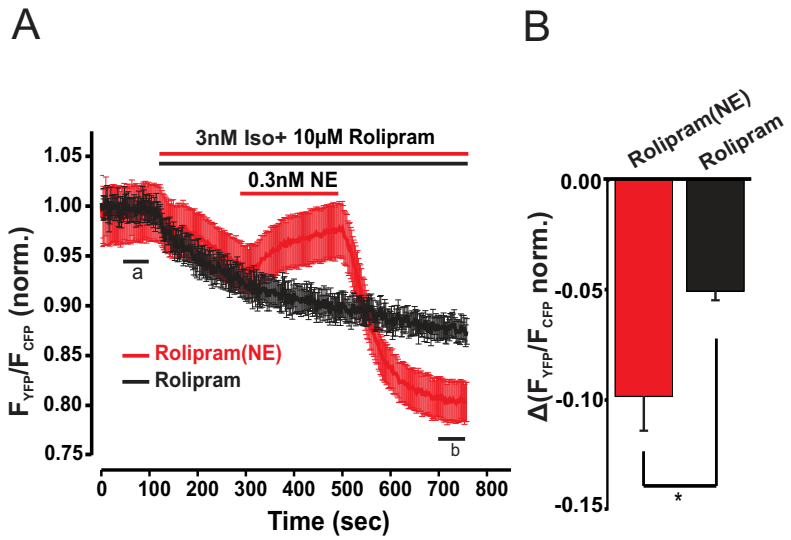

Figure 20: PDE4 inhibition did not attenuate G_i-induced cAMP rebound stimulation.

Exploring the effects of PDE4 inhibition on cAMP rebound stimulation was measured in HEK293T cells expressing Epac1-camps, AC5 and α_{2A}-AR. **A,** Averaged FRET data showing that the cAMP rebound stimulation after withdrawal of NE-induced α_{2A}-AR activation was not sensitive to inhibition of PDE4 with rolipram. The FRET signal of Epac1-camps was normalized to initial values. **B,** Alterations in FRET of the experiments shown in *A* were quantified as (F_{YFP}/F_{CFP} norm. at time point *b*) - (F_{YFP}/F_{CFP} norm. at time point *a*). All results are plotted as mean±S.E.M. (n=6-7). To avoid saturation of the sensor upon treatment with the PDE4 inhibitor, cells were pre-incubated with the inverse β-receptor agonist alprenolol for 20 to 30min.

4.7 G_i-induced cAMP rebound responses are mediated via Gβγ

As mentioned earlier**,** Gβγ facilitation of $G\alpha_s$-stimulated AC4 and possibly AC7 could be another possible mechanism for G_i-induced cAMP rebound responses (Bett *et al.*, 2002). So far, it was not demonstrated that AC7 is directly stimulated by Gβγ. Therefore, we first asked whether a Gβγ-dependent mechanism is involved in G_i-induced cAMP rebound stimulation. To test this mechanism, cells were transfected to express Epac1-camps, AC5, and α_{2A}-AR. In order to check for the importance of Gβγ signaling, cells were pre-incubated with the Gβγ inhibitor gallein (which blocks all Gβγ-dependent signaling (Lehamann *et al.*, 2008)) for 40min and G_i-induced cAMP rebound responses were compared with control conditions. Intriguingly, application of gallein significantly attenuated the G_i-induced cAMP rebound stimulation (black trace) compared to the control condition (red trace). These data support the hypothesis that Gβγ-dependent mechanisms are involved in the G_i-induced cAMP rebound stimulation (Fig. 21).

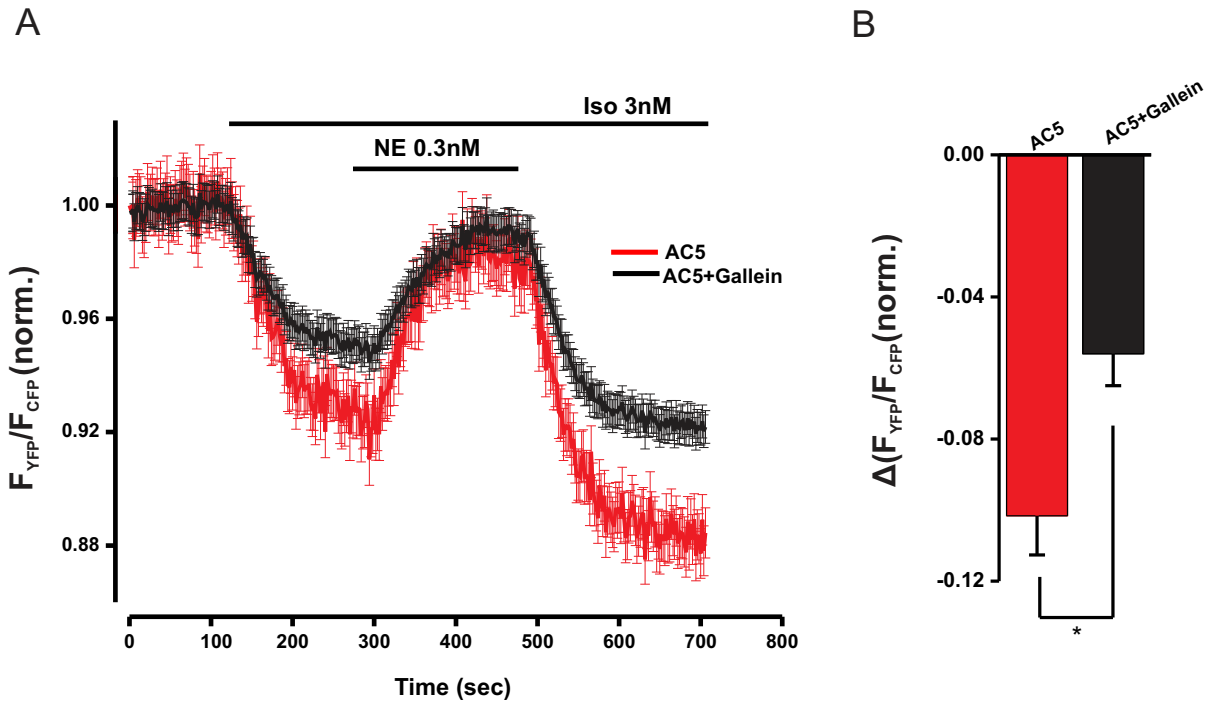

Figure 21: G_i-induced cAMP rebound responses are mediated by Gβγ

A, Epac1-camps based measurement of G_i-induced cAMP rebound stimulation was performed in HEK293T cells transfected with α_{2A}-AR and AC5. Cells were pre-incubated with 1µM of the gallein (Gβγ inhibitor) or vehicle for 40min (n=6-8). The averaged data demonstrate a loss of the cAMP rebound response after withdrawal of NE in cells treated with gallein. **B,** Experimental data derived from **A** were quantified in respect to Iso-mediated alterations of F_{YFP}/F_{CFP} (norm.) after withdrawal of ACh (F_{YFP}/F_{CFP} at time point b - F_{YFP}/F_{CFP} at time point a). Results are plotted as mean±S.E.M.

As a positive control of gallein, its effect on the interaction between PLCβ$_2$ and Gβγ was measured. It was shown previously that Gβ$_1$γ$_2$ activates PLCβ$_2$ (Wang *et al.*, 1999). In order to study the interaction between PLCβ$_2$ and Gβγ, cells were transfected to express PLCβ$_2$-Cerulean, YFP-tagged Gα$_q$, M$_3$-R, Gβ$_1$ and Gγ$_2$. Cells were then stimulated with ACh, resulting in activation of PLCβ$_2$. However, application of gallein significantly abolished the interaction of Gβγ with PLCβ$_2$ (Fig. 22).

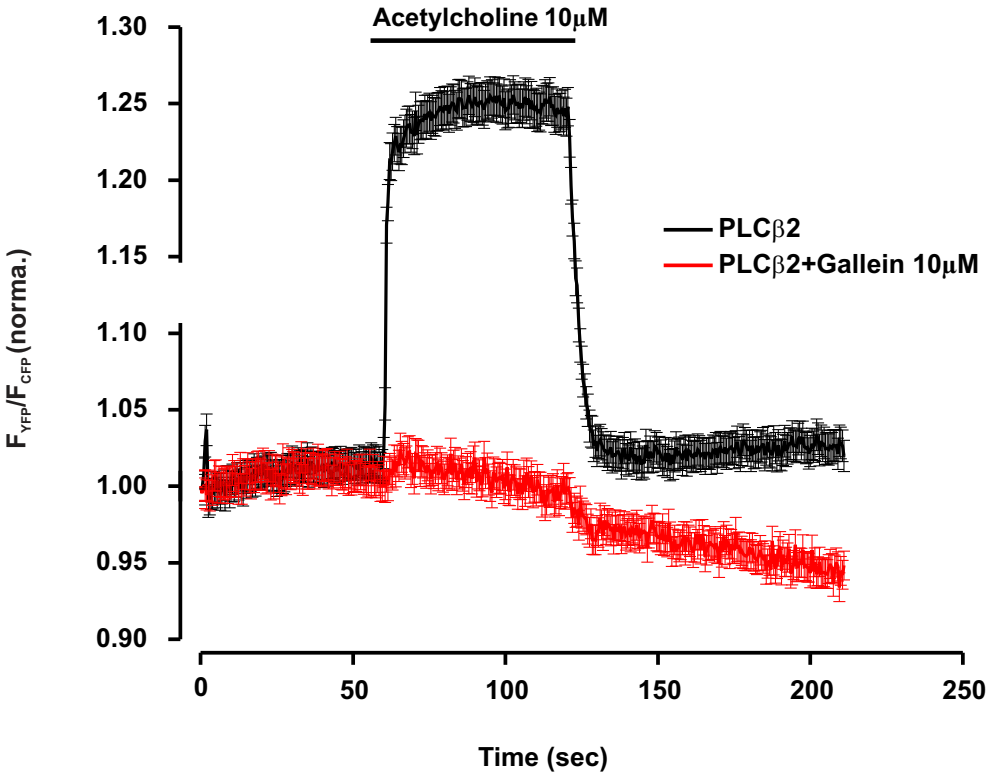

Figure 22: Galleine effectively inhibitied the interaction between PLCβ and Gβγ

Averaged FRET data showing inhibition of the interaction of PLCβ and Gβγ were measured in cells expressing PLCβ$_2$-Cerulean, Gq-YFP, M$_3$-R, Gβ$_1$ and Gγ$_2$. Cells were pre-incubated with 10µM gallein (G$_{βγ}$ inhibitor) or vehicle for 40min (n=7-8). Cells were then stimulated with 10µM ACh leading to effective interaction of PLCβ with Gβγ. However, application of gallein significantly inhibited this interaction. Results are plotted as mean±S.E.M.

In order to ensure that the G$_i$-induced cAMP rebound responses were specifically due to activation of Gβγ signaling, HEK cells were transfected to overexpress Gβγ together with Epac1-camps and AC5. By this treatment, we expected an enhancement of the G$_i$-induced rebound stimulation after termination of NE application. Surprisingly, cells overexpressing Gβγ exhibited inhibitory effects (black trace) on G$_i$-induced cAMP rebound levels compared to the control condition (red trace) indicating that Gβγ was not mediating G$_i$-induced cAMP rebound responses. Indeed, these data are conflicting with the results obtained with gallein. These conflicting results are remained an a open question and potential discrepancy is discussed in the discussion part.

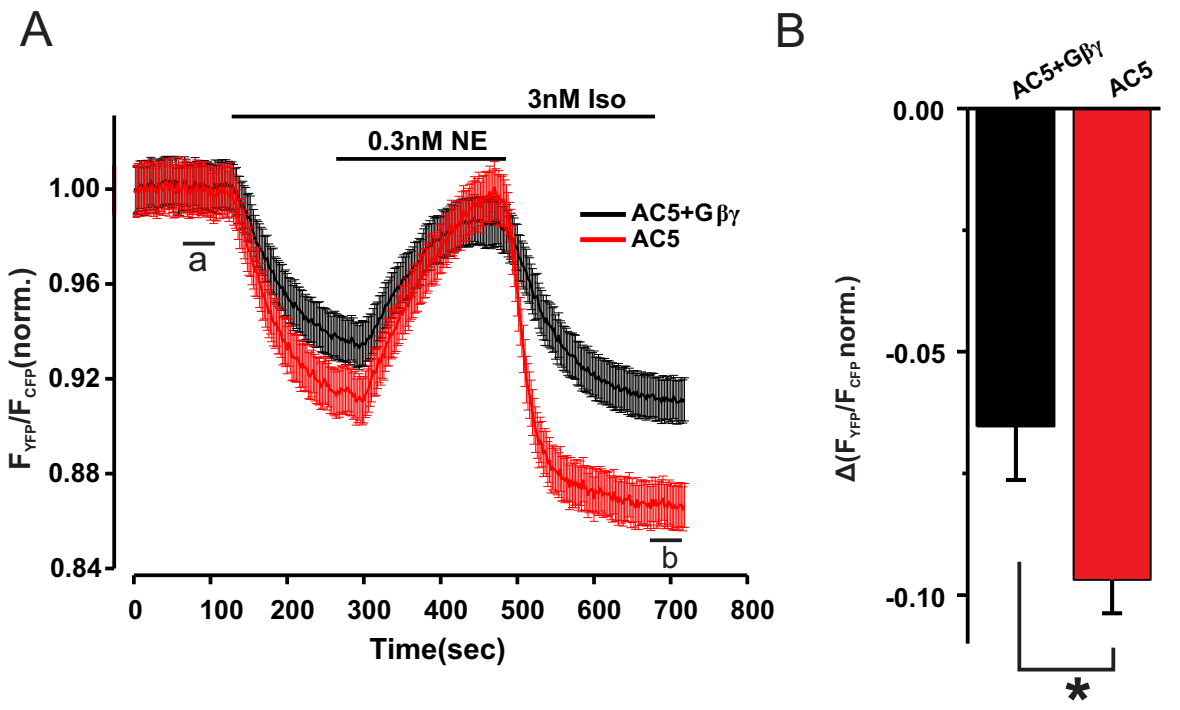

Figure 23: Gβγ overexpression reduced the G_i-induced cAMP rebound stimulation in HEK cells.

A, Averaged FRET recordings showing alterations in cAMP induced by application and subsequent withdrawal of 0.3nM NE were measured in HEK293T cells expressing Epac1-camps, α_{2A}-AR and AC5 with or without overexpression of Gβγ. The FRET signal of Epac1-camps was normalized to initial values. **B,** Iso-evoked alterations in FRET of the experiments shown in *A* were quantified as (F_{YFP}/F_{CFP} norm. at time point *b*) - (F_{YFP}/F_{CFP} norm. at time point *a*). All results are plotted as mean±S.E.M. (n=10-11).

Nevertheless, the experiments involving Gβγ inhibition by gallein suggested that a Gβγ-dependent mechanism is involved in G_i-induced cAMP rebound stimulation. However, it was not clear if this cAMP rebound stimulation was due to Gβγ-mediated activation of AC4. Therefore, we next asked whether Gβγ-mediated activation of AC4 was involved in G_i-induced cAMP rebound stimulation. In order to investigate this, cells were transfected to overexpress Epac1-camps and α_{2A}-AR with or without AC4 and cAMP levels were measured. Intriguingly, cells expressing AC4 showed significantly reduced cAMP rebound stimulation. By comparing cAMP rebound responses in HEK cells that had been transfected with AC4, AC5 or AC6, only cells expressing AC5 and AC6 induced a cAMP rebound stimulation (Fig. 24). Functional expression of AC4 was indicated by a lack of G_i-mediated inhibition, and there was no cAMP rebound stimulation at all. However, the cAMP levels were significantly reduced in AC4-expressing cells suggesting that Gβγ-mediated stimulation

of AC4 is not involved in G_i-induced cAMP rebound stimulation, which argues against the hypothesis that G_i-induced cAMP rebound stimulation is induced by Gβγ-activated AC4.

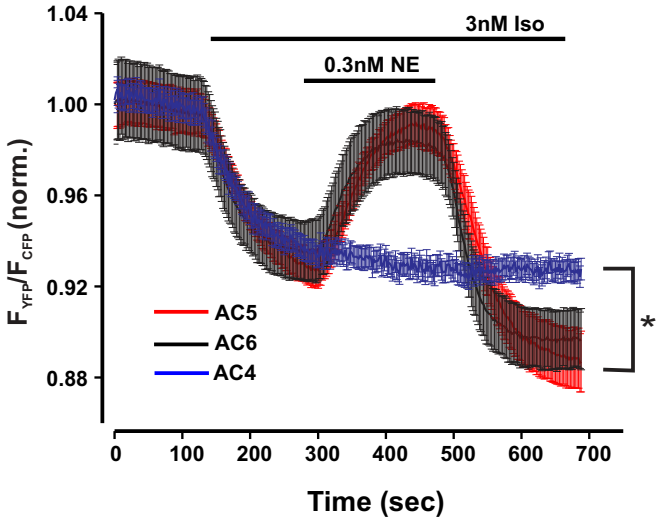

Figure 24: G_i-induced cAMP rebound stimulation is not mediated by Gβγ-activated AC4

A, Averaged FRET recordings showing G_i-induced cAMP rebound stimulation was measured in HEK293T cells overexpressing AC4, AC5 or AC6 together with Epac1-camps and α_2-AR. Cells expressing AC5 (red trace) and AC6 (black line) produced G_i-induced cAMP rebound stimulation but not AC4 expression (blue line). The FRET signal of Epac1-camps was normalized to initial values and quantified. All results are plotted as mean±S.E.M. (n=7-8).

It is not clear why Gβγ-activated AC4 produced lower cAMP levels than AC5-expressing cells but based on the results with gallein, one could conclude that Gβγ-dependent signaling is involved in G_i-induced cAMP rebound stimulation. Furthermore, it has been reported previously that Gβγ can conditionally stimulate AC5 in Sf9 cells (Katada *et al.*, 1987). In order to address the question whether Gβγ-activated AC5 is mediating G_i-induced cAMP rebound stimulation, HEK cells were transfected with a mutant AC5 lacking amino acids 66-137 which constitute the Gβγ binding site (AC5Δ66-137) mutant together with Epac1-camps and measured G_i-induced cAMP levels. The AC5Δ66-137 mutant showed significantly less FRET between AC5 and Gβγ interaction than full-length AC5 (Sadana *et al.*, 2008).

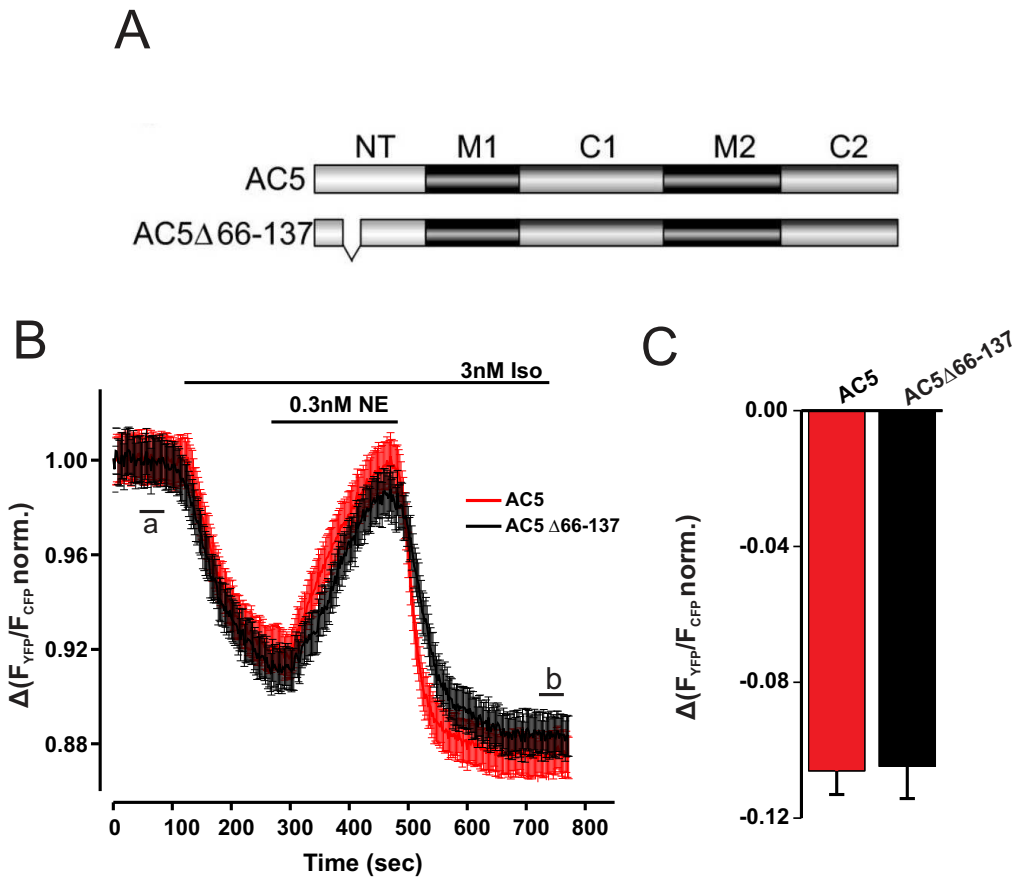

Figure 25: G_i-induced cAMP rebound stimulation is not mediated by Gβγ-induced activation of AC5.

A, Scheme illustrates full length AC5 and the βγ binding site deletion mutant AC5Δ66-137. **B,** Averaged FRET recordings comparing G_i-induced cAMP rebound levels was measured in HEK293T cells expressing AC5Δ66-137 or full length AC5 together with Epac1-camps and α_{2A}-AR which were subsequently subjected to the cAMP rebound stimulation protocol. The FRET signal of Epac1-camps was normalized to initial values. **C,** Experimental data derived from *A* were quantified with respect to Iso-mediated alterations of F_{YFP}/F_{CFP} (norm.) after withdrawal of NE (F_{YFP}/F_{CFP} at time point b - F_{YFP}/F_{CFP} at time point a). All results are plotted as mean±S.E.M. (n=5-6). Fig. A is adapted from Sadana *et al*., 2011.

Cells expressing full length AC5 produced cAMP rebound stimulation after termination of NE (Fig. 25 red trace). However, cells expressing the AC5Δ66-137 mutant did not show attenuated G_i-induced cAMP rebound stimulation after termination of NE (Fig. 25 black trace). This suggests that the cAMP rebound stimulation is not mediated by direct Gβγ activation of AC5. These results argue against the hypothesis that a Gβγ-dependent AC mechanism is involved in G_i-induced cAMP rebound stimulation. Therefore, it can be concluded that Gβγ-facilitation of $G\alpha_s$-stimulated AC4 is not a primary mechanism for G_i-induced cAMP rebound responses despite the fact that Gβγ inhibition studies (Fig. 21)

revealed that a Gβγ-mediated signaling mechanism is involved in G_i-induced cAMP rebound stimulation. This G_i-induced cAMP rebound stimulation might be due to either an indirect Gβγ stimulation of adenylyl cyclases or an activation of different Gβγ-dependent mechanisms. For example, Gβγ-dependent stimulation of phospholipase C activity and subsequent activation of protein kinase C leads to activation of AC5/6 and thereby increases cAMP levels (Calpham & Neer, 1997). In addition to PKC, Gβγ also directly activates phosphoinositide-3 (PI3) kinase (Viard *et al.*, 1999). Indeed, our previous gallein data also suggested that Gβγ-dependent PI3 kinase might be involved in cAMP rebound stimulation (Fig. 21) (Ukhanov *et al.*, 2011). Therefore, the next aim was to identify which signaling cascade is responsible for G_i-induced cAMP rebound effects.

4.8 Effects of PKA on G_i-induced cAMP rebound responses in HEK cells.

It is known that cAMP-dependent protein kinase A (PKA) is activated by cAMP and regulates many physiological responses (Tasken *et al.*, 2004). It was shown previously that a selective PKA inhibitor (H-89) diminished G_i-induced cAMP rebound stimulation via a cAMP-dependent PKA mechanism in atrial myocytes (Wang & Lipsius, 1995). Therefore, we decided to investigate whether PKA has any effect on G_i-induced cAMP rebound responses. In order to check PKA involvement, Epac1-camps, AC5, and α_{2A}-AR expressing cells were pre-incubated with or without a specific PKA inhibitor (KT5720) for 30 min and the G_i-induced cAMP rebound responses were compared with control conditions. It has been shown previously that PKA inhibitor H-89 significantly attenuated β_2-AR mediated cAMP levels (Penn *et al.*, 1999), therefore we chose a different PKA inhibitor (KT5720) to study PKA effects on G_i-induced cAMP rebound stimulation. Application of 1µM KT5720 did not affect G_i-induced cAMP rebound stimulation (Fig. 26 black trace). As a control, cells that had not been incubated with KT5720 produced cAMP rebound stimulation (Fig. 26 gray trace). This result argues against a role of PKA on G_i-induced cAMP rebound stimulation. From this observation, it can be concluded that G_i-induced rebound stimulation is not specifically mediated by PKA.

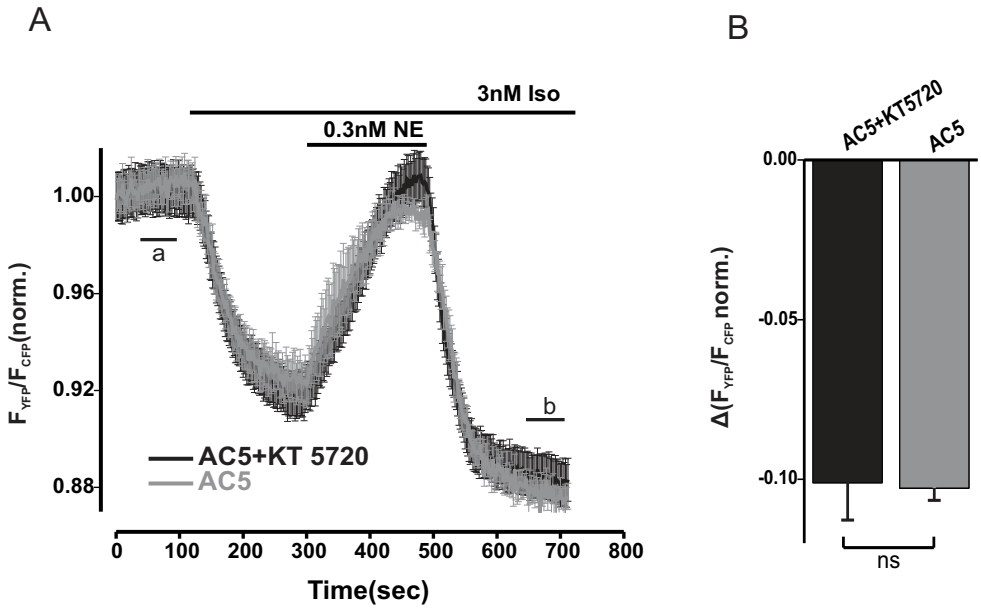

Figure 26: Protein kinase A inhibition did not attenuate G_i-induced cAMP rebound stimulation.

A, Averaged FRET recordings showing alterations in cAMP induced by application and subsequent withdrawal of 0.3nM NE was measured in HEK cells transfected with Epac1-camps, α_{2A}-AR and AC5 (n=6-7). The FRET signal of Epac1-camps was normalized to initial values. Cells were pre-incubated with 1µM of the PKA-specific inhibitor KT5720 or vehicle for 30min prior to the experiment (n=6-8). **B),** Experimental data derived from ***A*** were quantified with respect to Iso-mediated alterations of F_{YFP}/F_{CFP} (norm.) after withdrawal of NE (F_{YFP}/F_{CFP} at time point b - F_{YFP}/F_{CFP} at time point a). Results are plotted as mean±S.E.M.

To show that KT5720 indeed inhibited PKA, the PKA-specific FRET biosensor AKAR4 was used. AKAR4 consist of a phosphopeptide binding domain (FHA1), a consensus region of PKA substrates and sandwiched with donor fluorophore (cerulean) and an acceptor fluorophore (cp venus). When PKA is inactive, the donor and acceptor fluorophores are far apart, resulting in low FRET. Upon phosphorylation by PKA, the substrate region binds the FHA1, bringing the donor and acceptor fluorophores together and resulting in high FRET (Depry *et al.*, 2011). Cells were stimulated with 1µM Iso which leads to activation of PKA. However, the application of 1µM of the PKA inhibitor KT5720 significantly inhibited PKA activation (Fig. 27). Under basal conditions, the AKAR4 sensor-expressing cells displayed higher PKA activity. Therefore, in order to avoid saturation of the sensor, cells were pre-incubated with a lower concentration (50nM) of PKA inhibitor prior to the experiment. In addition, we next tested whether the cAMP rebound response was translated into PKA activity.

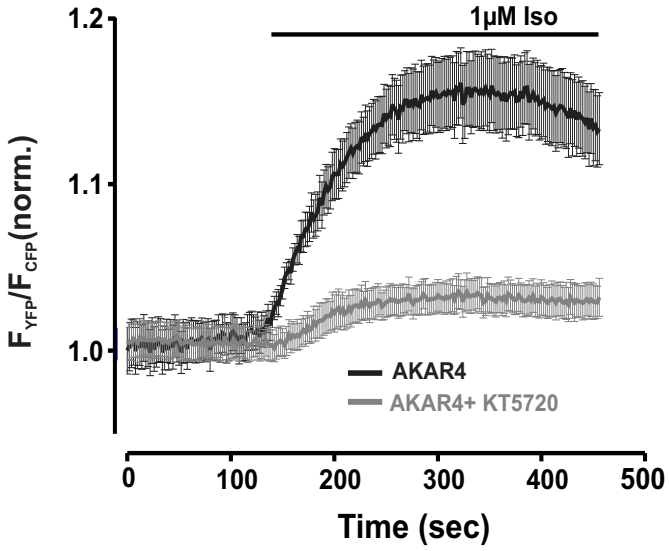

Figure 27: KT5720 effectively inhibited PKA activation.

HEK293T cells were transfected with 1µg of PKA-specific FRET-based sensor AKAR4. To avoid saturation of the sensor, cells were pre incubated with a low (submaximal) concentration of KT5720 (50nM) prior to the experiment. Cells were then stimulated with 1µM of Iso leading to activation of PKA. Application of 1µM KT5720 (PKA inhibitor) attenuated FRET increases (n=5). All results are plotted as mean±S.E.M

To measure PKA activity, the PKA specific FRET biosensor AKAR4 was used. In order to measure PKA activity, cells were transfected to express AKAR4, AC5, and α_{2A}-AR. As mentioned above, to avoid saturation of sensor, cells were pre-incubated with a lower concentration of KT5720 (50nM) which was present throughout the whole experiment. Cells expressing AC5 produced a PKA rebound stimulation upon washout of the α_{2A}-AR agonist NE (black trace) (Fig. 28). Furthermore, the G_i-induced PKA rebound stimulation was significantly diminished in cells expressing empty vector (pcDNA3) instead of AC5 (gray trace) (Fig. 28)

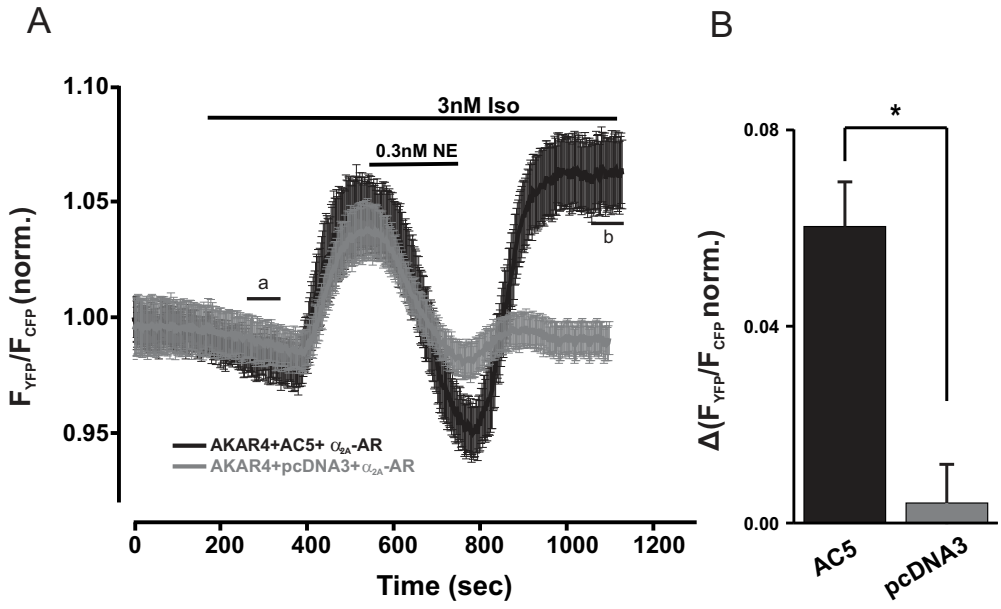

Figure 28: G_i activation induced PKA rebound responses.

A, Averaged FRET data are showing G_i-induced alterations in PKA activity induced by application and subsequent withdrawal of 0.3nM NE was measured in HEK cells transfected with PKA-specific sensor (AKAR4) and α_{2A}-AR with or without AC5 (n=6-7). Rebound effects occurred in the cells which had been transfected with AC5. Cells not transfected with AC5 not produced rebound response. The FRET signal of AKAR4 was normalized to initial values. **B**, Quantification of Iso-evoked alterations in cAMP between indicated time points (b-a) of the experiment shown in *A*. All results are plotted as mean±S.E.M

In addition, G_i-induced cAMP rebound levels were also measured by using another FRET-based cAMP bio-sensor, based on the hyperpolarization-activated cyclic nucleotide-gated channel (HCN) (HCN2-camps). Cells were transfected with AC5 and α_{2A}-AR and either Epac1-camps or HCN2-camps. As expected, cells expressing Epac1-camps produced cAMP rebound stimulation after termination of NE (red trace), whereas cells expressing HCN2-camps also produced similar cAMP rebound stimulation upon NE washout (black trace) (Fig. 29). There was no difference between cells expressing HCN2-camps or Epac1-camps (Fig. 29), indicating that G_i-induced cAMP rebound responses are not specific for the Epac-based cAMP sensor.

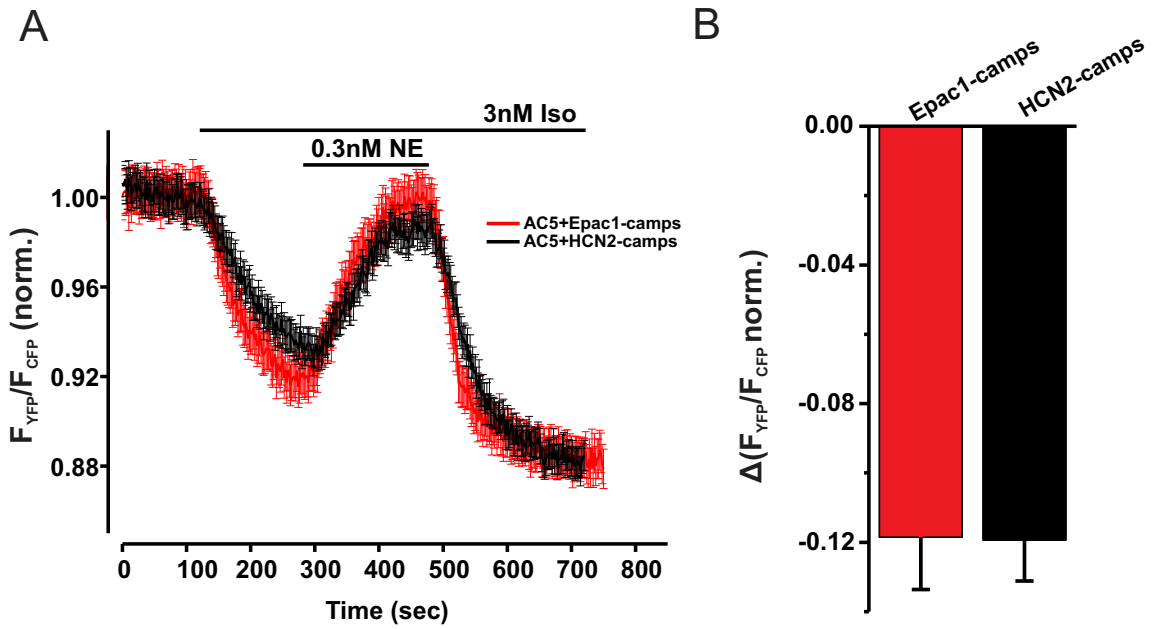

Figure 29: G_i-induced a cAMP rebound stimulation in HCN2-camps expressed HEK cells.

HEK293T cells were transfected with AC5, α_{2A}-AR and either HCN2-camps or Epac1-camps. **A**, Averaged FRET data comparing G_i-induced cAMP levels between HCN2-camps and Epac1-camps-expressing cells. **B,** Iso-evoked alterations in cAMP were quantified between indicated time points (b-a) of the experiments shown in *A*. Results are plotted as mean±S.E.M.

4.9. Effects of protein kinases on G_i-induced cAMP rebound stimulation in HEK cells

As mentioned earlier, signaling via inhibitory G proteins leads to regulation of several different pathways, most of which are mediated via Gβγ subunits including PKC, PKG and PI3K (Calpharm & Neer *et al*., 1997; Viard *et al*., 1999). Therefore, we first asked whether major protein kinases (including PKC, PLC, and PKG) are involved in G_i-induced cAMP rebound responses. In order to test the involvement of protein kinases, cells were transfected to express Epac1-camps, AC5, and α_{2A}-AR. Cells were then pre-incubated with or without the broad-spectrum protein kinase inhibitor staurosporine (which inhibits many kinases including PKA, PKC and PKG) for 30min and G_i-induced cAMP rebound responses were compared with control conditions. Treatment with 1µM staurosporine did not show any impact on G_i-induced cAMP rebound stimulation (black trace) compared to the control condition (gray trace) (Fig. 30). There was no difference in G_i-induced cAMP rebound stimulation between staurosporine-treated and control cells (Fig. 30). These results are consistent with earlier findings that PKC inhibition does not affect G_i-induced rebound stimulation of L-type Ca^{2+} currents in ventricular myocytes (Belevych *et al*., 2001).

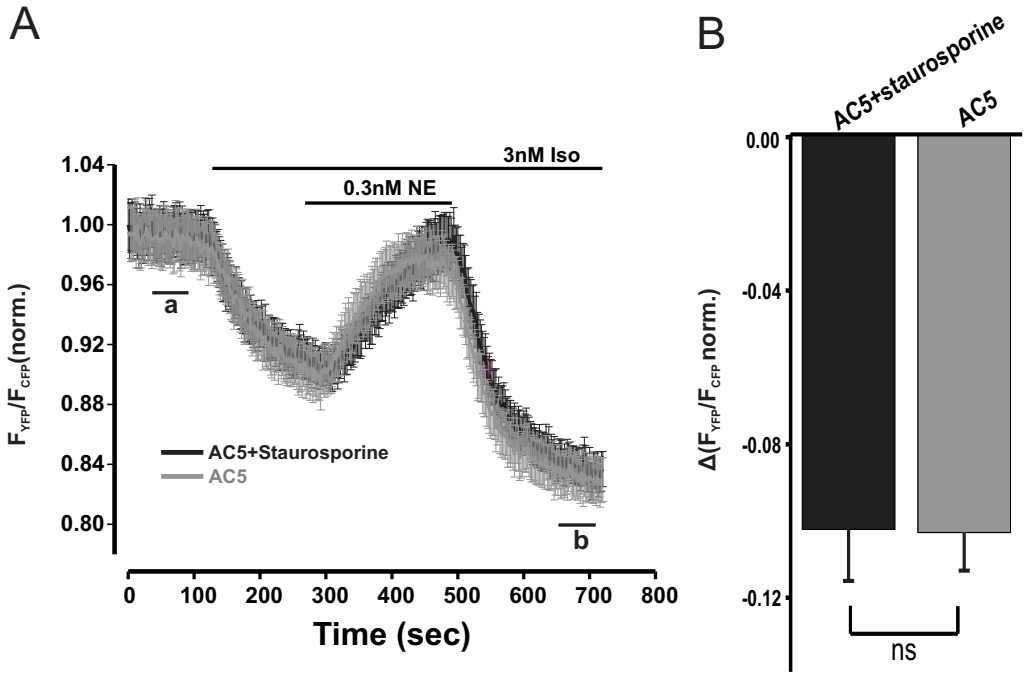

Figure 30: Staurosporine did not affect G_i-induced cAMP rebound stimulation.

HEK293T cells were transfected with α_{2A}-AR, Epac1-camps and AC5. **A,** Averaged FRET recordings show G_i-induced cAMP rebound stimulation induced by application and subsequent withdrawal of 0.3nM NE. Cells were pre-incubated with 1µM of the non-selective protein kinase inhibitor staurosporine or vehicle (n=8-10) for 30min prior to the experiment. **B,** Iso-evoked alterations in FRET subsequent to withdrawal of NE were quantified at indicated time points (b-a) of the experiments shown in *A.* Results are plotted as mean±S.E.M.

To show that staurosporine treatment was effective, it was tested for its ability to inhibit PKC by using the PKC-specific FRET biosensor Eevee-PKC. Eevee-PKC consists of a phosphopeptide binding domain (FHA1), a consensus region of PKC substrates and sandwiched with donor fluorophore (YPet) and acceptor fluorophore (EYFP). When PKC is inactive, the donor and acceptor fluorophores are far apart, resulting in low FRET. Upon phosphorylation by PKC, the substrate region binds the phosphopeptide binding domain FHA1, bringing the donor and acceptor fluorophores together and resulting in high FRET (Komatsu *et al*., 2011). HEK293 cells were transfected with a plasmid encoding the Eevee-PKC sensor. Cells were stimulated by applying 10µM of the PKC-specific activator TPA (or PMA) resulting in activation of PKC. However, 1µM staurosporine (PKC inhibitor) significantly inhibited TPA-mediated PKC activation (Fig. 31). From these experiments, it can be concluded that G_i-induced cAMP rebound stimulation is not mediated by PKA, PKC, PKG and other staurosporine sensitive kinases.

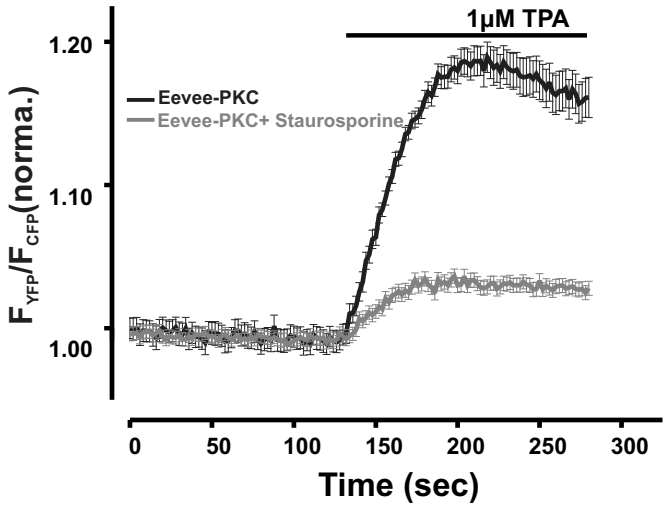

Figure 31: Staurosporine effectively inhibitied PKC activity.

Averaged FRET data showing PKC inhibition were measured in cells expressing the PKC-based FRET-sensor Eevee-PKC. Cells were stimulated with 1µM TPA (PKC specific activator) leading to activation of PKC. However, pre-treatment with 1µM staurosporine (PKC inhibitor) attenuated the TPA response (n=5). Results are plotted as mean±S.E.M.

4.10. Effects of PI3K on G_i-induced cAMP rebound stimulation in HEK cells.

It is known that class 1B PI3Ks (also known as PI3Kγ) are activated via PTX-sensitive $G\alpha_i$-coupled GPCRs. This activation of PI3Kγ is linked to a direct association of its catalytic domain with βγ subunits of inhibitory G proteins (G_i) (Stoyanov *et al*., 1995; Viard *et al*., 1999). However, our previous results also suggested that βγ dependent PI3K signaling is involved in cAMP rebound stimulation (Fig. 21). Therefore, it was decided to study the involvement of PI3K on G_i-induced cAMP rebound stimulation. In order to investigate the involvement of PI3K on cAMP rebound effects, cells expressing Epac1-camps, α_{2A}-AR and AC5 were pre-incubated with 1µM of the PI3K-specific inhibitor wortmannin, and G_i-induced cAMP rebound responses were compared with control conditions. Notably, application of 1µM wortmannin significantly reduced G_i-induced cAMP rebound responses (red traces) compared to the control conditions (black trace) (Fig. 32).

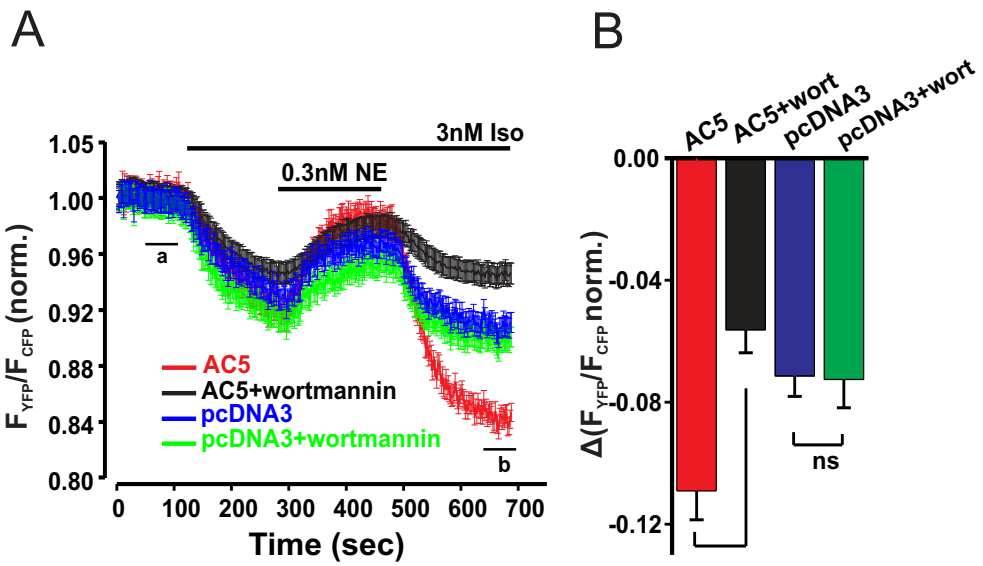

Figure 32: AC5-dependent G_i-induced cAMP rebound stimulation in HEK cells requires PI3K activation.

A, Epac1-camps based measurements of cAMP rebound responses were performed in cells transfected with α_{2A}-AR with or without AC5 as indicated. Cells were either pre-incubated with 1µM of the PI3K-specific inhibitor wortmannin or vehicle for 30min (n=10-11). Averaged data demonstrate a loss of the cAMP rebound response after withdrawal of NE due to wortmannin in cells expressing AC5. **B,** Iso-evoked alterations in F_{YFP}/F_{CFP} (norm.) were quantified and compared for the indicated conditions (b-a). Results are plotted as mean±S.E.M.

The reduction of FRET decreased from 11.2±1.2% to 5.6±1.5%. Based on *in vitro* cAMP calibrations of Epac1-camps, it was estimated that wortmannin reduced the cAMP concentrations from 4.1µM to levels of about 0.7µM. Interestingly, exposure to wortmannin significantly reduced G_i-induced cAMP rebound stimulation only in cells expressing AC5. In cells expressing empty vector (pcDNA3, green trace) instead of AC5 wortmannin did not show any effect on cAMP rebound stimulation compared to the control condition (blue trace) (Fig. 32).

Since AC6-expressing cells also produced cAMP rebound stimulation, we asked whether wortmannin had any effect on cAMP rebound stimulation. In order to investigate wortmannin effects on AC6, cells were transfected with Epac1-camps, α_{2A}-AR and with or without AC6 and tested for G_i-induced regulation of cAMP levels.

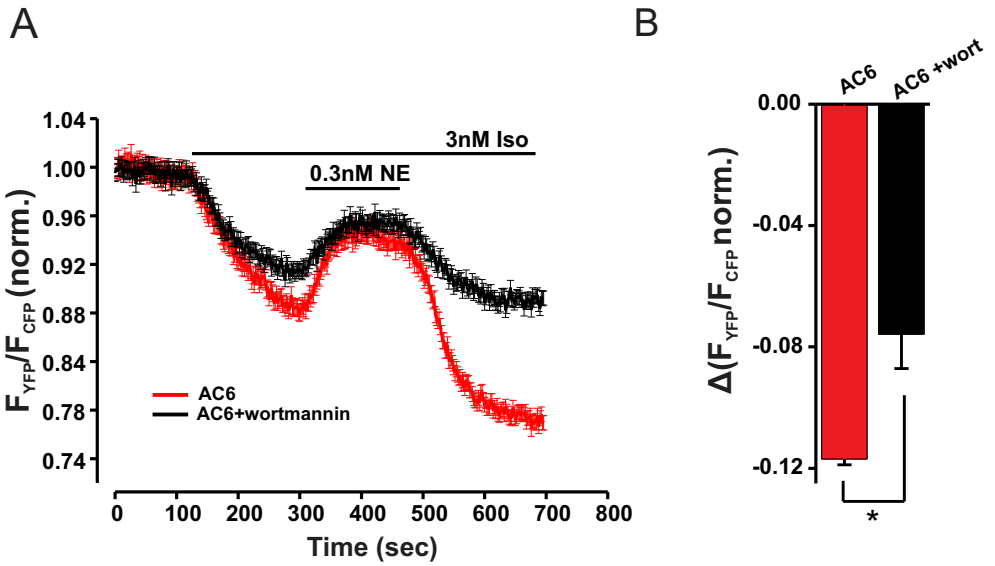

Figure 33: AC6-dependent G_i-induced cAMP rebound stimulation in HEK cells requires PI3K activation.

A, Epac1-camps-based measurements of cAMP rebound stimulation was performed in cells transfected with α_{2A}-AR with or without AC6 as indicated. Cells were either pre-incubated with 1µM of the PI3K-specific inhibitor wortmannin or vehicle for 30min (n=6-7). Averaged data demonstrate a loss of cAMP rebound response after withdrawal of NE due to wortmannin treatment. **B**, Iso-evoked alterations in FRET subsequent to withdrawal of NE were quantified at indicated time points (b-a) of the experiments shown in *A*. Results are plotted as mean±S.E.M.

In order to test for wortmannin effects on AC6, cells were pre-incubated with wortmannin for 30min and G_i-induced cAMP rebound responses were compared with control conditions. Notably, application of 1µM wortmannin significantly diminished G_i-induced cAMP rebound stimulation (black trace) compared to control conditions (red trace) (Fig. 33). Reduction of FRET decreased from 11.8±0.92% to 0.72±1.3%. Based on *in vitro* cAMP calibrations of Epac1-camps, it was estimated that wortmannin reduced the cAMP concentrations from 4.3µM to 0.74µM. These data suggest that a Gβγ-dependent PI3K pathway is involved in G_i-induced cAMP rebound stimulation of AC5/6-expressing cells.

An interesting observation shown in Fig. 32 and 33 was that exposure to wortmannin had a tendency to lower β_2-AR mediated rise in cAMP levels in cells expressing AC5/6. However, wortmannin did not show any effect on β_2-AR mediated rice in cAMP levels in cells expressing empty vector (pcDNA3) (Fig. 31). These data indicate that PI3Ks regulate ACs either directly or indirectly. To further confirm the effects of wortmannin on β_2-AR mediated increase in cAMP levels, cells were transfected to express AC4, AC5 or AC6 together with

Epac1-camps. Exposure to 1µM wortmannin significantly lowered β_2-AR mediated increase in cAMP levels only in cells expressing AC5 and AC6 (Fig. 34 B-C). Indeed, wortmannin did not reduce β_2-AR mediated increase in cAMP levels in cells expressing AC4; it rather showed a tendency to higher cAMP production in response to the β_2-AR agonist Iso (Fig. 34 A). These results further confirm that PI3K is regulating ACs. However, it is not clear whether PI3 kinases are directly or indirectly regulating ACs.

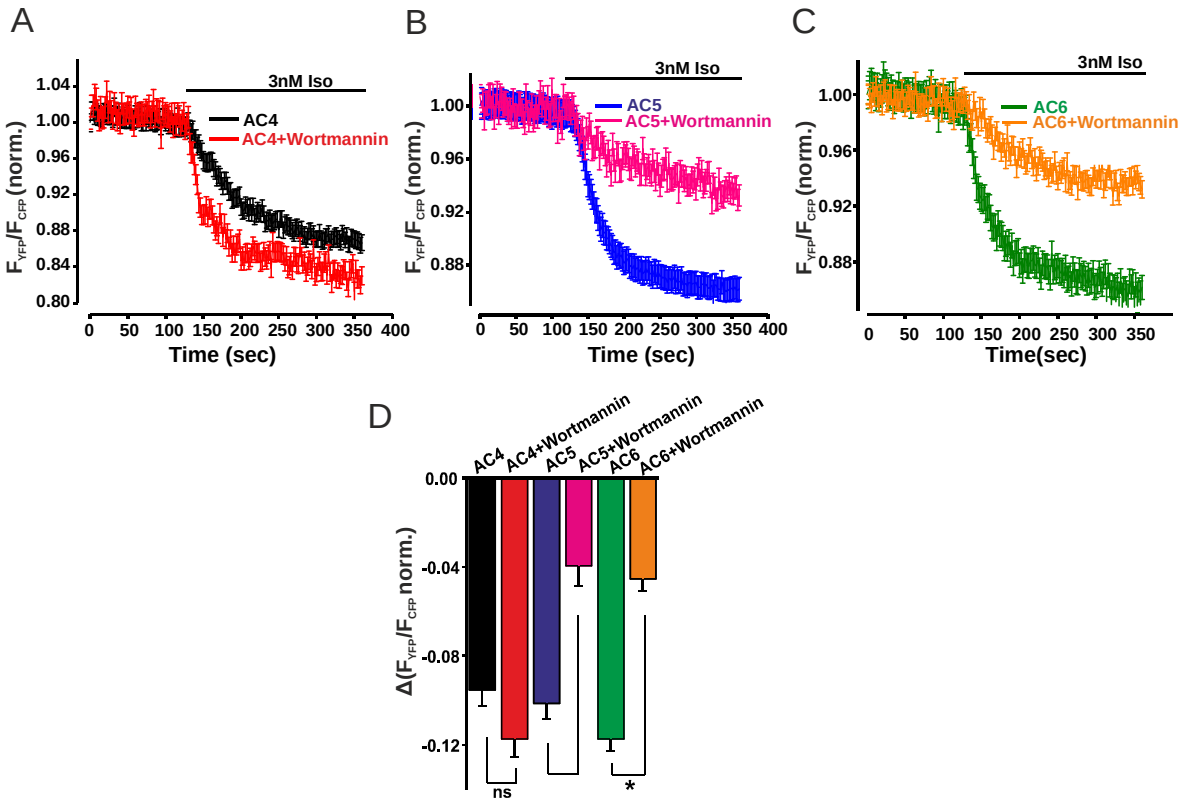

Figure 34: Activation of AC5 and AC6 is sensitive to wortmannin.

A, Epac1-camps expressing cells were subjected to FRET-based recording of $G\alpha_s$-induced cAMP levels illustrating the effect of 3nM Iso on cAMP levels. Cells were transfected with AC4, AC5 or AC6 as indicated and either treated with 1µM wortmannin or vehicle (n=7). **B**, Iso-evoked alterations in FRET induced by application of Iso were quantified as shown in *A*. Results are plotted as mean±S.E.M.

As a positive control for wortmannin, PI3K inhibition was tested by using a PIP_3 translocation sensor (AKT-PH-YFP). This sensor specifically binds PIP_3 at the plasma membrane through its PH domain. Wortmannin should reduce the cellular PIP_3 content, thereby resulting in cytoplasmic localization of the AKT-PH-YFP sensor.

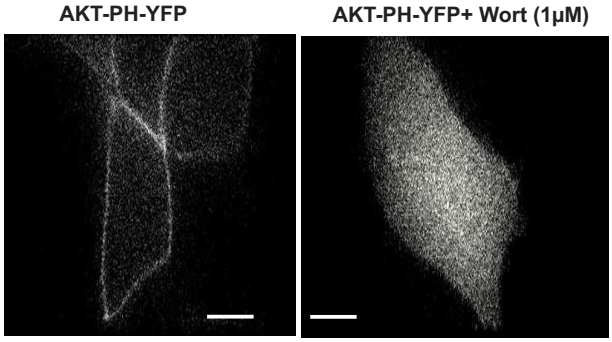

Figure 35: AKT-PH-YFP sensor displayed high basal PIP_3 levels in HEK293T cells.

Representative confocal images are AKT-PH-YFP transfected HEK293T cells. Cells were imaged before and after pre-treatement of 1µM wortmannin. In cells treated with vehicle the sensor was already located at the plasma membrane indicating high basal PIP_3 levels. Cells were relocated to the cytosol in treatement with wortmannin. Scale bars 10µm.

In order to further check for inhibition of receptor-mediated PI3K activity, cells were transfected to express AKT-PH-YFP. Cells were then pre-incubated with a lower concentration of wortmannin (50nM) in order to relocate AKT-PH-YFP to the cytosol (Fig. 36 A); otherwise the sensor was already localized to the membrane indicating high basal PIP_3 levels (Fig. 35). Cells were then stimulated with platelet-derived growth factor (PDGFBB) which is well known to activate PI3K in many cells including HEK293T cells (Gao *et al*., 2011) resulting in Akt translocation (translocation from the cytosol to the plasma membrane (Fig. 36A)) as reflected by decreasing the ratio of cytosolic AKT-PH-YFP relative to total cell fluorescence, which indicates increasing PIP_3 levels (black trace) (Fig. 36B). However, application of 1µM wortmannin completely prevented Akt translocation to the plasma membrane (gray trace) (Fig 36B).

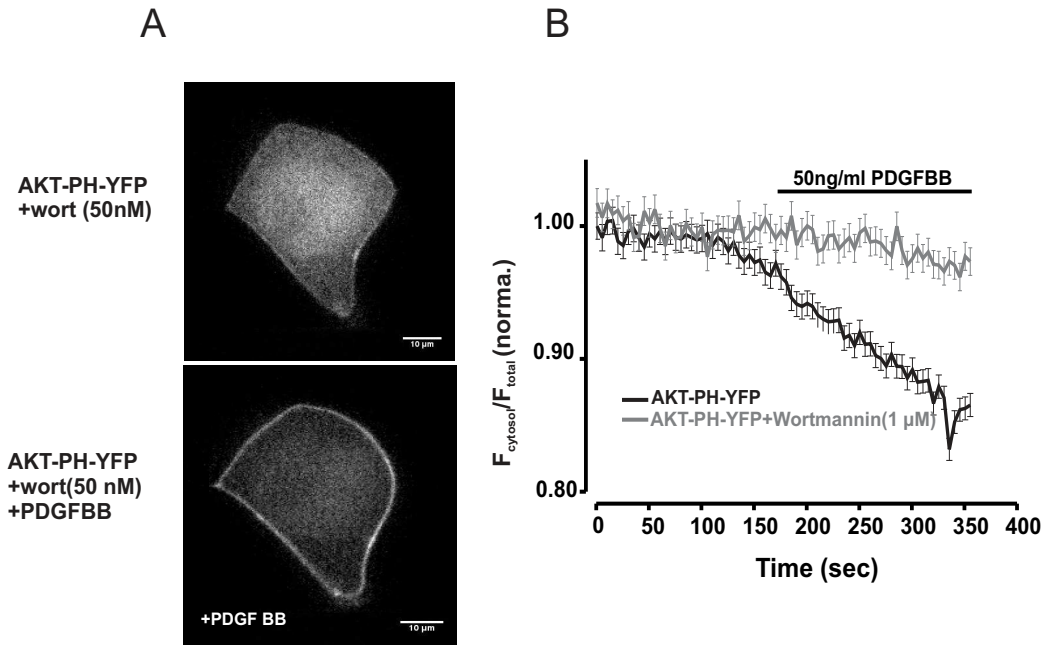

Figure 36: Wortmannin effectively inhibitied the PI3K activation.

HEK293T cells were expressed with PIP_3-dependent translocation sensor (AKT-PH-YFP) and then cells were incubated with a low concentration of wortmannin (50nM) in order to allow for partial translocation of AKT-PH-YFP. **A,** Representative confocal images of AKT-PH-YFP localization in HEK293T cells prior and after exposure to 50ng/ml of the PI3K activator PDGFBB **B,** Averaged data (n=14-16) showing the time course of membrane translocation of AKT-PH-YFP in response to PDGF-R stimulation and inhibition in response to 1µM wortmannin by plotting the fractional cytosolic YFP-staining. Due to movements of the cell during the experiment it was more reliable to measure cytosolic versus whole cell fluorescence compared to membrane staining. Scale bars 10µm.

4.11. Effects of PIP_3 on G_i-induced cAMP rebound stimulation in HEK cells.

Activation of PI3K leads to the generation of $PI(3,4,5)P_3$ and $PI(3,4)P_2$. Therefore, we next asked which phosphoinositol species is involved in PI3K-dependent cAMP rebound responses. In order to study this, cells were transfected to overexpress the PIP_3-specific phosphatase PTEN, which is known to dephosphorylate PIP_3, thereby decreasing PIP_3 levels (Maehama *et al.*, 1998). Intriguingly, overexpression of PTEN significantly attenuated G_i-induced cAMP rebound levels as reflected by a decrease in FRET ratio in cells expressing AC5. The FRET ratio was reduced by 12.1±0.93% to 7.8±1.4%. Based on Epac-camps1 calibration curves it was estimated that the cAMP concentrations after NE withdrawal are reduced from 6.0µM to 1.0µM (Fig. 37). Similar to wortmannin, cells overexpressing PTEN also show lower β_2-AR mediated increases in cAMP levels. These results indicate that the generation of PIP_3 is required for cAMP rebound responses.

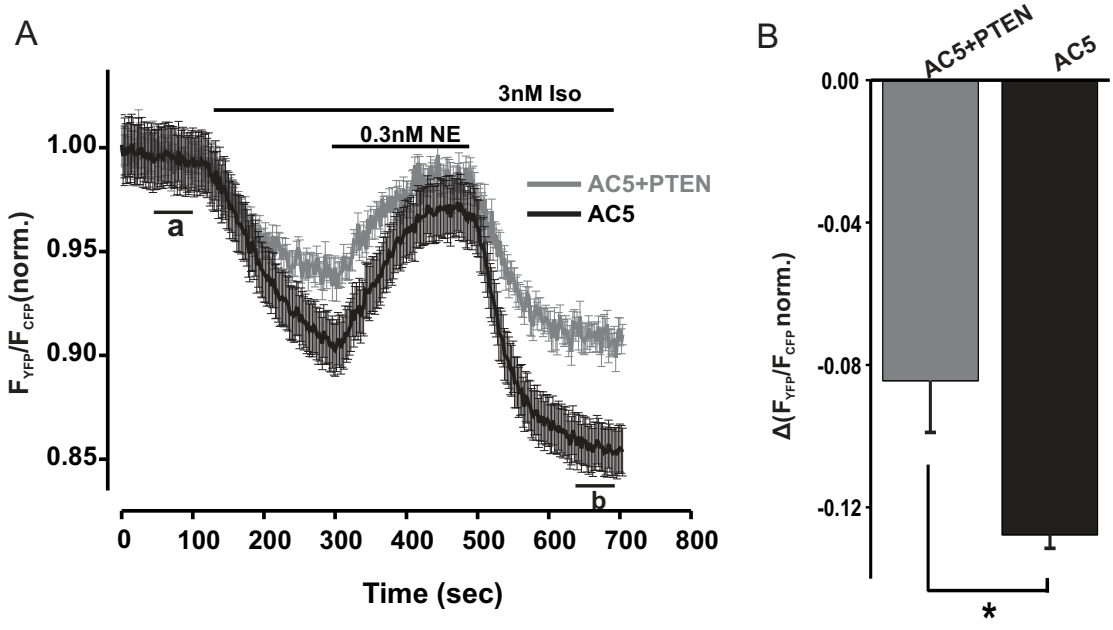

Figure 37: Overexpression of PTEN reduced G_i-induced cAMP rebound stimulation in HEK cells.

A, Averaged FRET data showing G_i-mediated alterations of cAMP responses induced by application and subsequent withdrawal of 0.3nM NE were measured in cells expressing Epac1-camps, AC5, α_{2A}-AR and PTEN (grey) or empty vector (black). The data show a loss of the cAMP rebound response after withdrawal of NE due to PTEN overexpression (n=7-8). **B**, Iso-evoked alterations in FRET subsequent to withdrawal of NE were quantified at indicated time points (b-a) of the experiments shown in *A*. Results are plotted as mean±S.E.M.

4.12. Effects of PI(3,4)P_2 on G_i-induced cAMP rebound stimulation in HEK cells.

As mentioned above, activation of PI3K also generates PI(3,4)P_2. A major pathway leading to PI(3,4)P_2 is the dephosphorylation of PI(3,4,5)P_3 by the 5-phosphatase SHIP2 (Damen *et al*., 1996). In order to test the involvement of PI(3,4)P_2, cells expressing Epac1-camps, AC5 and α_{2A}-AR were pre-incubated with or without the SHIP2 inhibitor AS 1949490 and G_i-induced cAMP rebound responses were compared. Application of 1µM AS 1949490 did not show any affect on G_i-induced cAMP rebound stimulation, which indicates that PI(3,4)P_2 signaling is not involved in PI3K-dependent cAMP rebound responses (Fig. 38). Therefore, it is concluded that G_i-induced cAMP rebound responses are likely dependent on PIP_3.

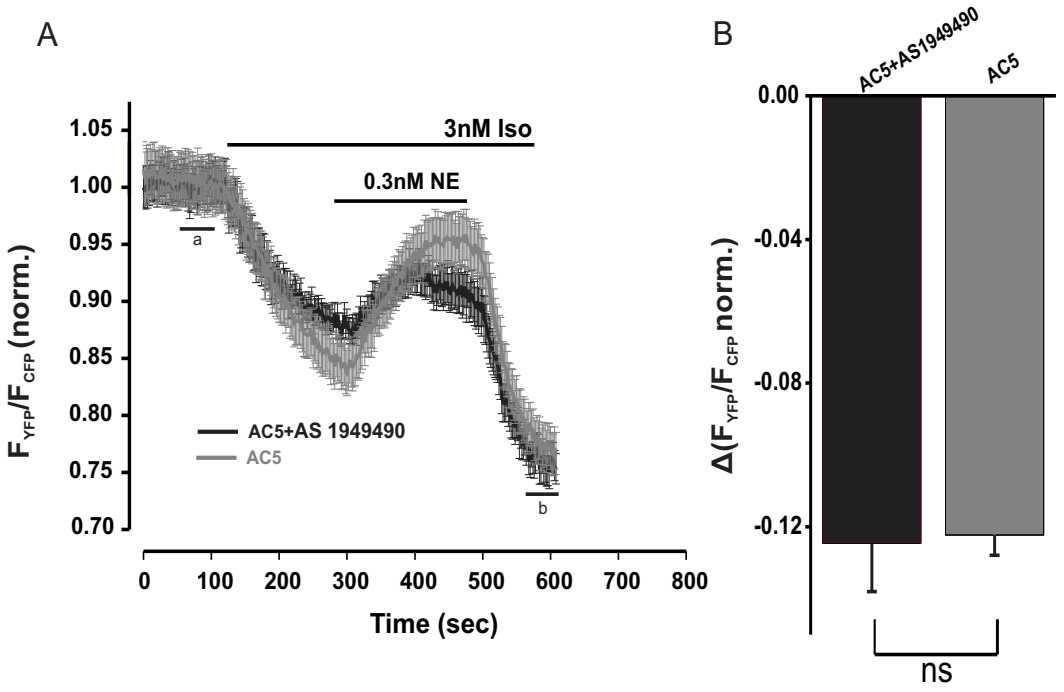

Figure 38: SHIP2 inhibition did not attenuate G_i-induced cAMP rebound stimulation in HEK cells.

A, Averaged FRET data showing G_i-mediated alterations of cAMP rebound responses induced by application and subsequent withdrawal of 0.3nM NE was measured in cells expressing Epac1-camps, AC5 and α_{2A}-AR. Cells were pre-incubated with AS 1949490 (SHIP2 inhibitor) or vehicle (n=5-6). **B,** Iso-evoked FRET changes were quantified as alterations in F_{YFP}/F_{CFP} (norm.) and plotted for the indicated conditions (b-a). Results are plotted as means±S.E.M.

4.13. Effects of AKT on G_i-induced cAMP rebound responses in HEK cells.

Furthermore, it was tested whether important downstream effectors of PIP_3 are involved in the generation of cAMP rebound responses. It is known that activation of PIP_3 further stimulates downstream effectors such as PDK1 and Akt (Stoke *et al.*, 1997; Klippel *et al.*, 1997). Therefore, we asked whether PIP_3 downstream signaling is involved in the PI3K-dependent cAMP rebound stimulation. In order to investigate this, the influence of Akt on G_i-induced cAMP rebound stimulation was tested. To measure Akt effects, cells expressing Epac-1camps, AC5 and α_{2A}-AR were pre-incubated with the Akt-specific inhibitor SH-5, and G_i-induced cAMP rebound responses were compared with control conditions. Application of 10µM of SH-5 did not show any effect on G_i-induced cAMP rebound stimulation (gray trace) compared to control conditions (black trace) (Fig. 39). This result indicates that Akt and its downstream signaling are not involved in PI3K-dependent cAMP rebound responses.

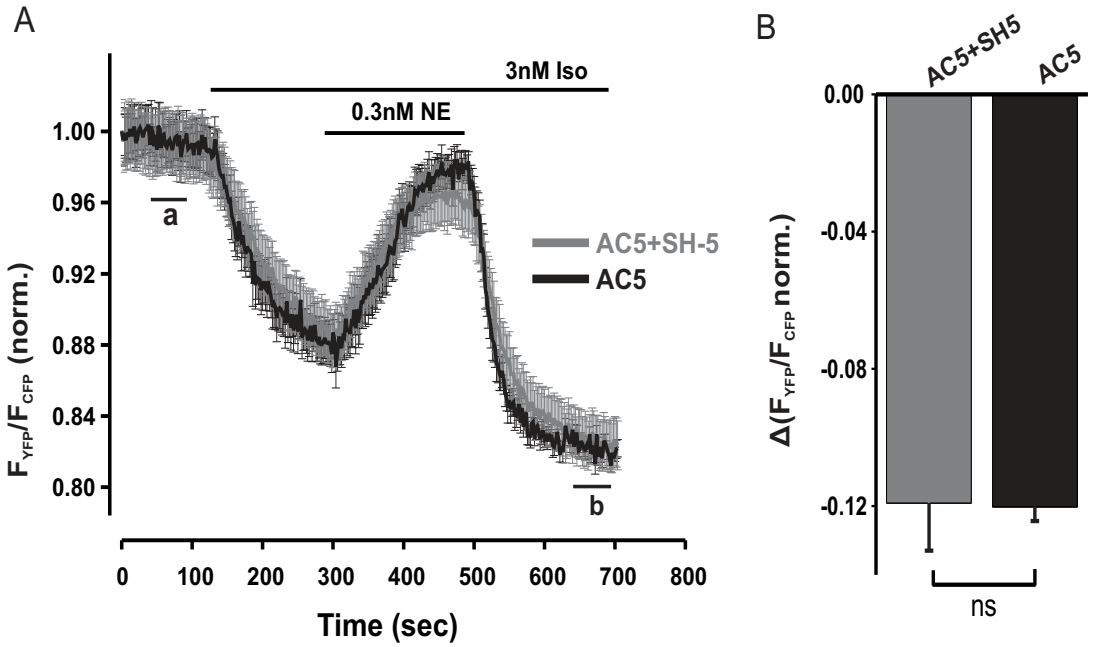

Figure 39: Akt inhibition did not affect G_i-induced cAMP rebound stimulation in HEK cells.

A, Averaged FRET data showing G_i-mediated alterations of cAMP rebound responses induced by application and subsequent withdrawal of 0.3nM NE was measured in cells expressing Epac1-camps, AC5 and α_{2A}-AR. Cells were pre-incubated with SH-5 or vehicle (n=6-7). **B,** Experimental data derived from *A* were quantified with respect to Iso-mediated alterations of F_{YFP}/F_{CFP} (norm.) after withdrawal of NE (F_{YFP}/F_{CFP} at time point b - F_{YFP}/F_{CFP} at time point a). Results are plotted as mean±S.E.M.

As a positive control for SH-5, we tested Akt inhibition by utilizing the PIP_3-dependent translocation sensor (AKT-PH-YFP). To study Akt inhibition, cells expressing the AKT-YFP-PH sensor were stimulated with platelet-derived growth factor (PDGFBB) resulting in Akt translocation as indicated by increase in PIP_3 levels (black trace). However, application of 10µM Akt specific inhibitor SH-5 significantly attenuated Akt translocation as indicated by reduction of PIP_3 levels (gray trace) (Fig. 40). In addition, the data obtained with the non-selective kinase inhibitor staurosporine and PTEN (which also inhibits PDK1) already indicate that PDK1 is not involved in G_i-induced cAMP rebound responses (Fig. 30). Therefore, based on these results it is concluded that PIP_3 either directly or indirectly mediates G_i-induced cAMP rebound responses.

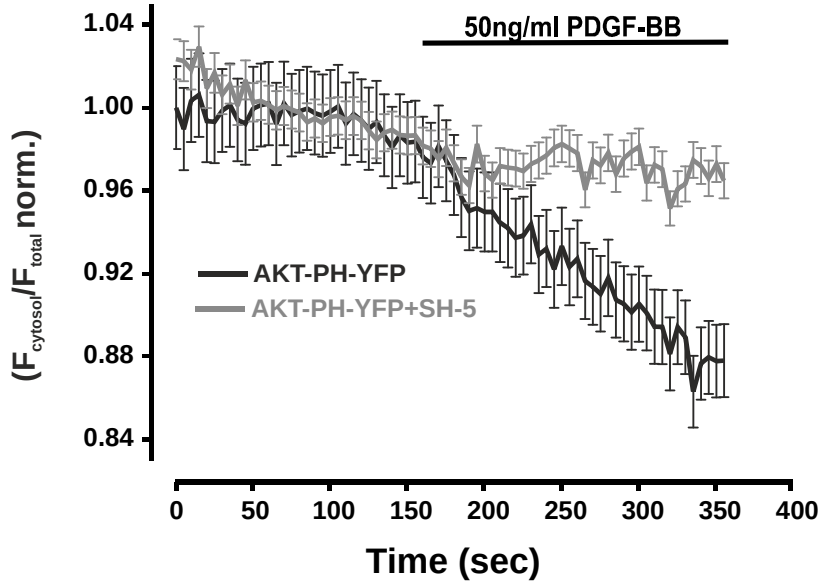

Figure 40: SH-5 effectively inhibited Akt activation.

Representative average data showing the SH5-mediated blockade of Akt translocation in HEK293T cells expressing a PIP_3-dependent translocation sensor (AKT-PH-YFP). Prior to the experiment, cells were pre-incubated with low concentrations of wortmannin (50nM) in order to allow for partial translocation of AKT-PH-YFP. Cells were then stimulated with 50ng/ml of the PI3K-specific activator PDGFBB leading to translocation of Akt from cytosol to plasma membrane as determined by plotting the ratio of cytosolic AKT-PH-YFP relative to total cell fluorescence. However, application of 1µM SH-5 (Akt inhibitor) completely abolished PDGF-induced membrane targeting of AKT-PH-YFP (n=5).

4.14. G_i-mediated PIP_3 activation via Gβγ.

The above data suggested that G_i-induced cAMP rebound stimulation leads to production of PIP_3. It is known from the literature that activation of PTX-sensitive G_i-coupled GPCRs activates PI3Kγ. This PI3Kγ activation has been linked to a direct association of its catalytic domain with the βγ subunits of G proteins (Stoyanov *et al*., 1995). Therefore, it was investigated whether the moderate G_i-coupled GPCR (α_{2A}-AR) stimulation used in the cAMP rebound stimulation protocol described above actually leads to an increase of PIP_3. To test this, we tested NE-mediated translocation of AKT-PH-YFP in HEK cells. As mentioned above in the absence of wortmannin, AKT-PH-YFP sensor is already completely localized to the plasma membrane. In order to achieve a cytosolic localization of the sensor in unstimulated cells, these experiments were carried out in the presence of a low concentration of wortmannin (50nM). Cells were then stimulated with NE, resulting in increasing PIP_3 levels (red trace) (Fig. 41 B) as reflected by translocation of the AKT-PH-YFP sensor from the cytosol to the plasma membrane (Fig. 41A).

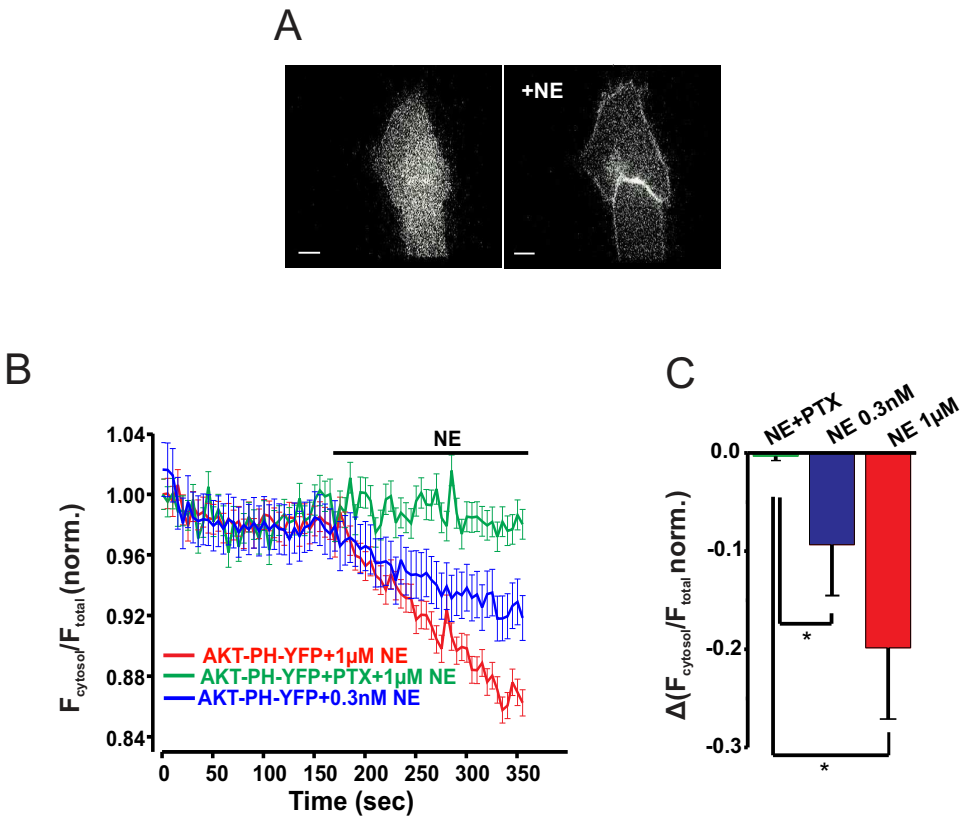

Figure 41: α_{2A}-AR receptor stimulation leads to elevation of PIP_3 levels.

A, Depicted are confocal images of HEK293T cells transfected with the PIP_3 sensitive AKT-PH-YFP translocation sensor, AC5, and α_{2A}-AR. Cells were pre-incubated with low concentrations of wortmannin (50nM) in order to relocate AKT-PH-YFP to the cytosol (left). Cells were then stimulated with 1µM NE leading to membrane targeting of AKT-PH-YFP (right). **B**, Depicted are averaged data for AKT-PH-YFP translocation to the plasma membrane by plotting the ratio of cytosolic AKT-PH-YFP relative to total cell fluorescence. To increase cytosolic AKT-PH-YFP localization cells were pre-incubated with 50nM wortmannin and stimulated with 1µM (red (n=10) and green (n=5) trace) or 0.3nM NE (blue traces (n=4)). Pretreatment with PTX (30ng/ml for >4h) abolished NE-induced membrane targeting of AKT-PH-YFP (green trace). **C**, NE-induced alterations in $YFP_{(cytosol)}/YFP_{(whole\ cell)}$ were quantified. Results are plotted as mean±S.E.M. Scale bar 10µm.

These results clearly demonstrated that stimulation of the α_{2A}-AR increases PIP_3 levels. To demonstrate that this increase of PIP_3 levels was mediated via PTX-sensitive proteins, cells were pre-incubated with PTX. As expected, the increase in PIP_3 levels induced by activation of $G\alpha_i$-coupled receptors was completely abolished by pre-treatment with PTX (green trace) (Fig. 41B-C).

However, PI3Kγ is also directly activated by Gβγ (Stoyanov *et al.*, 1995). Therefore, we asked whether Gβγ is involved in PI3K activation. In order to address this question, G_i-

mediated PI3K activation was measured in HEK cells by using the AKT-PH-YFP translocation sensor. To study the involvement of Gβγ, cells were then pre-incubated with the Gβγ inhibitor gallein. Exposure to the α_{2A}-AR agonist NE led to activation of PI3K. However, pre-incubation with 10µM gallein significantly reduced PI3K activation (Fig. 42). Based on these results, it can be concluded that PI3K is mediating G_i-induced cAMP rebound responses of AC5/6 expressing cells.

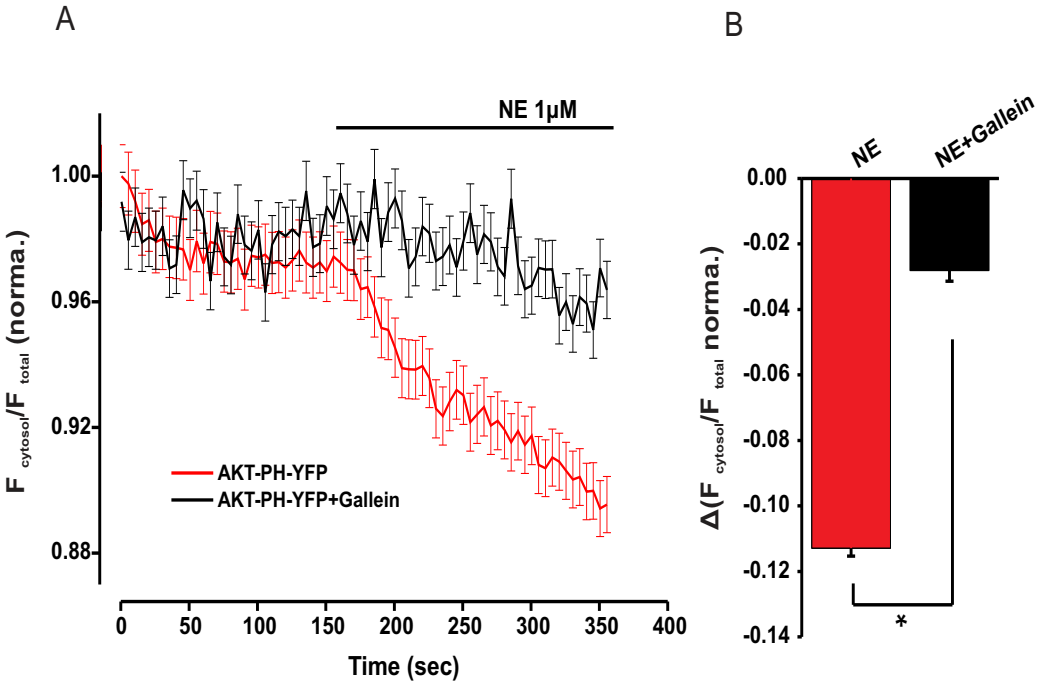

Figure 42: G_i-activation leads to elevation of PIP_3 levels via Gβγ.

A, Averaged AKT-PH-YFP translocation data showing Gβγ-dependent alterations of PIP_3 induced by application of 0.3nM NE in cells expressing AKT-PH-YFP. Cells were then stimulated with NE leading to activation of PIP_3. However, subsequent preincubation and application of 10µM gallein (Gβγ inhibitor) significantly reduced NE-stimulated PIP_3 activation. **B**, NE-induced alterations in $YFP(_{cytosol})/YFP(_{whole\ cell})$ were quantified. Results are plotted as mean±S.E.M (n=3-5).

4.15. Elevation of PIP_3 potentiates $G\alpha_s$-enhanced cAMP levels.

The translocation assay revealed that G_i-induced cAMP rebound responses are mediated by PIP_3 primarily in AC5/6-expressing cells. Therefore, the next aim was to determine whether elevations of PIP_3 induced by other means than G_i protein activation would indeed sensitize AC5. In order to test this hypothesis, HEK293T cells expressing Epac1-camps, AC5, and α_{2A}-AR were stimulated with platelet-derived growth factor (PDGFBB) (which is known to activate PI3K) and G_s-enhanced cAMP levels were measured. Stimulation of Epac1-camps

expressing cells with 50ng/ml PDGFBB significantly increased $G\alpha_s$-enhanced cAMP levels (red trace) compared to a control condition (black trace) (Fig. 43A- B).

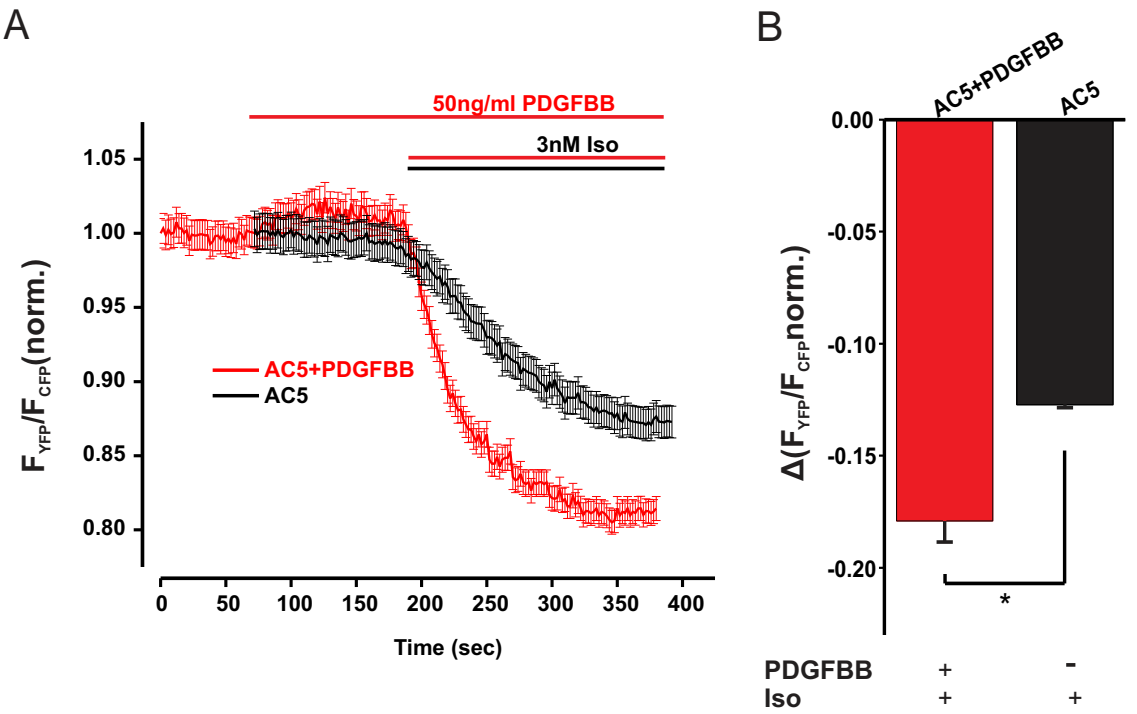

Figure 43: Elevation of PIP_3 causes sensitization of AC5

A, Averaged FRET data showing effects of PDGF-receptor-mediated PIP_3 production on Iso-mediated cAMP responses were measured in AC5-expressing cells (n=8-10). Cells expressing Epac1-camps were (red) or were not (black) incubated with 50 ng/mL PDGFBB at the indicated time point during FRET imaging. **B**, PDGF-induced FRET changes after application of Iso of the experiments shown in *A* were quantified. Results are plotted as mean±S.E.M.

These results suggest that ACs, specifically AC5/6 are regulated by PIP_3. Furthermore, these results strongly support the hypothesis that PIP_3 is mediating the G_i-induced cAMP rebound responses in AC5-expressing cells.

4.16. Effects of PI3K on G_i-induced cAMP rebound responses in cardiac myocytes.

Since the role of PIP_3 for G_i-mediated cAMP rebound responses was so far only shown in a heterologous expression system, the next aim was to test whether the ACh-induced cAMP rebound phenomenon is also mediated by PIP_3 in atrial cardiac myocytes

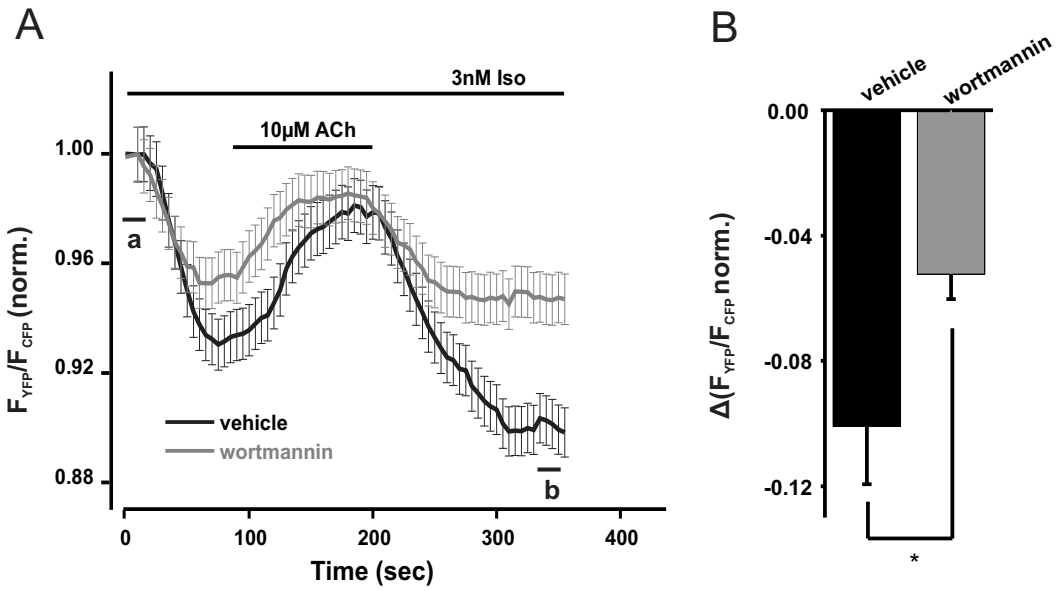

Figure 44: Wortmannin abolishes G_i-induced cAMP rebound responses in atrial myocytes.

A, Isolated murine atrial myocytes from Epac1-camps expressing mice were pre-incubated with 1µM wortmannin or vehicle for 30min and subsequently subjected to the cAMP-rebound stimulation protocol as described in Fig.9A. Averaged FRET data demonstrate a loss of the cAMP rebound response after withdrawal of ACh in cells pre-treated with 1µM of wortmannin (n=6-9). **B,** Experimental data derived from *A* were quantified with respect to Iso-mediated alterations of F_{YFP}/F_{CFP} norm. after withdrawal of ACh (F_{YFP}/F_{CFP} at time point b - F_{YFP}/F_{CFP} at time point a). Results are plotted as mean±S.E.M.

In order to test this, Epac1-camps expressing transgenic mouse atrial cells were pre-incubated with the PI3K inhibitor wortmannin and the G_i-induced cAMP rebound stimulation was measured. These experiments were performed in collaboration with Dr. Viaceslav O. Nikolaev work group. Notably, application of 1µM wortmannin significantly reduced the ACh-induced cAMP rebound levels (gray trace) compared to control conditions (black trace) (Fig. 44). This result suggests that also in murine atrial myocytes, cAMP rebound responses are largely dependent on PIP_3-mediated adenylyl cyclase sensitization. Intriguingly, wortmannin had a tendency to lower AC activity in response to β-adrenergic receptor stimulation (Fig. 44), similar to what was observed in AC5-expressing HEK293T cells (Fig. 32).

5. Discussion

cAMP together with Ca^{2+} is the most prominent cytosolic second messenger in virtually all cells, which is generated by ACs through stimulatory G protein $G\alpha_s$. cAMP regulates many different functions of the cell; consequently, dysfunction of cAMP regulation is involved in the pathology of many different diseases. Previously a cAMP rebound stimulation was identified after termination of $G\alpha_i$-stimulation in cardiac myocytes as well HEK293T cells but the mechanism is still under debate (Ono *et al*., 1994; Wang *et al*., 1995; Belevych *et al*., 2000; Milde *et al.,* 2013). However, while studying the mechanism of this long known cAMP rebound phenomenon after termination of $G\alpha_i$-stimulation in cardiac myocytes, we discovered a novel regulatory pathway that requires PI3 kinase activity and leads to sensitization of ACs, primarily AC5 and AC6 (Fig. 45).

5.1 G_i-induced cAMP rebound responses are specific for AC5 and AC6 in HEK293T and HeLa cells.

The G_i-induced cAMP rebound responses were originally described in cardiac myocytes. Similar to myocytes, the cAMP rebound responses were also described in HEK293T cells after termination of G_i stimulation by using real-time cAMP imaging with a FRET-based cAMP biosensor (Epac1-camps) (Milde *et al*., 2013). Primarily the cAMP rebound responses could be reproduced after withdrawal of Gi/o stimulation in two different heterologous overexpression systems (HEK293T and HeLa cells) (Fig. 8 and 16). These cAMP rebound effects were seen only when cells expressed AC5 and AC6, but not when expressing empty vector instead of AC5 or AC6 or in cells expressing AC4 (Fig. 10, 11 and 24), which supports the hypothesis that cAMP rebound responses are AC5/6 dependent (Belevych *et al*., 2001; Bett *et al*., 2001). Indeed, native HEK293T and HeLa cells expressed AC5 and AC6 only to a low extent, and the contribution of endogenous AC5/6 to functional cAMP production was minor. Due to lack of suitable AC5/6 specific antibodies for the detection of protein expression, we studied AC5/6 mRNA expression levels and found detectable amounts of AC5/6 in HEK and HeLa cells upon transfection (Fig. 17). During the investigation of G_i-induced cAMP rebound responses, it was noted that cAMP rebound responses were not observed at maximally stimulating concentrations of Iso. These results are in line with earlier findings that cAMP rebound stimulation of the Cl^- current was not observed if $G\alpha_s$ stimulation was fully activated by maximally stimulating concentrations of Iso (1µM) in guinea-pig ventrucular myocytes (Zakharov *et al*., 1997). These observations hinted towards

the rebound stimulation is due to facilitation of cAMP-dependent responses (Wang & Lipsius, 1995).

Cells expressing a different G_i coupled receptor (α_{2A}-AR) instead of the M_2-R also produced similar cAMP rebound responses upon termination of treatment with the α_{2A}-adrenergic receptor agonist NE (Fig. 12). cAMP rebound effects could also be elicited in cells expressing the $G\alpha_s$-coupled dopamine D_1 receptor in combination with the $G\alpha_i$-coupled α_{2A}-AR. In these cells, a similar degree of cAMP rebound responses was observed upon termination of $G\alpha_i$-activation compared to the β_2-adrenergic receptor (Fig. 13). These results suggest that G_i-induced cAMP rebound responses are not receptor specific. In addition it was found that the G_i-induced cAMP rebound responses were sensitive to PTX. PTX-treated HEK cells were significantly inhibited in their ability to produce G_i-induced cAMP rebound responses (Fig. 14). These results are consistent with earlier findings that G_i-induced rebound stimulation of L-type Ca^{2+} current in atrial myocytes and cAMP-activated Cl^--current in ventricular myocytes are attenuated by PTX treatment (Wang & Lipsus, 1995; Belevych *et al.*, 1997). This observation indicated that cAMP rebound levels are mediated by PTX-sensitive Gi/o proteins. Importantly, G_i-induced cAMP rebound responses were observed not only at the level of cAMP, but also by using AKAR4, a FRET reporter of PKA activity (Fig. 28). In addition, G_i-induced cAMP rebound responses were also observed using HCN2-camps (a different cAMP FRET-biosensor) (Fig. 29)

However, the intracellular concentration of cAMP can be increased not only by stimulation of AC activity but also by an inhibition of PDE activity. It has been previously reported that the PDE3 dependent NO-cGMP pathway was involved in G_i-induced cAMP rebound increase in cat atrial myocytes (Wang *et al.*, 1995; Wang *et al.*, 1998). However, our results clearly argue against a major contribution of PDEs in cAMP rebound response: Inhibition of major PDE isoforms such as PDE3 and PDE4 did not attenuate the cAMP rebound response (Fig. 19 and 20). These results are in line with previous studies that PDE3-dependent NO-cGMP signaling is not involved in G_i-induced rebound cAMP effects in ventricular myocytes (Bett *et al.*, 2002; Zakharov *et al.*, 1997). In addition, inhibition of PKA is known to stimulate PDE4 activity but this had no detectable effect on the observed rebound responses. Furthermore, the fact that in a heterologous expression system the rebound response was completely absent when cAMP was produced via AC4 argues against a major role of PDEs in the generation of cAMP rebound stimulation. Therefore, it can be concluded that PDE3-

dependent NO-cGMP signaling does not contribute to ACh-induced inhibition of cAMP rebound stimulation.

By expressing different inhibitory $G\alpha_i$ proteins, we ruled out that cAMP rebound responses were restricted to certain G_i subtypes (Fig. 15). Furthermore, significantly lower cAMP rebound responses were observed when inhibiting Gβγ with galleine (Fig. 21), which suggests that a Gβγ-dependent mechanism is involved in cAMP rebound responses. These results are consistent with a proposed mechanism that Gβγ facilitation of $G\alpha_s$-stimulated AC2/4 leads to cAMP rebound responses (Bett *et al*., 2001; Belevych *et al.,* 2001). In addition, overexpression of G protein βγ subunits showed a significant reduction of G_i-induced cAMP rebound response (Fig. 23). This argues against the results showing that the βγ inhibitor gallein significantly reduced cAMP rebound responses (Fig. 21). However, it is not clear why βγ overexpression had an inhibitory effect on G_i-induced cAMP rebound responses. One explanation could be that long term stimulation of PI3K with βγ could lead to desensitization of its production or it's down stream signaling. However, this negative discrepancy still remains an open question. It was noted during the investigation of G_i-induced cAMP rebound stimulation that G_i-induced cAMP rebound stimulation is long lasting (around 10-15 min) (data not shown). This observation is consistent with earlier findings that Gβγ-mediated stimulatory responses do not deactivate as quickly as inhibitory effects (Harvey *et al.,* 2007). These data further strengthen the hypothesis that a Gβγ-dependent signaling mechanism is involved in cAMP rebound responses. Surprisingly, G_i-induced cAMP rebound responses were significantly reduced when cells expressed AC4 (Fig. 24), which argues against the proposed mechanism that Gβγ-facilitated $G\alpha_s$-stimulated AC4 is involved in generation of the cAMP rebound responses. However, it has been reported previously that Gβγ conditionally activates AC5, resulting in an increase in cAMP levels. By using an AC5 mutant with the Gβγ binding site deleted, AC5Δ66-137 (Sadana *et al*., 2007), we ruled out the possible involvement of Gβγ activation of AC5 in G_i-induced cAMP rebound responses. A similar degree of cAMP rebound responses was observed in cells expressing the AC5Δ66-137 mutant compared to cells expressing full-length AC5 (Fig. 25). These results explain that the G_i-induced cAMP rebound responses are not directly mediated by Gβγ-activated ACs.

Then the question arises, why do we see a significant reduction in cAMP rebound responses by Gβγ inhibition? There is a possible explanation for this. It could be that the cAMP

rebound stimulation may not actually directly involve Gβγ-dependent activation of ACs; perhaps another Gβγ-dependent mechanism is involved such as Gβγ-dependent stimulation of phospholipase C (PLC) activity and subsequent activation of protein kinase C (PKC) (Clapham & Neer, 1997) or a Gβγ-activated phosphoinositide 3 kinase-dependent signaling pathway (Vidar *et al.,* 1998). Indeed, our Gβγ inhibition data (βγ inhibitor gallein significantly inhibits Gβγ activated PI3K) (Fig. 20) also hinted that Gβγ activated PI3K is involved in G_i-induced cAMP rebound stimulation (Ukhanov *et al*., 2011)

5.2 PIP_3 mediated G_i-induced cAMP rebound responses.

Interestingly, the PI3K inhibitor wortmannin significantly lowered α_{2A}-AR-induced cAMP rebound responses of AC 5/6 (Fig. 32, 33), which supports the hypothesis that Gβγ activated PI3K signaling was involved in G_i-induced cAMP rebound responses. These results are consistent with earlier findings, which reported that relaxin-mediated stimulation of cAMP was inhibited by PI3K inhibitors (LY294002 and wortmannin) in THP-1 cells (Nguyen *et al*., 2003 and 2005). On the other hand, these findings are contrary to a previous report that cardiac-specific PI3Kγ-KO mice exhibit an increase in basal contractility (Patrucco *et al*., 2004). However, the effect of PI3K inhibition on basal cAMP levels is not clear in most cell types or tissues, not even cells that vastly express AC5/6. Indeed, similar stimulatory effects were observed upon wortmannin treatment in the case of AC4-expressing cells in response to β_2-adrenergic stimulation (Fig. 34). Furthermore, wortmannin had no effects on cells expressing empty vector instead of AC5 or AC6, suggesting that wortmannin effects were specific to AC5 or AC6 in HEK cells. In addition, using the well established PIP_3 sensor AKT-PH-YFP, we were able to demonstrate that stimulation of α_{2A}-adrenergic receptors under conditions very similar to those used to study rebound stimulation indeed led to an increase in PIP_3 production (Fig. 41). The PIP_3 levels required for AC5/6 specific stimulation are obviously higher than those needed for translocation of the AKT-PH domain. This could be deduced from the observation that overall PI3K activity in the absence of Gi/o stimulation had to be reduced in order to see Gi/o mediated translocation of the AKT-sensor (Fig. 36). In addition, the Gβγ inhibitor gallein completely abolished $G\alpha_i$-mediated PI3K activity, which further confirmed PI3K signaling through Gβγ. However, these results are preliminary, and additional experiments are needed to substantiate them (Fig. 42). Furthermore, wortmannin pretreatment did not only fully inhibit cAMP rebound responses in AC5 expressing HEK cells but also completely abolished this response in adult mouse atrial myocytes (Fig. 44). These findings suggest that G_i-mediated cAMP rebound responses are mediated via a Gβγ-

PI3K dependent pathway, both in cardiac myocytes and in heterologous expression systems. In atrial myocytes, AC5 and AC6 are predominantly expressed (Dhein *et al*., 2001; Defer *et al*., 2000; Mattick *et al*., 2007). This evidence for functional expression of AC5/6 in atrial myocytes comes from the the observation of robust inhibition in response to activation of inhibitory G protein (G_i), which indicates AC5 and AC6 regulation via PTX-sensitive G_i protein (Fig. 8A). Furthermore, termination of G_i activation leads to cAMP rebound responses. In mouse ventricular myocytes, we observed only very minor cAMP rebound responses after withdrwal of muscarinic receptor agonist. This low cAMP rebound responses might be due to a relatively lower expression of M_2-R in ventricular myocytes compared to atrial myocytes and also suggest that basal cAMP levels might be higher in atrial myocytes (Deighton *et al*., 1990; Zakharov *et al*., 1997). Using both PTEN overexpression (which is a phosphatidylinositol-3,4,5-trisphosphate 3-phosphatase, thereby lowering PIP_3 levels (Maehama *et al.*, 1998)) and SHIP2 inhibition (a phosphatidylinositol-3,4,5-trisphosphate 5-phosphatase catalyzing the conversion of PIP_3 into $PI(3,4)P_2$ (Damen *et al.*, 1996)), we identified PIP_3 as the major phosphoinositol species that is involved in PI3K-dependent cAMP rebound responses (Fig. 37 and 38). However, our PTEN overexpression results are also contrary to a previous finding, which reported that functional impairment of PTEN leads to a decrease in cardiac contractility (Crackower *et al*., 2002). One explanation for this opposing effect could be that PI3Kγ not only regulates PIP_3 levels but rather provides a scaffold for other important regulatory proteins including PDEs (Gregg *et al*., 2010).

It has been previously reported that in THP-1 cells, relaxin stimulates PI3K activity, thereby enhancing AC activity resulting in increased cAMP levels. The authors further showed that these increased cAMP levels were mediated by PIP_3 activated PDK1 downstream target, PKC ζ (Nguyen *et al*., 2005). However, our PTEN, staurosporine and KT5270 (even though this compound is sold as a PKA inhibitor, it also inhibits PDK1) data indicated already that PDK1 and its downstream targets are not involved in G_i-induced cAMP rebound responses (Fig. 26 and 30). Furthermore, Akt-specific inhibitors also failed to attenuate the G_i-induced cAMP rebound stimulation (Fig. 39). Therefore, a possible involvement of PIP_3 downstream signaling on G_i-induced cAMP rebound effects could be ruled out. Instead, our data suggest that PIP_3 itself either directly or indirectly mediates cAMP rebound responses.

In addition, the broad-spectrum kinase inhibitor staurosporine failed to affect G_i-induced cAMP rebound responses (Fig. 30). These results indicate that G_i-induced cAMP rebound responses are not mediated by PKC, PKG and other staurosporine-sensitive kinases and also

rule out the possible Gβγ-dependent activation of PKC as a source for G_i-induced cAMP rebound responses. This finding is in line with earlier findings that a protein kinase C inhibitor did not block the cAMP rebound response of L-type Ca^{2+} currents induced by stimulation of muscarinic acetylcholine receptors in ventricular myocytes (Belevych *et al.*, 2001).

In addition to PKC signaling, we ruled out a possible involvement of PKA signaling on the G_i-induced cAMP rebound response by PKA inhibition by showing that G_i-induced cAMP rebound responses were not affected by the PKA inhibitor KT5720 (Fig. 26).

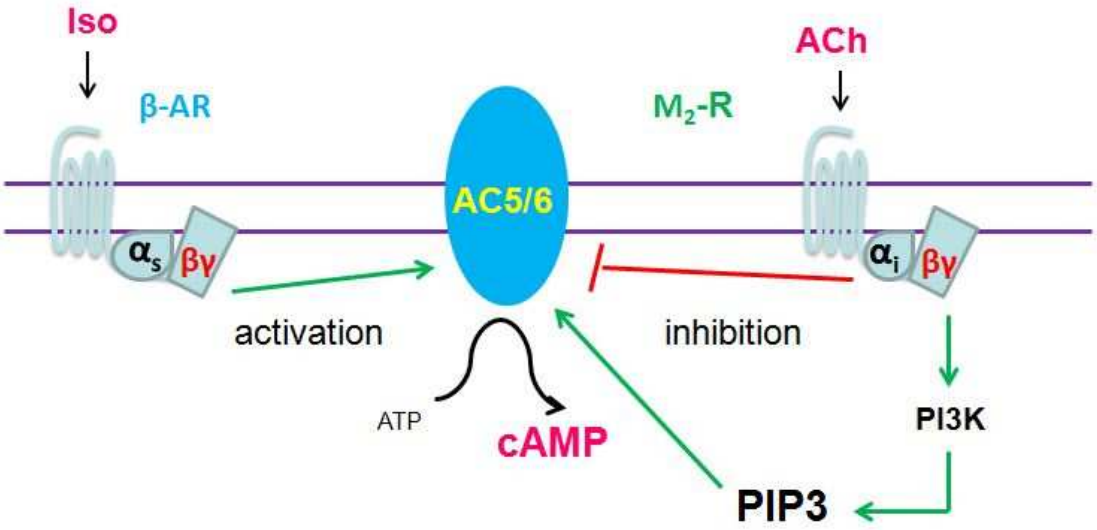

Figure 45: Proposed PIP_3 pathway which is responsible for G_i-induced cAMP rebound stimulation.

This finding seems to be contradictory to previous findings that a selective PKA inhibitor diminished the cAMP rebound responses which led to the claim that cAMP rebound responses are mediated via a G protein/adenylate cyclase/cAMP-dependent PKA signaling pathway in atrial myocytes (Wang & Lipsius, 1995).

Importantly, exposure to wortmannin significantly lowered β-adrenergic enhanced cAMP levels only in cells expressing AC5 and AC6. Indeed, wortmannin did not reduce β_2-adrenergic enhanced cAMP levels in cells transfected with AC4; there was rather a tendency towards faster cAMP production in response to Iso (Fig. 34). These findings led us to conclude that PIP_3 regulates primarily AC5 and AC6. This conclusion is strengthened by the

observation that the activation of PI3K in a G_i-independent manner through PDGF receptor stimulation also resulted in a stimulation of AC5 (Fig. 43).

Due to the general importance of PI3K signaling in various tissues and cell types, we predict that PIP_3 dependent AC regulation represents an important novel regulatory mechanism to fine tune cAMP homeostasis in cells. However, this study did not investigate whether PIP_3 has a direct effect on the level of adenylyl cyclases or whether any unidentified PIP_3-dependent regulatory proteins will indirectly mediate this effect. The next step should be to investigate these uncovered questions in the future.

5.4. Concluding remarks

This work reported mechanisms underlying the well described cAMP rebound phenomenon after withdrawal of muscarinic stimulation in atrial myocytes by real-time cAMP imaging using the FRET-based cAMP biosensor Epac1-camps. By means of the heterologous expression system, we identified that muscarinic receptor-induced cAMP rebound responses were mediated via PTX-sensitive/AC5/6 dependent signaling and identified the involvement of the Gi-mediated PI3K pathway. Our results led us to conclude that AC5/6 but not AC4 is under the control of a novel PIP_3 dependent regulation. These results could provide the mechanism underlying long known physiological phenomena such as postvagal tachycardia and arrhythmogenic mechanisms in the heart. Due to the general importance of PI3K signaling and broad expression of AC5/6 in various tissues and cell types we predict that PIP_3 dependent AC regulation represents an important novel regulatory mechanism to fine-tune cAMP homeostasis in cells. Future studies have to reveal whether PIP_3 regulates AC5/6 activity by direct interaction with the cyclase or exert its function via interaction with unknown AC-regulating proteins.

5.5. Key findings

In this present study, three major findings were discovered in receptor-mediated regulation of cAMP levels

- A PTX-sensitive AC5/6-dependent pathway underlies the G_i-induced cAMP rebound stimulation in intact cells.
- This pathway is initiated via Gβγ-mediated activation of PI3K both in mouse atrial myocytes as well in HEK293T cells.
- Elevation of PIP_3 enhances AC5/6 activity and leads to pronounced physiologically relevant alterations of cytosolic cAMP levels.

6. Summary

A wide variety of signaling substances such as hormones, neurotransmitters, odorants and chemokines control intracellular signaling by regulating the production of the second messenger cAMP. By activating Epac, PKA and cyclic nucleotide-gated ion channels, the production of cAMP alters a wide range of biological processes including cell division and metabolism. A number of GPCRs controls intracellular cAMP levels via stimulatory or inhibitory G proteins via adenylyl cyclases. The function of the broadly expressed AC5 and AC6 is enhanced by stimulatory ($G\alpha_s$) or attenuated by inhibitory ($G\alpha_i$) G proteins. Mechanistically both inhibition and stimulation is mediated via a direct protein-protein interaction. In addition to this direct regulation, several previous studies reported a cAMP rebound stimulation after withdrawal of G_i stimulation in cardiac myocytes for which the mechanism is debated (Hartzell, 1988; Wang & Lipsius, 1995). A similar cAMP rebound response was observed previously in our lab after termination of α_{2A}-AR adrenergic receptor activation in HEK293T cells (Markus *et al*., 2013). The present study was aimed at investigating mechanisms underlying G_i-induced cAMP rebound effects.

Many genetically encoded biosensors have been developed based on fluorescence resonance energy transfer (FRET) to visualize the spatiotemporal dynamics of various intracellular signals including second messengers. FRET-based cAMP biosensor (Epac1-camps) as well as heterologous overexpression system was used to investigate the mechanisms underlying G_i-mediated cAMP rebound stimulation in cardiac myocytes and also in heterologous expression system. When studying the mechanism of the long-known phenomenon of cAMP rebound stimulation after withdrawal of G_i stimulation in cardiac myocytes, we observed a PTX-sensitive/G_i-mediated/ adenylyl cyclase (type 5/6)/ cAMP-dependent pathway for this cAMP rebound stimulation.

In addition, we observed that inhibition of $G\beta\gamma$ by gallein led to an attenuation of the AC5-mediated cAMP rebound response, although, overexpression of AC4 did not produce additional cAMP stimulation. This implies that different $G\beta\gamma$-mediated signaling pathways may exist. Interestingly, we observed that PI3K inhibitor attenuates AC5/6-dependent cAMP rebound effects. This indicated that G_i-mediated cAMP rebound response was mediated via the PI3K-dependent pathway. Indeed, overexpression of PIP_3-specific phosphatase PTEN confirmed that PIP_3 itself either directly or indirectly mediated Gi-dependent cAMP rebound

responses. Additionally, inhibition of PIP_2-specific phosphatase SHIP and downstream events of PIP_3-dependent regulation of Akt further confirm the influence of PIP_3 on cAMP rebound levels. Indeed, surpassing G_i-mediated PI3K activation through PDGF-receptor stimulation strengthens this pathway. In addition, we confirmed that inhibition of PI3K also prevented cAMP rebound response after withdrawal of ACh in atrial myocytes. We suppose that the novel PIP_3 dependent regulation of AC5/6 might represent a missing mechanism that explains physiological phenomena such as post vagal tachycardia.

7. Zusammenfassung

Eine große Bandbreite von Signalmolekülen – darunter Hormone, Neurotransmitter, Geruchsstoffe und Chemokine – kontrollieren intrazelluläre Signale durch die Regulation des sog. zweiten Botenstoffs cAMP. Die Produktion von cAMP beeinflusst verschiedenste biologische Prozesse wie die Zellteilung und Stoffwechsel. Dies geschieht unter anderem durch die Aktivierung von Epac, PKA und cyclisch Nukleotid-gesteuerte Ionenkanäle. Eine Reihe von GPCR kontrolliert das intrazelluläre cAMP-Niveau mittels des Einflusses von stimulatorischen oder inhibitorischen G-Proteinen auf die Adenylylcyclasen. Die Aktivität der weit verbreiteten AC5 und AC6 wird durch stimulatorische G-Proteine ($G\alpha_s$) erhöht, während sie durch inhibitorische G-Proteine ($G\alpha_i$) verringert wird. Mechanistisch werden Inhibition und Stimulation durch direkte Protein/Protein-Interaktionen vermittelt. Zusätzlich zu dieser direkten Regulation wurde in anderen vorangegangenen Studien eine cAMP-Rebound-Stimulation beschrieben. Diese trat in Kardiomyocyten auf, sobald die Aktivierung von G_i-Proteinen beendet wurde. Der zugrundeliegende Mechanismus ist umstritten (Hartzell, 1988; Wang *et al.,* 1995). Ein ähnliches cAMP-Rebound-Verhalten wurde auch bereits in unserem Labor in HEK293T-Zellen beobachtet, nachdem die Stimulation α_{2A}-adrenerger Rezeptoren beendet wurde (Milde *et al*., 2013). Daher zielte die vorliegende Arbeit auf die Untersuchung des zugrundeliegenden Mechanismus dieses G_i-Protein-induzierten cAMP-Rebound-Effekts.

Es wurden viele genetisch kodierte Biosensoren entwickelt, die auf dem Förster/Fluoreszenz-Resonanzenergietransfer (FRET) beruhen und mit denen die zeitliche und räumliche Dynamik von verschiedenen intrazellulären Signalen, einschließlich denen der zweiten Botenstoffe, sichtbar gemacht werden konnte. Der FRET-basierte cAMP-Biosensor Epac1-camps wurde zusammen mit heterologen Überexpressionsmodellen benutzt, um den Mechanismus der Gi-Protein-vermittelten cAMP-Rebound-Stimulation in Kardiomyocyten und anderen lebenden Zellen zu untersuchen. Während der Untersuchung dieses wohlbekannten cAMP-Rebound-Phänomens beobachteten wir einen PTX-empfindlichen, Gi-Protein-vermittelten Typ5/6-Adenylylcyclase/cAMP-abhängigen Signalweg.

Zusätzlich dazu stellten wir fest, dass die Inhibition von $G\beta\gamma$-Untereinheiten durch Gallein zu einer Verringerung der AC5-vermittelten cAMP-Rebound-Antwort führte, während die Überexpression von AC4 keine zusätzliche Stimulation von cAMP bewirkte. Dies legt nahe,

dass verschiedene Gβγ-vermittelte Signalwege existieren. Bemerkenswerterweise beobachteten wir auch, dass, PI3K den AC5/6-abhängigen cAMP-Rebound-Effekt abschwächte. Dies deutete darauf hin, dass die G_i-vermittelte cAMP-Rebound-Antwort einem PI3K-abhängigen Signalweg unterliegt. Tatsächlich bestätigte die Überexpression der PIP_3-spezifischen Phosphatase PTEN, dass PIP_3 selbst, entweder direkt oder indirekt, die Gi-abhängige cAMP-Rebound-Antwort vermittelt. Der Einfluss von PIP_3 auf die cAMP-Rebound-Niveaus wurde zusätzlich durch die Inhibition der PIP_2-spezifischen Phosphatase SHIP und weiterer Vorgänge unterhalb der PIP_3-abhängigen Regulation von Akt bestätigt. Außerdem konnte der Signalweg verstärkt werden, wenn die Gi-abhängige PI3K-Aktivierung durch die Stimulation des PDGF-Rezeptors umgangen wurde. Zusätzlich dazu konnten wir bestätigen, dass auch in atrialen Myocyten die Inhibierung der PI3K die Ausbildung der cAMP-Rebound-Antwort verhinderte, nachdem Acetylcholin entfernt wurde. Wir vermuten, dass diese neu beschriebene PIP_3-abhängige Regulation der AC5/6 jenen unbekannten Mechanismus darstellt, der physiologischen Phänomenen wie der post-vagalen Tachikardie zu Grunde liegt.

8. References

Ahlquist RP. (1948) A study of the adrenotropic receptors. *Am J Physiol.* **153**:586-600.

Alberts B, Johnson A, Lewis J, Raff M, Roberts K, and Walter P. (2012) Molecular biology of the cell. New York: Garland Science.

Aman MJ, Lamkin TD, Okada H, Kurosaki T, and Ravichandran KS. (1998) The inositol phosphatase SHIP inhibits Akt/PKB activation in B cells. *J Biol Chem.* **273**:33922-8.

Arai K, Maruyama Y, Nishida M, Tanabe S, Takagahara S, Kozasa T, Mori Y, Nagao T, and Kurose H. (2003) Differential requirement of Gα12, Gα13, Gαq, and Gβγ for endothelin-1-induced c-Jun NH2-terminal kinase and extracellular signal-regulated kinase activation. *Mol.Pharmacol.* **63**:478-488.

Asboth G, Price SA, Bellinger J, Ledger W, Barlow DH, and Bernal AL. (2001) Characterization of adenylyl cyclases in cultured human granulosa cells. *Reproduction.* **121**:217-218.

Azzi M, Charest PG, Angers S, Rousseau G, Kohout T, Bouvier M, and Pineyro G. (2003) Beta-arrestin-mediated activation of MAPK by inverse agonists reveals distinct active conformations for G protein-coupled receptors. *Proc Natl Acad Sci U S A.* **100:**11406-11411.

Baillie GS, Scot JD, and Houslay MD. (2005) Compartmentalisation of phosphodiesterases and protein kinase A: opposites attract. *FEBS Lett.* **579**:3264-3270.

Bakalyar HA, and Reed RR. (1990) Identification of a specialized adenylyl cyclase that may mediate odorant detection. *Science.* **250**:1403-1406.

Baker LP, Nielsen MD, Impey S, Metcalf MA, Poser SW, Chan G, Obrietan K, Hamblin MW, and Storm DR. (1998) Stimulation of type 1 and type 8 Ca2+/calmodulinsensitive adenylyl cyclases by the Gs-coupled 5 hydroxytryptamine subtype 5 HT7A receptor. *J Biol Chem.* **273**:17469-17476.

Barry PH, and Lynch JW. (2005) Ligand-gated channels. *IEEE Trans.Nanobioscience.* **4**:70-80.

Bauman AL, Soughayer J, Nguyen BT, Willoughby D, Carnegie GK, Wong W, Hoshi N, Langeberg LK, Cooper DM, Dessauer CW, and Scott JD. (2006) Dynamic regulation of cAMP synthesis through anchored PKA-adenylyl cyclase V/VI complexes. *Mol Cell.* **23**:925-31.

Bayewitch ML, Avidor-reiss T, Levy R, Pfeuffer T, Nevo I, Simonds WF, and Vogel Z. (1998) Inhibition of adenylyl cyclase isoforms V and VI by various Gbetagamma subunits. *FASEB J.* **12**:1019–1025.

Beavo JA, Conti M, and Heaslip RJ. (1994) Multiple cyclic nucleotide phosphodiesterases. *Mol Pharmacol.* **46:**399-405.

Beavo JA, Hansen RS, Harrison SA, Hurwitz RL, Martins TJ, and Mumby MC. (1982) Identification and properties of cyclic nucleotide phosphodiesterases. *Mol Cell Endocrinol*. **28**: 387-410.

Belevych AE, and Harvey RD (2000) Muscarinic inhibitory and stimulatory regulation of the L-type Ca^{2+} current is not altered in cardiac ventricular myocytes from mice lacking endothelial nitric oxide synthase. *J Physiol.* **528**: 279–289.

Belevych AE, Sims C, and Harvey RD. (2001) ACh-induced rebound stimulation of L-type Ca^{2+} current in guinea-pig ventricular myocytes, mediated by Gbetagamma-dependent activation of adenylyl cyclase. *J Physiol.* **536:**677–692.

Berman DM, Kozasa T, and Gilman AG. (1996) The GTPase-activating protein RGS4 stabilizes the transition state for nucleotide hydrolysis. *J Biol Chem.* **271**:27209-12.

Berridge MJ. (2005) Unlocking the secrets of cell signaling. *Annual Review of Physiology.* **67**:1–21.

Bett GC, Dai S, and Campbell DL. (2002) Cholinergic modulation of the basal L-type calcium current in ferret right ventricular myocytes. *J Physiol.* **542**:107-117.

Bolland S, Pearse RN, Kurosaki T, and Ravetch JV. (1998) SHIP modulates immune receptor responses by regulating membrane association of Btk. *Immunity*. **8:**509-16.

Börner S, Schwede F, Schlipp A, Berisha F, Calebiro D, Lohse MJ, and Nikolaev VO. (2011) FRET measurements of intracellular cAMP concentrations and cAMP analog permeability in intact cells. *Nat Protoc***. 6**:427-38.

Brady JD, Rich ED, Martens JR, Karpen JW, Varnum MD, and Brown RL. (2006) Interplay between PIP_3 and calmodulin regulation of olfactory cyclic nucleotide-gated channels. *Proc Natl Acad Sci U S A.* **103**:15635-15640.

Brazil DP, Yang ZZ, and Hemmings BA. (2004) Advances in protein kinase B signalling: AKTion on multiple fronts. *Trends Biochem Sci*. **29**:233-42.

Bryan NS, Bian K, and Murad F. (2009) Discovery of the nitric oxide signaling pathway and targets for drug development. *Front Biosci.* **14**:1–18.

Buck J, Sinclair ML, Schapal L, Cann MJ, and Levin LR. (1999) Cytosolic adenylyl cyclase defines a unique signaling molecule in mammals. *Proc Natl Acad Sci U S A.* **96**:79-84.

Buck J, Sinclair ML, Schapal L, Cann MJ, and Levin LR. (1999) Cytosolic adenylyl cyclase defines a unique signaling molecule in mammals. *Proc Natl Acad Sci USA.* **96**:79–84.

Buhl AM, Johnson NL, Dhanasekaran N, and Johnson GL. (1995) Gα12 and Gα13 stimulate Rho-dependent stress fiber formation and focal adhesion assembly. *J Biol Chem.* **270**: 24631-24634.

Bünemann M, Frank M, and Lohse MJ (2003). Gi protein activation in intact cells involves subunit rearrangement rather than dissociation. *Proc Natl Acad Sci U S A.* **100**: 16077-16082.

Burke GH, and Calaresu FR. (1972) An experimental analysis of the tachycardia that follows vagal stimulation. *J Physiol*. **226**:491-510

Calebiro D, Nikolaev VO, Gagliani MC, de Filippis T, Dees C, Tacchetti C, Persani L, and Lohse MJ. (2009) Persistent cAMP-signals triggered by internalized G-protein-coupled receptors. *PLoS Biol.* **7.** 1000172.

Cali JJ, Zwaagstra JC, Mons N, Cooper DM, and Krupinski J. (1994) Adenylyl cyclase type VIII. A Ca2+/calmodulin-stimulated enzyme expressed in discrete regions of rat brain. *J Biol Chem.* **269**:12190-12195.

Cantley LC, and Neel BG. (1999) New insights into tumor suppression: PTEN suppresses tumor formation by restraining the phosphoinositide 3-kinase/AKT pathway. *Proc Natl Acad Sci U S A*. **96**:4240-4245.

Card GL, England BP, Suzuki Y, Fong D, Powell B, Lee B, Luu C, Tabrizizad M, Gillette S, Ibrahim PN, Artis DR, Bollag G, Milburn MV, Kim SH, Schlessinger J, and Zhang KY (2004) Structural basis for the activity of drugs that inhibit phosphodiesterases. *Structure.* **12:**2233-2247.

Caulfield MP, Robbins J, Higashida H, and Brown DA. (1993) Postsynaptic actions of acetylcholine: the coupling of muscarinic receptor subtypes to neuronal ion channels. *Prog Brain Res*. **98**:293-301.

Celli BR, and MacNee W. (2004) Standards for the diagnosis and treatment of patients with COPD: a summary of the ATS/ERS position paper. *Eur Respir J.* **23**:932-46.

Chen CA, and Manning DR. (2001) Regulation of G-proteins by covalent modification. *Oncogene*. **20**:1643-1652.

Chen Y, Cann MJ, Litvin TN, Iourgenko V, Sinclair ML, Levin LR, and Buck J. (2000) Soluble adenylyl cyclase as an evolutionarily conserved bicarbonate sensor. *Science.* **289**:625–628.

Choi EJ, Xia Z, and Storm DR. (1992) Stimulation of the type III olfactory adenylyl cyclase by calcium and calmodulin. *Biochemistry.* **31**:6492–6498.

Christensen AE, Selheim F, de Rooij J, Dremier S, Schwede F, Dao KK, Martinez A, Maenhaut C, Bos JL, Genieser HG, and Døskeland SO. (2003) cAMP analog mapping of Epac1 and cAMP kinase. Discriminating analogs demonstrate that Epac and cAMP kinase act synergistically to promote PC-12 cell neurite extension. *J Biol Chem*. **278**:35394-402.

Clapham DE, and Neer EJ (1997) G protein βγ subunits. *Annu Rev of Pharmacol Toxicol.* **37**:167-203.

Cooper DM. (2003) Regulation and organization of adenylyl cyclases and cAMP. *Biochem J.* **375**:517-529.

Cooper GM. *The Cell: A Molecular Approach.* Sunderland, MA: Sinauer Associates, Inc, 2013. Print.

Coppe D, and Steer ML. (1978) Adenyl cyclase. *Int. J Oral Surg.* **7**:43-51.

Crackower MA, Oudit GY, Kozieradzki I, Sarao R, Sun H, Sasaki T, Hirsch E, Suzuki A, Shioi T, Irie-Sasaki J, Sah R, Cheng HY, Rybin VO, Lembo G, Fratta L,Oliveira-dos-Santos AJ, Benovic JL, Kahn CR, Izumo S, Steinberg SF, Wymann MP, Backx

PH, and Penninger JM. (2002) Regulation of myocardial contractility and cell size by distinct PI3K-PTEN signaling pathways. *Cell.* **110:**737-749.

Cully M, You H, Levine AJ, and Mak TW. (2006) Beyond PTEN mutations: the PI3K pathway as an integrator of multiple inputs during tumorigenesis. *Nat Rev Cancer*. **6**: 184–192.

Cumbay MG, and Watts VJ. (2004) Novel regulatory properties of human type 9 adenylate cyclase. *J Pharmacol Exp Ther*. **310:**108–115.

Currie KP. (2010) G protein modulation of CaV2 voltage-gated calcium channels. *Channels (Austin).* **4**: 497-509.

Cvejic S, Jiang Y, and Huang X. (2000) Signaling of G_12 family of G-proteins through a tyrosine kinase and a Ras-GAP. *Trends Cardiovasc.Med.* **10**:160-165.

Damen JE, Liu L, Rosten P, Humphries RK, Jefferson AB, Majerus PW, and Krystal G. (1996) The 145-kDa protein induced to associate with Shc by multiple cytokines is an inositol tetraphosphate and phosphatidylinositol 3,4,5-triphosphate 5-phosphatase. *Proc Natl Acad Sci U S A.* **93**:1689-93.

de Rooij J, Rehmann H, van Triest M, Cool RH, Wittinghofer A, and Bos JL. (2000) Mechanism of regulation of the Epac family of cAMP-dependent RapGEFs. *J Biol Chem*. **275**:20829-36.

de Rooij J, Zwartkruis FJ, Verheijen MH, Cool RH, Nijman SM, Wittinghofer A, and Bos JL. (1998) Epac is a Rap1 guanine-nucleotide-exchange factor directly activated by cyclic AMP. *Nature.* **396:**474–47.

Defer N, Best-Belpomme M, and Hanoune J. (2000) Tissue specificity and physiological relevance of various isoforms of adenylyl cyclase. *Am J Physiol Renal Physiol.* **279:**400-416.

Degerman E, Belfrage P, and Manganiello VC. (1997) Structure, localization, and regulation of cGMP-inhibited phosphodiesterase (PDE3). *J Biol Chem*. **272**: 6823-6.

Deighton NM, Motomura S, Borquez D, Zerkowski HR, Doetsch N, and Brodde OE (1990) Muscarinic cholinoceptors in the human heart: demonstration, subclassification, and distribution. *Naunyn Schmiedebergs Arch Pharmacol.* **341**:14-21.

Depry C, Allen MD, and Zhang J. (2011) Visualization of PKA activity in plasma membrane microdomains. *Mol Biosyst.* **7**:52-8.

Dessauer CW, and Gilman AG (1997) The catalytic mechanism of mammalian adenylyl cyclase. Equilibrium binding and kinetic analysis of P-site inhibition. *J Biol Chem.* **272:**27787-27795.

Dessauer CW, and Nguyen BT. (2005) Relaxin stimulates multiple signaling pathways: activation of cAMP, PI3K, and PKCzeta in THP-1 cells. *Ann NY Acad Sci*. **1041**:272–279.

Dessauer CW, Tesmer JJ, Sprang SR, and Gilman AG. (1998) Identification of a Giα binding site on type V adenylyl cyclase. *J Biol Chem*. **273**:25831-25839.

Dhein S, van Koppen CJ, and Brodde OE. (2001). Muscarinic receptors in the mammalian heart. *Pharmacol Res.* **44**:161-182.

Diel S, Klass K, Wittig B, and Kleuss C. (2006) Gβγ activation site in adenylyl cyclase type II. Adenylyl cyclase type III is inhibited by Gβγ. *J Biol Chem.* **281**:288-294

DiFrancesco D, and Tortora P. (1991) Direct activation of cardiac pacemaker channels by intracellular cyclic AMP. *Nature*. **351**:145-7.

Endoh M, Maruyama M, and Iijima T. (1985) Attenuation of muscarinic cholinergic inhibition by islet-activating protein in the heart. *Am J Physiol*. **249**:309-20

Engelman E, and Marsala C. (2013) Efficacy of adding clonidine to intrathecal morphine in acute postoperative pain: meta-analysis. *Br J Anaesth.* **110**:21-7.

Engelman JA, Luo J, and Cantley LC. (2006) The evolution of phosphatidylinositol 3-kinases as regulators of growth and metabolism. *Nat Rev Genet.* **7**:606–619.

Erin JK, Richard JS, Jennifer MK, Danielle LH, Krista LA, Elliot RB, Kelvin C, Kanchana KG, Philip SL, Jessica RL, Arthur KS, Nicholas RV, and Christopher DD. (2012) First Messengers. In: eLS. John Wiley & Sons Ltd, Chichester. http://www.els.net [doi: 10.1002/9780470015902.a0024167]

Evanko DS, Thiyagarajan MM, Takida S, and Wedegaertner PB. (2005) Loss of association between activated Gαq and Gβγ disrupts receptor-dependent and receptor-independent signaling. *Cell Signal.* **17**:1218-1228.

Feinstein PG, Schrader KA, Bakalyar HA, Tang WJ, Krupinski J, Gilman AG, and Reed RR. (1991) Molecular cloning and characterization of a $Ca^{2+/}$calmodulinin sensitive adenylyl cyclase from rat brain. *Proc Natl Acad Sci U S A.* **88**:10173-10177.

Feldman DS, Zamah AM, Pierce KL, Miller WE, Kelly F, Rapacciuolo A, Rockman HA, Koch WJ, and Luttrell LM. (2002) Selective inhibition of heterotrimeric Gs signaling. Targeting the receptor-G-protein interface using a peptide minigene encoding the G_s carboxyl terminus. *J Biol Chem.* **277**:28631-28640.

Ferrandon S, Feinstein TN, Castro M, Wang B, Bouley R, Potts JT, Gardella TJ, and Vilardaga JP. (2009) Sustained cyclic AMP production by parathyroid hormone receptor endocytosis. *Nat Chem Biol.* **10**:734-42.

Finn JT, Grunwald ME, and Yau KW. (1996) Cyclic nucleotide-gated ion channels: an extended family with diverse functions. *Annu Rev Physiol.* **58**:395-426.

Florio VA, and Ross EM. (1983) Regulation of the catalytic component of adenylate cyclase. Potentiative interaction of stimulatory ligands and 2′,5′-dideoxyadenosine. *Mol. Pharmacol.* **24**:195-202.

Francis SH, and Corbin JD. (1999) Cyclic nucleotide-dependent protein kinases: intracellular receptors for cAMP and cGMP action. *Crit Rev Clin Lab Sci* **36:**275–328.

Frank M, Thumer L, Lohse MJ, and Bünemann M. (2005) G Protein activation without subunit dissociation depends on a G{alpha}(i)-specific region. *J Biol Chem.* **280**: 24584-24590.

Fraser LR, Adeoya-Osiguwa S, Baxendale RW, Mededovic S, and Osiguwa OO. (2005) First messenger regulation of mammalian sperm function *via* adenylyl cyclase/cAMP. *J Reprod Dev.* **51**:37-46.

Fredriksson R, Lagerstrom MC, Lundin LG, and Schioth HB. (2003) The G-protein coupled receptors in the human genome form five main families. Phylogenetic analysis, paralogon groups, and fingerprints. *Mol Pharmacol.* **63**: 1256-1272.

Gancedo, J. M. (2013). Biological roles of cAMP: variations on a theme in the different kingdoms of life. *Biol Rev Camb Philos. Soc.* **88**: 645-68.

Gao BN, and Gilman AG. (1991) Cloning and expression of a widely distributed adenylyl cyclase type IV. *Proc Natl Acad Sci U.S.A.* **88**: 10178-10182.

Gao X, Sadana R, Dessauer CW, and Patel TB. (2007) Conditional stimulation of adenylyl cyclase type V and VI by βγ-dimers. *J Biol Chem.* **282**: 294-302.

Gao X, Lowry PR, Zhou X, Depry C, Wei Z, Wong GW, and Zhang J. (2011) PI3K/Akt signaling requires spatial compartmentalization in plasma membrane microdomains. *Proc Natl Acad Sci USA.* **108**:14509-12514.

Gilmour RF Jr, and Zipes DP. (1985) Positive inotropic effect of acetylcholine in canine cardiac Purkinje fibers. *Am J Physiol*. **249:** 735-40.

Gloerich M, and Bos JL. (2010) Epac: defining a new mechanism for cAMP action. *Annu. Rev. Pharmacol. Toxicol.* **50**: 355-375.

Gohla A, Offermanns S, Wilkie TM, and Schultz G. (1999) Differential involvement of Gα12 and Gα13 in receptor-mediated stress fiber formation. *J Biol Chem.* **274**:17901-17907

Gomeza J, Zhang L, Kostenis E, Felder CC, Bymaster FP, Brodkin J, Shannon H, Xia B, Duttaroy A, Deng CX, and Wess J. (2001) Generation and pharmacological analysis of M2 and M4 muscarinic receptor knockout mice. *Life Sci.* **68**:2457-66.

Gregg CJ, Steppan J, Gonzalez DR, Champion HC, Phan AC, Nyhan D, Shoukas AA, Hare JM, Barouch LA, and Berkowitz DE. (2010) β2-adrenergic receptor-coupled phosphoinositide 3-kinase constrains cAMP-dependent increases in cardiac inotropy through phosphodiesterase 4 activation. *Anesth Analg.* **111**:870-877.

Guyton A, and Hall J. (2006) Chapter 10: Rhythmical Excitation of the Heart. In Gruliow, Rebecca. *Textbook of Medical Physiology* (Book) (11th ed.). Philadelphia, Pennsylvania: Elsevier Inc. p. 122.

Hanoune J, and Defer N. (2001) Regulation and role of adenylyl cyclase isoforms. *Annu Rev Pharmacol Toxicol.* **41**:145-74.

Hartzell HC. (1988) Regulation of cardiac ion channels by catecholamines, acetylcholine and second messenger systems. *Prog Biophys Mol Biol* **52**:165–247.

Harvey RD, and Belevych AE. (2003) Muscarinic regulation of cardiac ion channels. *Br. J. Pharmacol* **139:**1074–1084.

Hazeki O, and Ui M. (1981) Modification by islet-activating protein of receptor-mediated regulation of cyclic AMP accumulation in isolated rat heart cells. *J Biol Chem*. **256**: 2856-62.

Hein L, Altman JD, and Kobilka BK. (1999). Two functionally distinct alpha2-adrenergic receptors regulate sympathetic neurotransmission. *Nature.* **402**:181-184.

Hein P, Rochais F, Hoffmann C, Dorsch S, V. Nikolaev VO, Engelhardt S, Berlot CH, Lohse MJ, and Bünemann M (2006). Gs activation is time-limiting in initiating receptor-mediated signaling. *J Biol Chem.* **281**:33345-33351.

Hill, J., Howlett, A. and Klein, C. (2000) Nitric oxide selectively inhibits adenylyl cyclase isoforms 5 and 6. *Cell Signal.* **12**:233-237.

Hirsch E, Lembo G,Montrucchio G, Rommel C, Costa C, and Barberis L. (2006) Signaling through PI3Kgamma: a common platform for leukocyte, platelet and cardiovascular stress sensing. *Thrombosis and Haemostasis* **95**:29-35.

Hofmann F, Ammendola A, and Schlossmann J. (2000) Rising behind NO: cGMP-dependent protein kinases. *J Cell Sci*.**113**:1671-6.

Hofmann F. (2005) The biology of cyclic GMP-dependent protein kinases. *J Biol Chem* **280**:1–4.

Hollenberg M, Carriere S, and Barger AC. (1965) Biphasic action of acetylcholine on ventricular myocardium. *Circ Res*. **16**:527-36.

Holz GG, Kang G, Harbeck M, Roe MW, and Chepurny OG (2006) Cell physiology of cAMP sensor Epac. *J Physiol.* **577**:5-15.

Hommers LG, Klenk C, Dees C, and Bünemann M. (2010) G proteins in reverse mode: receptor-mediated GTP release inhibits G protein and effector function. *J. Biol. Chem.* **285**:8227-8233.

Hu CL, Chandra R, Ge H, Pain J, Yan L, Babu G, Depre C, Iwatsubo K, Ishikawa Y, Sadoshima J, Vatner SF, and Vatner DE. (2009) Adenylyl cyclase type 5 expression

during cardiac development and stress. *Am J Physiol Heart Circ Physiol.* **297**:1776-1782.

Hulme EC. (1990) Muscarinic acetylcholine receptors: typical G-coupled receptors. *Symp Soc Exp Biol*. **44**:39-54

Insel PA, and Ostrom RS. (2003) Forskolin as a tool for examining adenylyl cyclase expression, regulation, and G-protein signaling. *Cell Mol.Neurobiol.* **23**, 305-314.

Ishikawa Y, Katsushika S, Chen L, Halnon NJ, Kawabe J, and Homcy CJ. (1992) Isolation and characterization of a novel cardiac adenylyl cyclase cDNA. *J Biol Chem.* **267**:13553-13557.

Iwami G, Kawabe J, Ebina T, Cannon PJ, Homcy CJ, and Ishikawa Y. (1995) Regulation of adenylyl cyclase by protein kinase A. *J Biol Chem*. **270**:12481–12484.

Iyengar R. (1993) Multiple families of Gs-regulated adenylyl cyclases. *Adv.Second Messenger Phosphoprotein Res.* **28**:27-36.

Jacoby E, Bouhelal R, Gerspacher M, and Seuwen K. (2006) The 7 TM G-protein-coupled receptor target family. *ChemMedChem*. **8**:761-82.

Jaiswal BS, and Conti M. (2003) Calcium regulation of the soluble adenylyl cyclase expressed in mammalian spermatozoa. *Proc Natl Acad Sci USA.* **100**:10676-10681.

Janetopoulos C, Jin T, and Devreotes P. (2001) Receptor-mediated activation of heterotrimeric G-proteins in living cells. *Science*. **291**:2408-11.

Jastrzebska B, Fotiadis D, Jang GF, Stenkamp RE, Engel A, and Palczewski K. (2006) Functional and structural characterization of rhodopsin oligomers. *J Biol Chem.* **281**: 11917-11922.

Jeon YH, Heo YS, Kim CM, Hyun YL, Lee TG, Ro S, and Cho JM. (2005) Phosphodiesterase: overview of protein structures, potential therapeutic applications and recent progress in drug development. *Cell Mol Life Sci.* **62:**1198-1220.

Jiang A, Craxton A, Kurosaki T, and Clark EA. (1998) Different protein tyrosine kinases are required for B cell antigen receptor-mediated activation of extracellular signalregulated kinase, c-Jun NH2-terminal kinase 1, and p38 mitogen-activated protein kinase. *J Exp Med.* **188**:1297-1306.

Jiang Z, and Zhou Y. (2006) Using silico methods predicting ligands for orphan GPCRs. *Curr Protein Pept Sci*. **7**:459-64.

Johnson RA, Désaubry L, Bianchi G, Shoshani I, Lyons E Jr, Taussig R, Watson PA, Cali JJ, Krupinski J, Pieroni JP, and Iyengar R. (1997) Isozyme-dependent sensitivity of adenylyl cyclases to P-site-mediated inhibition by adenine nucleosides and nucleoside 3′-polyphosphates. *J Biol Chem.* **272**:8962-8966.

Jones DT, and Reed RR. (1989) Golf: An olfactory neuron specific-g protein involved in odorant signal transduction. *Science*. **244**:790–795.

Jungmichel S, Sylvestersen KB, Choudhary C, Nguyen S, Mann M, and Nielsen ML. (2014) Specificity and commonality of the phosphoinositide-binding proteome analyzed by quantitative mass spectrometry. *Cell rep.* **6**:578-91.

Kalesnikoff J, Sly LM, Hughes MR, Büchse T, Rauh MJ, Cao LP, Lam V, Mui A, Huber M, and Krystal G. (2003) The role of SHIP in cytokine-induced signaling. *Rev Physiol Biochem Pharmacol.* **149**: 87–103.

Kamenetsky M, Middelhaufe S, Bank EM, Levin LR, Buck J, and Steegborn C. (2006) Molecular details of cAMP generation in mammalian cells: a tale of two systems. *J Mol Biol*. **362**:623-39.

Katada T, Kusakabe K, Oinuma M, and Ui M. (1987) A novel mechanism for the inhibition of adenylate cyclase via inhibitory GTP-binding proteins. Calmodulin-dependent inhibition of the cyclase catalyst by the beta gamma-subunits of GTP-binding proteins. *J Biol Chem*. **262**:11897-900.

Kaupp UB, and Seifert R. (2002) Cyclic nucleotide-gated ion channels.*Physiol Rev*. **82**:769-824.

Kawabe J, Iwami G, Ebina T, Ohno S, Katada T, Ueda Y, Homcy CJ, and Ishikawa Y. (1994) Differential activation of adenylyl cyclase by protein kinase C isoenzymes. *J Biol Chem*. **269:**16554–16558.

Kirstein M, Rivet-Bastide M, Hatem S, Bénardeau A, Mercadier JJ, and Fischmeister R. (1995) Nitric oxide regulates the calcium current in isolated human atrial myocytes. *J Clin Invest*. **95**:794-802.

Klippel A, Kavanaugh WM, Pot D, and Williams LT. (1997) A specific product of phosphatidylinositol 3-kinase directly activates the protein kinase Akt through its pleckstrin homology domain. *Mol Cell Biol.* **17**:338-344.

Kneussel M. (2005) Postsynaptic scaffold proteins at non-synaptic sites. The role of postsynaptic scaffold proteins in motor-protein-receptor complexes. *Embo Rep.* **6**:22-27.

Komatsu N, Aoki K, Yamada M, Yukinaga H, Fujita Y, Kamioka Y, and Matsuda M. (2011) Development ofan optimized backbone of FRET biosensors for kinases and GTPases. *Mol Biol Cell*. **22**:4647-56.

Krieglstein K, Strelau J, Schober A, Sullivan A, and Unsicker K. (2002) TGF-_ and the regulation of neuron survival and death. *J Physiol Paris.* **96**:25-30.

Kristelly R, Gao G, and Tesmer JJ. (2004) Structural determinants of RhoA binding and nucleotide exchange in leukemia-associated Rho guanine-nucleotide exchange factor. *J Biol Chem.* **279**:47352-47362.

Krupinski J, Coussen F, Bakalyar HA, Tang WJ, Feinstein PG, Orth K, Slaughter C, Reed RR, and Gilman AG. (1989) Adenylyl cyclase amino acid sequence: possible channel- or transporter-like structure. *Science.* **244**:1558-1564.

Kume S, Saneyoshi T, and Mikoshiba K. (2000) Desensitization of IP3-induced Ca2+ release by overexpression of a constitutively active G_q-subunit converts ventral to dorsal fate in Xenopus early embryos. *Dev Growth Differ.* **42**:327-335.

Kurosu H, Maehama T, Okada T, Yamamoto T, Hoshino S, Fukui Y, Ui M, Hazeki O, and Katada T. (1997) Heterodimeric phosphoinositide 3-kinase consisting of p85 and p110beta is synergistically activated by the betagamma subunits of G proteins and phosphotyrosyl peptide. *J Biol Chem.* **272**: 24252-6.

Lagerström MC, and Schiöth HB. (2008) Structural diversity of G protein-coupled receptors and significance for drug discovery. *Nat Rev Drug Discov.* **7**:339-57.

Landry Y, Niederhoffer N, Sick E, and Gies JP. (2006) Heptahelical and other G-proteincoupled receptors (GPCRs) signaling. *Curr.Med Chem.* **13**:51-63.

Lee CH, Park D, Wu D, Rhee SG, and Simon MI. (1992) Members of the Gq alpha subunit gene family activate phospholipase C beta isozymes. *J Biol Chem.* **267**:16044-7.

Lee DA, and Higginbotham EJ. (2005) Glaucoma and its treatment: a review. *Am J Health Syst Pharm.* **62:**691-9.

Lehmann DM, Seneviratne AM, and Smrcka AV. (2008) Small molecule disruption of G protein beta gamma subunit signaling inhibits neutrophil chemotaxis and inflammation. *Mol Pharmacol.* **73:**410-8.

Lehmann KG, Lane JG, Piepmeier JM, and Batsford WP. (1987) Cardiovascular abnormalities accompanying acute spinal cord injury in humans: incidence, time course and severity. *J Am Coll Cardiol*. **10**:46-52

Levy JV, and Killebrew E. (1971) Inotropic effects of prostaglandin E2 on isolated cardiac tissue. *Proc Soc Exp Biol Med*. **136**:1227-31.

Li DM, and Sun H. (1997) TEP1, encoded by a candidate tumor suppressor locus, is a novel protein tyrosine phosphatase regulated by transforming growth factor beta. *Cancer Res.* **57**:2124-9.

Li J, Yen C, Liaw D, Podsypanina K, Bose S, Wang SI, Puc J, Miliaresis C, Rodgers L, McCombie R, Bigner SH, Giovanella BC, Ittmann M, Tycko B, Hibshoosh H, Wigler MH, and Parsons R. (1997) PTEN, a putative protein tyrosine phosphatase gene mutated in human brain, breast, and prostate cancer. *Science*. **275**:1943-7.

Lin Y, and Smrcka AV. (2011) Understanding molecular recognition by G protein βγ subunits on the path to pharmacological targeting. *Mol Pharmacol.* **80**:551-557.

Lincoln TM, Wu X, Sellak H, Dey N, and Choi CS. (2006) Regulation of vascular smooth muscle cell phenotype by cyclic GMP and cyclic GMP-dependent protein kinase. *Front Biosci.* **11**:356-367.

Linder, JU. (2006) Class III adenylyl cyclases: molecular mechanisms of catalysis and regulation. *Cell Mol Life Sci.* **63**:1736-1751.

Lindvall J, and Islam TC. (2002) Interaction of Btk and Akt in B cell signaling. *Biochem Biophys Res Commun*. **293**:1319-26.

Lioubin MN, Algate PA, Tsai S, Carlberg K, Aebersold A, and Rohrschneider LR. (1996) p150Ship, a signal transduction molecule with inositol polyphosphate-5-phosphatase activity. *Genes Dev*. **10**:1084-95.

Löffelholz K, and Pappano AJ. (1985) The parasympathetic neuroeffector junction of the heart. *Pharmacol Rev*. **37**:1-24.

Lohmann SM, and Walter U. (2005) Tracking functions of cGMP-dependent protein kinases (cGK). *Front Biosci.* **10**:1313-1328.

Lohse MJ, Nuber S, and Hoffmann C. (2012). Fluorescence/bioluminescence resonance energy transfer techniques to study G-protein-coupled receptor activation and signaling. *Pharmacol. Rev.* **64**:299-336.

Ludwig A, Zong X, Stieber J, Hullin R, Hofmann F, and Biel M. (1999) Two pacemaker channels from human heart with profoundly different activation kinetics. *EMBO J.* **18**: 2323-2329.

Lugnier C, and Komas N. (1993) Modulation of vascular cyclic nucleotide phosphodiesterases by cyclic GMP: role in vasodilatation. *Eur Heart J.* **14**:141-148.

MacDermott AB, Role LW, and Siegelbaum SA. (1999) Presynaptic ionotropic receptors and the control of transmitter release. *Annu Rev Neurosci.* **22:**443-485.

Macrez-Lepretre N, Kalkbrenner F, Schultz G, and Mironneau J. (1997) Distinct functions of Gq and G11 proteins in coupling _1-adrenoreceptors to Ca^{2+} release and Ca^{2+} entry in rat portal vein myocytes. *J Biol Chem.* **272**:5261-5268

Madiraju AK, Erion DM, Rahimi Y, Zhang XM, Braddock DT, Albright RA, Prigaro BJ, Wood JL, Bhanot S, MacDonald MJ, Jurczak MJ, Camporez JP, Lee HY, Cline GW, Samuel VT, Kibbey RG, and Shulman GI. (2014) Metformin suppresses

gluconeogenesis by inhibiting mitochondrial glycerophosphate dehydrogenase. *Nature*. **510:**542-6.

Maehama T, and Dixon JE. (1998) The tumor suppressor, PTEN/MMAC1, dephosphorylates the lipid second messenger, phosphatidylinositol 3,4,5-trisphosphate. *J Biol Chem*. **273**:13375-8.

Maffucci T, Brancaccio A, Piccolo E, Stein RC, and Falasca M. (2003) Insulin induces phosphatidylinositol-3-phosphate formation through TC10 activation. *EMBO Journal* **22**:4178–4189.

Maier U, Babich A, Macrez N, Leopoldt D, Gierschik P, Illenberger D, and Nürnberg B. (2000) Gβ5γ2 is a highly selective activator of phospholipid-dependent enzymes. *J Biol Chem.* **275**:13746-13754.

Maier U, Babich A, and Nürnberg B. (1999) Roles of non-catalytic subunits in Gbetagamma-induced activation of class I phosphoinositide 3-kinase isoforms beta and gamma. *J Biol Chem*. **274**:29311-7.

Maioli E, Torricelli C, and Fortino V. (2006) Functional interactions of protein kinase A and C in signalling networks: a recapitulation. *Cell Mol Life Sci*. **63**:637-41.

Manganiello VC, Taira M, Degerman E, and Belfrage P. (1995) Type III cGMP-inhibited cyclic nucleotide phosphodiesterases (PDE3 gene family). *Cell Signal*. **7**:445-55.

Martinez SE, Wu AY, Glavas NA, Tang XB, Turley S, Hol WG, and Beavo JA. (2002) The two GAF domains in phosphodiesterase 2A have distinct roles in dimerization and in cGMP binding. *Proc Natl Acad Sci USA*. **99**:13260-13265.

Mattick P, Parrington J, Odia E, Simpson A, Collins T, and Terrar D. (2007) Ca2+-stimulated adenylyl cyclase isoform AC1 is preferentially expressed in guinea-pig sino-atrial node cells and modulates the I(f) pacemaker current. *J Physiol*. **582:**1195-203.

McCudden CR, Hains MD, Kimple RJ, Siderovski DP, and Willard FS. (2005) G-protein signaling: back to the future. *Cell Mol Life Sci.* **62**:551-577.

Meigs TE, Fedor-Chaiken M, Kaplan DD, Brackenbury R, and Casey PJ. (2002) Gα12 and Gα13 negatively regulate the adhesive functions of cadherin. *J Biol Chem.* **277**: 24594-24600.

Merritt EA, Sarfaty S, Chang TT, Palmer LM, Jobling MG, Holmes RK, and Hol WG. (1995) Surprising leads for a cholera toxin receptor-binding antagonist: crystallographic studies of CTB mutants. *Structure.* **3**:561-570.

Metrich M, Berthouze E, Morel B, Crozatier A, Gomez M, and Lezoualc'h L. (2010). Role of the cAMP-binding protein Epac in cardiovascular physiology and pathophysiology. *Pflugers Arch.* **459**:535-546.

Michel JJ, and Scott JD. (2002) AKAP mediated signal transduction. *Annu Rev Pharmacol Toxicol*. **42**:235-57.

Michell RH. (2007) Evolution of the diverse biological roles of inositols. *Biochemical Society Symposium* **74**: 223-246.

Milde M, Rinne A, Wunder F, Engelhardt S, and Bünemann M. (2013) Dynamics of Gαi1 interaction with type 5 adenylate cyclase reveal the molecular basis for high sensitivity of Gi-mediated inhibition of cAMP production. *Biochem J.* **454**:515–523.

Milligan G, and Kostenis E. (2006) Heterotrimeric G-proteins: a short history. *Br J Pharmacol*. **147**:46-55.

Much B, Wahl-Schott C, Zong X, Schneider A, Baumann L, Moosmang S, Ludwig A, and Biel M. (2002) Role of subunit heteromerization and N-linked glycosylation in the formation of functional hyperpolarization-activated cyclic nucleotide-gated channels. *J Biol Chem.* **278**:43781-6.

Murad F, Chi YM, Rall TW, and Sutherland EW. (1962) Adenyl cyclase. III. The effect of catecholamines and choline esters on the formation of adenosine 3',5'-phosphate by preparations from cardiac muscle and liver. *J Biol Chem*. **237**:1233-8.

Murga C, Laguinge L, Wetzker R, Cuadrado A, and Gutkind JS. (1998) Activation of Akt/protein kinase B by G protein-coupled receptors. A role for alpha and beta gamma subunits of heterotrimeric G proteins acting through phosphatidylinositol-3-OH kinase gamma. *J Biol Chem* **273**:19080-19085.

Murthy KS, and Makhlouf GM. (1998) Regulation of adenylyl cyclase type V/VI in smooth muscle: interplay of inhibitory G protein and Ca2+ influx. *Mol Pharmacol*. **54**:122-8.

Myung CS, Lim WK, DeFilippo JM, Yasuda H, Neubig RR, and Garrison JC. (2006) Regions in the G_-subunit important for interaction with receptors and effectors. *Mol Pharmacol*. **69**:877-887.

Nakaki T, Nakadate T, and Kato R. (1980) Alpha 2-adrenoceptors modulating insulin release from isolated pancreatic islets. *Naunyn Schmiedebergs Arch Pharmacol.* **313**:151-3.

Nikolaev VO, Bünemann M, Hein L, Hannawacker A, and Lohse MJ (2004) Novel single chain cAMP sensors for receptor-induced signal propagation. *J Biol Chem* **279**:37215–37218.

Nikolaev VO, Bünemann M, Schmitteckert E, Lohse MJ, and Engelhardt S. (2006) Cyclic AMP imaging in adult cardiac myocytes reveals far-reaching beta1-adrenergic but locally confined beta2-adrenergic receptor-mediated signaling. *Circ. Res*. **99:**1084-1091.

Noebels JL. (2012) The Voltage-Gated Calcium Channel and Absence Epilepsy. 4th edition. Bethesda (MD): National Center for Biotechnology Information (US)

Nürnberg B, Gudermann T, and Schultz G. (1995) Receptors and G-proteins as primary components of transmembrane signal transduction. Part 2. G-proteins: structure and function. *J Mol Med.* **73**: 123-132.

Nürnberg B. (2004) The state of GPCR research in 2004. *Nat.Rev.Drug Discov.* **3**: 577-626

Obadiah J, Avidor-Reiss T, Fishburn CS, Carmon S, Bayewitch M, Vogel Z, Fuchs S, and Levavi-Sivan B. (1999) Adenylyl cyclase interaction with the D2 dopamine receptor family; differential coupling to Gi, Gz, and Gs. *Cell Mol Neurobiol.* **19**:653-664.

Ohno-Shosaku T, Hashimotodani Y, Maejima T, and Kano M. (2005) Ca^{2+} signaling and synaptic modulation: regulation of endocannabinoid-mediated synaptic modulation by Ca^{2+}. *Cell Calcium.* **38**:69-374.

Omori K, Kotera J. (2007) Overview of PDEs and their regulation. *Circ Res.***100**: 309-27.

Ono K, Noma A. (1994) Autonomic regulation of cardiac chloride current. *Jap J Physiol* **44**:193-198.

Papa S, Rasmo DD, Technikova-Dobrova Z, Panelli D, Signorile A, Scacco S, Petruzzella V, Papa F, Palmisano G, Gnoni A, Micelli L, and Sardanelli AM. (2012) Respiratory chain complex I, a main regulatory target of the cAMP/PKA pathway is defective in different human diseases. *FEBS Lett.* **586:**568-77.

Paterson JM, Smith SM, Harmar AJ, and Antoni FA. (1995) Control of a novel adenylyl cyclase by calcineurin. *Biochem Biophys Res Commun.* **214**:1000-1008.

Paterson JM, Smith SM, Simpson J, Grace OC, Sosunov AA, Bell JE, and Antoni FA. (2000) Characterisation of human adenylyl cyclase type IX reveals inhibition by Ca2+/Calcineurin and differential mRNA plyadenylation. *J.Neurochem.* **75**:1358-1367.

Patrucco E, Notte A, Barberis L, Selvetella G, Maffei A, Brancaccio M, Marengo S, Russo G, Azzolino O, Rybalkin SD, Silengo L, Altruda F, Wetzker R, Wymann MP, Lembo

G, and Hirsch E. (2004) PI3Kγ Modulates the Cardiac Response to Chronic Pressure Overload by Distinct Kinase-Dependent and -Independent Effects. *Cell.* **118**: 375-387.

Patschan D, Patschan S, Wessels JT, Becker JU, David S, Henze E, Goligorsky MS and Muller GA. (2010) Epac-1 activator 8-O-cAMP augments renoprotective effects of syngeneic [corrected] murine EPCs in acute ischemic kidney injury. *Am. J. Physiol. Renal Physiol.* **298**:78-85

Pavan B, Biondi C, and Dalpiaz A. (2009) Adenylyl cyclases as innovative therapeutic goals. *Drug Discov Today* **14**: 982-991.

Penn RB, Parent JL, Pronin AN, Panettieri RA Jr, and Benovic JL. (1999) Pharmacological inhibition of protein kinases in intact cells: antagonism of beta adrenergic receptor ligand binding by H-89 reveals limitations of usefulness. *J Pharmacol Exp Ther*. **288**:428-37.

Pian P, Bucchi A, Decostanzo A, Robinson RB, and Siegelbaum SA. (2002) Modulation of cyclic nucleotide-regulated HCN channels by PIP(2) and receptors coupled to phospholipase C. *Pflugers Arch*. **455**:125-45.

Pierce KL, Premont RT, and Lefkowitz RJ. (2002) Seventransmembrane receptors. *Nature Reviews Molecular Cell Biology*. **9**:639-650.

Pierre S, Eschenhagen T, Geisslinger G. and Scholich K. (2009) Capturing adenylyl cyclases as potential drug targets. *Nat Rev Drug Discov.* **8**:321-335.

Ponsioen B, Zhao J, Riedl J, Zwartkruis F, van der Krogt G, Zaccolo M, Moolenaar WH, Bos JL, and Jalink K. (2004) Detecting cAMP-induced Epac activation by fluorescence resonance energy transfer: Epac as a novel cAMP indicator. *EMBO Rep*. **5**:1176-80

Poppleton H, Sun H, Fulgham D, Bertics P, and Patel TB. (1996) Activation of Gsalpha by the epidermal growth factor receptor involves phosphorylation. *J Biol Chem.* **271**:6947-6951.

Postea O, and Biel M. (2011) Exploring HCN channels as novel drug targets. *Nat Rev Drug Discov*. **10**:903-14.

Premont RT, Matsuoka I, Mattei MG, Pouille Y, Defer N, and Hanoune J. (1996) Identification and characterization of a widely expressed form of adenylyl cyclase. *J Biol Chem.* **271**:13900-13907.

Qiao J, Mei FC, Popov VL, Vergara LA, and Cheng X. (2002) Cell cycle-dependent subcellular localization of exchange factor directly activated by cAMP. *J Biol Chem*. **277**:26581-6

Rabe KF. (2011) Update on roflumilast, a phosphodiesterase 4 inhibitor for the treatment of chronic obstructive pulmonary disease. *Br J Pharmacol*. **163**:53-67.

Rall TW. (1971) Formation and metabolism of cyclic AMP in the mammalian central nervous system. *Ann N Y Acad Sci.* **185**:520-530.

Rameh LE, and Cantley LC. (1999) The role of phosphoinositide 3-kinase lipid products in cell function. *J Biol Chem.* **274**:8347-50.

Rhee MH, Nevo I, Avidor-Reiss T, Levy R, and Vogel Z. (2000) Differential superactivation of adenylyl cyclase isozymes after chronic activation of the CB1 cannabinoid receptor. *Mol Pharmacol*. **57**:746-752.

Rhee SG. (2001) Regulation of phosphoinositide-specific phospholipase C. *Annu Rev.Biochem.* **70**: 281-312.

Roberts DJ, and Waelbroeck M. (2004) G-protein activation by G-protein coupled receptors: ternary complex formation or catalyzed reaction? *Biochem Pharmacol.* **68**:799-806.

Rochais F, Abi-Gerges A, Horner K, Lefebvre F, Cooper DM, Conti M, Fischmeister R, and Vandecasteele G. (2006) A specific pattern of phosphodiesterases controls the cAMP signals generated by different G_s-coupled receptors in adult rat ventricular myocytes. *Circ Res.* **98:**1081-1088.

Roseberry AG, Bünemann M, Elavunkal J, and Hosey MM. (2001). Agonist-dependent delivery of M(2) muscarinic acetylcholine receptors to the cell surface after pertussis toxin treatment. *Mol Pharmacol.* **59**:1256-1268.

Roskoski R Jr. (2005) Src kinase regulation by phosphorylation and dephosphorylation. *Biochem Biophys Res Commun.* **331**:1-14.

Ross EM, Maguire ME, Sturgill TW, Biltonen RL, and Gilman AG. (1977) Relationship between the β-adrenergic receptor and adenylyl cyclase. *J Biol Chem.* **252**:5761-5775.

Runne C, and Chen S. (2013) PLEKHG2 promotes heterotrimeric G protein βγ-stimulated lymphocyte migration via Rac and Cdc42 activation and actin polymerization. *Mol Cell Biol.* **33**: 4294-307.

Sadana R, Dascal N, and Dessauer CW. (2009) N terminus of type 5 adenylyl cyclase scaffolds Gs heterotrimer. *Mol Pharmacol.* **76**: 1256-1264.

Sands WA, Woolson HD, Milne GR, Rutherford C, and Palmer TM. (2006) Exchange protein activated by cyclic AMP (Epac)-mediated induction of suppressor of cytokine signaling 3 (SOCS-3) in vascular endothelial cells. *Mol Cell Biol.* **26:** 6333-46.

Scholich K, Barbier AJ, Mullenix JB, and Patel TB. (1997) Characterization of soluble forms of nonchimeric type V adenylyl cyclases. *Proc Natl Acad Sci U S A.* **94**:2915-2920.

Schulz S. (2005) C-type natriuretic peptide and guanylyl cyclase B receptor. *Peptides.* **26**: 1024-1034.

Scott JD, and Pawson T. (2000) Cell communication: the inside story. *Sci.Am.* **282**:72-79.

Seamon KB, Padgett W, and Daly JW. (1981) Forskolin: unique diterpene activator of adenylyl cyclase in membranes and in intact cells. *Proc Natl Acad Sci U S A.* **78**: 3363-3367.

Sharman JL, Benson HE, Pawson AJ, Lukito V, Mpamhanga CP, Bombail V, Davenport AP, Peters JA, Spedding M, Harmar AJ, and Nc I. (2013) IUPHAR-DB: updated database content and new features. *Nucleic Acids Res.* **41**(Database issue): D1083-1088.

Smrcka AV, and Sternweis PC. (1993) Regulation of purified subtypes of phosphatidylinositol-specific phospholipase C-β by Gα-subunits and Gβγ-dimers. *J Biol Chem.* **268**:9667-9674.

Song Y, Shryock JC, and Belardinelli L. (1998) Potentiating effect of acetylcholine on stimulation by isoproterenol of L-type Ca^{2+} current and arrhythmogenic triggered activity in guinea pig ventricular myocytes. *J Cardiovasc Electrophysiol.* **9**:718–726.

Sosunov SA, Kemaikin SP, Kurnikova IA, Antoni FA, and Sosunov AA. (2001) Expression of adenylyl cyclase type IX and calcineurin in synapses of the central nervous system. *Bull Exp Biol Med.* **131**:172-175.

Steiner D, Saya D, Schallmach E, Simonds WF, and Vogel Z. (2006) Adenylyl cyclase type VIII activity is regulated by Gβγ-subunits. *Cell Signal.* **18**: 62-68.

Stephens LR, Eguinoa A, Erdjument-Bromage H, Lui M, Cooke F, Coadwell J, Smrcka AS, Thelen M, Cadwallader K, Tempst P, and Hawkins PT. (1997) The G beta gamma sensitivity of a PI3K is dependent upon a tightly associated adaptor, p101. *Cell*. **89**:105-14.

Stokoe D, Stephens LR, Copeland T, Gaffney PR, Reese CB, Painter GF, Holmes AB, McCormick F, and Hawkins PT. (1999) Dual role of phosphatidylinositol-3,4,5-trisphosphate in the activation of protein kinase B. *Science.* **277**:567-70.

Stoyanov B, Volinia S, Hanck T, Rubio I, Loubtchenkov M, Malek D, Stoyanova S, Vanhaesebroeck B, Dhand R, Nürnberg B, Gierschik P, Seedorf K, Hsuan JJ, Waterfield MD, and Wetzker R. (1995) Cloning and characterization of a G protein-activated human phosphoinositide-3 kinase. *Science* **269**:690-693.

Strathmann MP, and Simon MI. (1991) Gα12 and Gα13-subunits define a fourth class of Gα-subunits. *Proc Natl Acad Sci U S A.* **88**:5582-5586.

Suire S, Coadwell J, Ferguson GJ, Davidson K, Hawkins P, and Stephens L. (2005) p84, a new Gbetagamma-activated regulatory subunit of the type IB phosphoinositide 3-kinase p110gamma. *Curr Biol.* **15**: 566–570.

Sunahara RK, Tesmer JJ, Gilman AG, and Sprang SR. (1997) Crystal structure of the adenylyl cyclase activator Gαs. *Science.* **278**: 1943-1947.

Surgand JS, Rodrigo J, Kellenberger E, and Rognan D. (2006) A chemogenomic analysis of the transmembrane binding cavity of human G-protein-coupled receptors. *Proteins*. **62**:509-538.

Sutherland EW, and Rall TW. (1960) Formation of adenosine-3,5-phosphate (cyclic adenylate) and its relation to the action of several neurohormones or hormones. *Acta Endocrinol.* **34**:171-174.

Sutherland EW, and Robison GA. (1966) The role of cyclic-3',5'-AMP in responses to catecholamines and other hormones. *Pharmacol Rev.* **18**:145-61.

Tang WJ, and Gilman AG (1991) Type-specific regulation of adenylyl cyclase by G protein bg subunits. *Science*. **254**:1500-1503.

Tang WJ, and Gilman AG (1995) Construction of a soluble adenylyl cyclase activated by Gsa and forskolin. *Science*. **268**:1769-1772.

Tang WJ, Krupinski J, and Gilman AG. (1991) Expression and characterization of calmodulin-activated (type I) adenylyl cyclase. *J Biol Chem.* **266**:8595–6803.

Taskén K, and Aandahl EM. (2004) Localized effects of cAMP mediated by distinct routes of protein kinase A. *Physiol Rev*. **84**: 137-67.

Taussig R, and Gilman AG. (1995) Mammalian membrane-bound adenylyl cyclases. *J Biol Chem.* **270:**1-4.

Taussig R, Tang WJ, Hepler JR, and Gilman AG. (1994) Distinct patterns of bidirectional regulation of mammalian adenylyl cyclases. *J Biol Chem*. **269**:6093–6100.

Thompson WJ, Epstein PM, and Strada SJ. (1979) Purification and characterization of high-affinity cyclic adenosine monophosphate phosphodiesterase from dog kidney. *Biochemistry*. **18**:5228-37.

Torphy TJ. (1998) Phosphodiesterase isozymes: molecular targets for novel antiasthma agents. *Am J Respir Crit Care Med*. **157**:351-70.

Uhlen M, Oksvold P, Fagerberg L, Lundberg E, Jonasson K, Forsberg M, Zwahlen M, Kampf C, Wester K, Hober S, Wernerus H, Björling L, and Ponten F. (2010) Towards a knowledge-based Human Protein Atlas. *Nat Biotechnol*. **28**: 1248-1250.

Ukhanov K, Brunert D, Corey EA, and Ache BW. (2011) Phosphoinositide 3-kinase-dependent antagonism in mammalian olfactory receptor neurons. *J Neurosci.* **31**:273-80.

Vassilatis DK, Hohmann JG, Zeng H, Li F, Ranchalis JE, Mortrud MT, Brown A, Rodriguez, SS, Weller JR, Wright AC, Bergmann JE, and Gaitanaris GA. (2003). The G protein-coupled receptor repertoires of human and mouse. *Proc Natl Acad Sci. U S A.* **100**: 4903-4908.

Viard P, Exner T, Maier U, Mironneau J, Nürnberg B, and Macrez N. (1999) Gβγ dimers stimulate vascular L-type Ca^{2+} channels via phosphoinositide 3-kinase. *FASEB J.* **13**:685-694.

von Hayn K, Werthmann RC, Nikolaev VO, Hommers LG, Lohse MJ, and Bünemann M. (2010) G_q-mediated Ca^{2+} signals inhibit adenylyl cyclases 5/6 in vascular smooth muscle cells. *Am j Physiol Cell Physiol.* **298:** 324-332.

Wachtel H. (1982) Characteristic behavioural alterations in rats induced by rolipram and other selective adenosine cyclic 3', 5'-monophosphate phosphodiesterase inhibitors. *Psychopharmacology*. **77**:309-16.

Wainger BJ, DeGennaro M, Santoro B, Siegelbaum SA, and Tibbs GR. (2001) Molecular mechanism of cAMP modulation of HCN pacemaker channels. *Nature*. **411**:805-10.

Waldman SA, Murad F. (1988) Biochemical mechanisms underlying vascular smooth muscle relaxation: the guanylate cyclase-cyclic GMP system. *J Cardiovasc Pharmacol*. **12**:115-8.

Walker EH, Pacold ME, Perisic O, Stephens L, Hawkins PT, Wymann MP, and Williams RL. (2000) Structural determinants of phosphoinositide 3-kinase inhibition by wortmannin, LY294002, quercetin, myricetin, and staurosporine. *Molecular Cell*. **6**: 909-919.

Walker EH, Perisic O, Ried C, Stephens L, and Williams RL. (1999) Structural insights into phosphoinositide 3-kinase catalysis and signalling. *Nature*. **402:** 313-320.

Wall MA, Coleman DE, Lee E, Iniguez-Lluhi JA, Posner BA, Gilman AG, and Sprang SR. (1995) The structure of the heterotrimer $G\alpha i_1\beta_1\gamma_2$. *Cell*. **83**: 1047-1058.

Walser R, Burke JE, Gogvadze E, Bohnacker T, Zhang X, Hess D, Küenzi P, Leitges M, Hirsch E, Williams RL, Laffargue M, and Wymann MP. (2013) PKCβ

phosphorylates PI3Kγ to activate it and release it from GPCR control. *PLoS Biol*. **11**: 1001587

Wang T, Pentyala S, Rebecchi MJ, and Scarlata S. (1999) Differential association of the pleckstrin homology domains of phospholipases C-beta 1, C-beta 2, and C-delta 1 with lipid bilayers and the beta gamma subunits of heterotrimeric G proteins. *Biochemistry*. **38**:1517-24

Wang YG, and Lipsius SL. (1996) A cellular mechanism contributing to postvagal tachycardia studied in isolated pacemaker cells from cat right atrium. *Circ Res*. **79**:109-14.

Wang YG, and Lipsius SL. (1995) Acetylcholine elicits a rebound stimulation of Ca^{2+} current mediated by pertussis toxin-sensitive G protein and cAMP- dependent protein kinase A in atrial myocytes. *Circ Res.* **76**: 634-644.

Wang YG, Rechenmacher CE, and Lipsius SL. (1998) Nitric oxide signaling mediates stimulation of L-type Ca^{2+} current elicited by withdrawal of acetylcholine in cat atrial myocytes. *J Gen Physiol* **111**:113–125.

Wang YX, Dhulipala PD, Li L, Benovic JL, and Kotlikoff MI. (1999) Coupling of M2 muscarinic receptors to membrane ion channels via phosphoinositide 3-kinase gamma and atypical protein kinase C. *J Biol Chem* **274:**13859–13864.

Wang D, Govindaiah G, Liu R, De Arcangelis V, Cox CL, and Xiang YK. (2010) Binding of amyloid beta peptide to beta2 adrenergic receptor induces PKA-dependent AMPA receptor hyperactivity. *FASEB J*. **24**: 3511–3521.

Watson AJ, Katz A, and Simon MI. (1994) A fifth member of the mammalian G_-subunit family. Expression in brain and activation of the _2 isotype of phospholipase C. *J Biol Chem.* **269**, 22150-22156

Watts VJ, and Neve KA. (2005) Sensitization of adenylyl cyclase by G_i/o-coupled receptors. *Pharmacol.Ther.* **106**: 405-421.

Webb BL, Hirst SJ, and Giembycz MA. (2000) Protein kinase C isoenzymes: a review oftheir structure, regulation and role in regulating airways smoothmuscle ton e and mitogenesis. *Br J Pharmacol.* **130**:1433-52.

Wei J, Wayman G, and Storm DR. (1996) Phosphorylation and inhibition of type III adenylyl cyclase by calmodulin-dependent protein kinase II in vivo. *J Biol Chem*. **271**:24231-24235.

Weitmann S, Schultz G, and Kleuss C. (2001) Adenylyl cyclase type II domains involved in Gβγ stimulation. *Biochemistry.* **40**:10853-10858

Whiting PJ, Bonnert TP, McKernan RM, Farrar S, Le Bourdelles B, Heavens RP, Smith DW, Hewson L, Rigby MR, Sirinathsinghji DJ, Thompson SA, and Wafford KA. (1999) Molecular and functional diversity of the expanding GABAA receptor gene family. *Ann N Y Acad Sci*. **868**: 645-653

Wickman K, Krapivinsky G, Corey S, Kennedy M, Nemec J, Medina I, and Clapham DE. (1999) Structure, G protein activation, and functional relevance of the cardiac G protein-gated K+ channel, IKACh. *Ann N Y Acad Sci*. **868**:386-98.

Williams ML, Hata JA, Schroder J, Rampersaud E, Petrofski J, Jakoi A, Milano CA, and Koch WJ. (2004) Targeted beta-adrenergic receptor kinase (betaARK1) inhibition by gene transfer in failing human hearts. *Circulation.* **109**: 1590–3.

Wittpoth C, Scholich K, Yigzaw Y, Stringfield TM, and Patel TB. (1999) Regions on adenylyl cyclase that are necessary for inhibition of activity by βγand Gαi-subunits of heterotrimeric G-proteins. *Proc Natl Acad Sci U S A.* **96**: 9551-9556

Worzfeld T, Wettschureck N, and Offermanns S. (2008) G(12)/G(13)-mediated signalling in mammalian physiology and disease. *Trends Pharmacol Sci.* **29**:582-9.

Wu D, Katz A, and Simon MI. (1993) Activation of phospholipase C-β2 by the Gα-subunit and Gβγ-dimers of trimeric GTP-binding protein. *Proc Natl Acad Sci U S A.* **90**: 5297-5301.

Wu EH, and Wong YH. (2005) Pertussis toxin-sensitive Gi/o proteins are involved in nerve growth factor-induced pro-survival Akt signaling cascade in PC12 cells. *Cell Signal.* **17**: 881-890.

Wymann MP, and Marone R. (2005) Phosphoinositide 3-kinase in disease: timing, location, and scaffolding. *Curr Opin Cell Biol.* **17**:141-9.

Yaksh TL, Dirksen R, and Harty GJ. (1985) Antinociceptive effects of intrathecally injected cholinomimetic drugs in the rat and cat. *Eur J Pharmacol.* **117**:81-8.

Yamauchi J, Kaziro Y, and Itoh H. (1999) Differential regulation of mitogen-activated protein kinase kinase 4 (MKK4) and 7 (MKK7) by signaling from Gβγ-subunit in human embryonal kidney 293 cells. *J Biol Chem.* **274**:1957-1965.

Yoshimura M, and Cooper DM. (1992) Cloning and expression of a Ca^{2+}-inhibitable adenylyl cyclase from NCB-20 cells. *Proc.Natl.Acad.Sci.U.S.A.* **89**: 6716-6720

Yu X, Duan KL, Shang CF, Yu HG, and Zhou Z. (2004) Calcium influx through hyperpolarization-activated cation channels (I(h) channels) contributes to activity-evoked neuronal secretion. *Proc Natl Acad Sci U S A.* **101**:1051-6.

Zahn K, Eckstein N, Tränkle C, Sadée W, and Mohr K. (2002) Allosteric modulation of muscarinic receptor signaling: alcuronium-induced conversion of pilocarpine from an agonist into an antagonist. *J Pharmacol Exp Ther.* **301**:720-8.

Zakharov SI, and Harvey RD. (1997) Rebound stimulation of the cAMP-regulated Cl^- current by acetylcholine in guinea-pig ventricular myocytes. *J Physiol.* **499**:105–120.

9. Curriculum Vitae

Name:	**Raghavender reddy Gopireddy**
Birthplace:	Hyderabad, India

Education:

2011-2015:	**PhD** in Prof. Moritz Büenemann lab, Department of Pharmacology and Clinical Pharmacy Phillips University, Marburg, Germany **Thesis title**: *Adenylyl cyclase 5/6 undelies PIP_3 dependent regulation.*
2008-2010:	**Masters** in Biomedicine at University of Skovde, Sweden. **Master thesis** in tha lab Prof. Dennis Larsson, Department of Biomedicine, University of Skovde, Sweden. **Master thesis title**: *Role of Caspase 3, 8 and 9 in 1,25-dihydroxy* vitamin *D3 mediated Apoptosis of Prostate Cancer cells.*
2007-2008:	Worked as a **Quality control analyst** at Dr. Reddy's Laboratories, Hyderabad, India
2003-2007:	**Bachelor of Pharmacy** from Osmania University, Hyderabad, India.

10. Publications

Adenylyl cyclases 5 and 6 underlie PIP_3-dependent regulation.

Reddy GR, Subramanian H, Birk A, Milde M, Nikolaev VO, Bünemann M.

FASEB J. 2015 Apr 30. ***Epub ahead of print***

11. Declaration

I solemnly declare that the work submitted here is result of my own investigation except otherwise stated. This work has not been submitted to any other university or institute towards the partial fulfillment of any degree.

Marburg, 12.06.2015

Gopireddy Raghavender reddy

12. Acknowledgements

I would like to express my deepest gratitude to my supervisor Prof. Dr. Moritz Bünemann for giving me the opportunity to perform this work in his research group and for his great support throughout my PhD and giving valuable inputs and encouragement without which this work would have been not possible. I also appreciated for his patience to answering all my questions.

I would like to thank Dr. Viaceslav O. Nikolaev, Hariharan Subramnian and Alexandra Birk for the collaboration on the cardiac myocyte and radilo ligand experiments.

I would like to thank Dr. Cornelius Krasel for answering any question I had.

I am very grateful for Dr. Cornelius Krasel, Dr. Shashi Chillapagari, Dr. Markus Milde, and Dr. Eva-Lisa Bodamann for proofreaded all this and I am very thankful for their comments. I am also thankful to Nikol Groning together with Emma Esser for their help with administrative things.

I would like to thank all other members of the Bünemann Lab for their help and creating friendly atmosphere. I would like to thank all other colleagues in the Institute of Pharmacology and Clinical Pharmacy in Marburg.

I would like to thank my best friend and fiancé Nayani Reddy for her continuous support and cheering me when things sometimes got rough. Last but not least, I would like to thank my parents and my sister for their love and moral support and understanding in all those years. I would also like to thank my friends in Marburg for making my stay a memorable one.